



UNIVERSIDADE D
COIMBRA

Eryk Carvalho Gomes Rodrigues Fernandes

**EMERGING CONTAMINANTS REMOVAL BY LIGHT
DRIVEN OZONATION AND BIOFILTRATION**

Master's thesis in the scientific area of Chemical Engineering supervised by Professor
Doctor Rui Carlos Cardoso Martins and Doctor João Manuel Ferreira Gomes and
submitted to the Department of Chemical Engineering, Faculty of Science and
Technology, University of Coimbra

September 2019

Eryk Carvalho Gomes Rodrigues Fernandes

Emerging contaminants removal by light driven ozonation and biofiltration

Master's thesis in the scientific area of Chemical Engineering, submitted to the Department of
Chemical Engineering, Faculty of Science and Technology, University of Coimbra

Supervisors

Professor Doctor Rui Martins

Doctor João Gomes

Coimbra, September 2019



UNIVERSIDADE D
COIMBRA

ACKNOWLEDGMENTS

It is the end of an incredibly complex and fulfilling chapter. In this 5 years, innumerable people, places and moments existed and will be forever in my memory. To the ones that always gave me total support, I will be forever thankful.

To the undeniable guidance and wisdom passed throughout all these years, I would like to thank all my family, specially my sister and mother.

I express all my gratitude to Professor Doctor Rui Martins and Doctor João Gomes for the shared knowledge and dedication, with your time and help it was possible to easily feel integrated in this new scenario.

I would like to thank Professor Doctor Ana Miguel for the great experience and availability, allowing me to learn and feel welcome in a totally different environment.

To all who I've shared unforgettable moments in and out of the laboratory, specially Patricia Almeida, Inês Ferreira and Nelson Assunção.

To the closest friends in this new country all these years, Jessica Fernandes, Claudia Gaspar, Eva Campos, Telma Vaz, João Pereira, Cecilia Freitas, Ana Serva and many others, thanks for the patience, shared moments and true friendship.

Sincerely,

Eryk Fernandes

ABSTRACT

The environmental problems faced nowadays are a direct response of the increasing industrial exploration of natural resources and the growing global population. These industries align with the current scientific development are responsible for the injection of different contaminants in many water bodies. Due to its persistent characteristic and the lack of efficient technologies to adequately remove them, these contaminants of emerging concern (CECs) enter in the water cycle, representing a great hazard to human and environmental health.

In this work, the use of advanced oxidation processes (AOPs), focusing on photocatalytic ozonation, have been vastly explored. Nitrogen doped catalysts were applied for the removal of a mixture of 5 parabens and the resulting solutions were evaluated according to different parameters. Ecotoxicity studies were conducted using different species to determine the toxicity levels after the treatments. AOPs were also applied the removal of *Escherichia coli* from different water matrices, and the invasive species *Corbicula fluminea* was investigated in parallel for the same disinfection propose and as a pest management strategy.

Photocatalytic ozonation reactions for the degradation of methyl-, ethyl-, propyl-, butyl- and benzylparaben as a mixture resulted in a considerable decrease of the ozone consumption compared to single ozonation, representing a great economic improvement, due to the cost of ozone production. In ecotoxicity studies, all treated solution had lower toxicity to the 3 investigated species compared with the initial parabens mixture solution.

The effect of different parameters over photocatalytic ozonation and parabens depletion were investigated. Neutral pH conditions improved the contaminants removal, achieving total elimination in 60 min, half the time needed for the unaltered pH solution (acidic pH). The presence of different ionic species, such as I^- , HCO_3^- , SO_4^{2-} and Cl^- also had a beneficial effect over the reactions, reducing the transferred ozone doses needed for total parabens removal. The degradation of the contaminants when spiked in two different water matrices, river water and a secondary wastewater, had a slight improvement, which indicates that, in real conditions, the process efficiency is still verified.

In disinfection tests, both single and photocatalytic ozonation completely removed *E. coli* from both studied matrices. The integrated process had a reduced ozone consumption, representing a higher energetic efficiency. Biofiltration using the invasive Asian clam was not able to completely remove bacteria from river water but had a 1.1 log reduction over the first 6 h of the tests. The use of *Corbicula fluminea* in this process is not yet optimized and the results are

preliminary, but still represent a great potential, not only as a low-cost disinfection technology but also as a pest management technique, avoiding the negative environmental and economic effects of the invasive species.

Keywords: Nitrogen doped; Photocatalytic ozonation; *Escherichia coli*; Biofiltration; *Corbicula fluminea*; Ecotoxicity tests;

RESUMO

Os atuais problemas ambientais enfrentados são uma consequência direta da crescente exploração industrial de recursos naturais e população mundial. As indústrias juntamente com o atual desenvolvimento científico são responsáveis pela inserção de diferentes contaminantes em diversos meios hídricos. Devido a elevada persistência nos meios e a falta de tecnologias eficientes para removê-los, estes contaminantes emergentes entram no ciclo da água, representando um grande perigo à saúde humana e ambiental.

Neste trabalho, o uso de processos de oxidação avançados, principalmente o processo integrado de fotocatalise e ozonólise, foi amplamente estudado. Catalisadores de base dióxido titânio dopados com diferentes concentrações de azoto foram aplicados na degradação de uma mistura contendo 5 parabenos. As soluções obtidas foram avaliadas consoante diferentes parâmetros. Estudos acerca da ecotoxicidade também foram realizados para determinar os níveis de toxicidade relativos a 3 diferentes espécies: *Allivibrio fischeri*, *Lepidium sativum* e *Corbicula fluminea*. Processos de oxidação também foram aplicados para a remoção da bactéria *Escherichia coli* de diferentes fontes hídricas, e estudados em conjunto com o uso da espécie invasora *Corbicula fluminea* em testes de biofiltração tanto quanto uma técnica de desinfecção quanto controlo e prevenção de pestes

Testes de ozonólise fotocatalítica para a degradação da mistura de metil-, etil-, propil-, butil e benzilparabeno resultaram na total remoção destes e utilizando uma quantidade total de ozono consideravelmente inferior a utilizado em reações de ozonólise simples. Este facto representa uma grande vantagem económica devido ao custo da produção do ozono. Estudos acerca da ecotoxicidade de todas as soluções tratadas demonstraram um carácter menos toxico perante as 3 espécies investigadas.

Os efeitos de diferentes parâmetros sobre as reações de ozonólise fotocatalítica e a remoção dos parabenos. Valores neutros de pH melhoraram a remoção dos contaminantes, atingindo completa eliminação em 60 min, sendo este a metade do tempo necessário para a reações sem alteração do pH (pH ácido). A presença de diferentes iões, como I^- , HCO_3^- , SO_4^{2-} e Cl^- , também tiveram um efeito benéfico sobre as reações, reduzindo a quantidade de ozono transferida necessária para a remoção total dos parabenos. Os contaminantes também foram dissolvidos em água do rio e em um efluente secundário, obtendo uma taxa de degradação levemente superior, o que indica que mesmo em condições de tratamento reais, a eficiência do processo se mantém.

Nos testes de desinfecção realizados, reações de ozonólise simples e fotocatalítica foram capazes de eliminar totalmente a bactéria investigada de ambas as matrizes estudadas. Contudo, o processo integrado obteve uma redução do consumo de ozono, representando uma maior eficiência energética. Testes de biofiltração utilizando a espécie de amêijoia asiática invasora não obtiveram a completa remoção da bactéria presente na solução de água do rio, porém ainda obteve uma redução logarítmica de 1.1 nas primeiras 6 h. O uso da bivalve *Corbicula fluminea* neste processo não se encontra totalmente otimizada e os resultados obtidos ainda são preliminares, porém ainda representa um grande potencial para esta aplicação, não somente como uma tecnologia de desinfecção de baixo custo, mas também como uma estratégia de prevenção e controle de pestes, evitando os seus impactos ambientais e económicos.

Palavras-Chave: Nitrogénio dopado; Ozonólise fotocatalítica; *Escherichia coli*; Biofiltração; *Corbicula fluminea*; Testes de Ecotoxicidade;

INDEX

1. INTRODUCTION	1
1.1. Work Motivation and Scope	1
1.2. Thesis Objectives	4
1.3. Thesis Structure.....	4
2. THEORETICAL BACKGROUND AND FRAMEWORK	5
2.1. Parabens	5
2.2. Microorganisms.....	6
2.3. Photocatalytic Ozonation	6
2.4. Biofiltration.....	9
2.5. Toxicity Assessment	10
3. STATE OF THE ART	11
3.1. Parabens Degradation.....	11
3.2. Bacteria Removal	15
4. MATERIALS AND METHODS	19
4.1. Catalysts Synthesis.....	19
4.1.1. Method 1.....	19
4.1.2. Method 2.....	19
4.2. Catalysts Characterization.....	19
4.2.1. Specific Surface Area (S_{BET})	19
4.2.2. X-Ray Diffraction.....	20
4.2.3. Raman Spectroscopy	20
4.3. Asian Clams Gathering	20
4.4. Experimental Procedures	20
4.4.1. Parabens Oxidation Reactions	20
4.4.2. Bacteria Disinfection Tests.....	21
4.5. Analytical Methods	22
4.5.1. High-Performance Liquid Chromatography (HPLC).....	22
4.5.2. Chemical Oxygen Demand (COD).....	23
4.5.3. Total Organic Carbon (TOC).....	23
4.5.4. Ionic Chromatography	23
4.6. Toxicity Assessment	23
4.6.1. <i>Lepidium sativum</i>	23
4.6.2. <i>Allivibrio fischeri</i>	24
4.6.3. <i>Corbicula fluminea</i>	24

5. PHOCATALYTIC OZONATION FOR PARABENS REMOVAL	25
5.1. Method 1	25
5.1.1. Catalysts Characterization	25
5.1.2. Parabens Degradation	29
5.1.3. Chemical Oxygen Demand (COD) and Total Organic Carbon (TOC) Removals	32
5.1.4. Toxicity Evaluation	34
5.2. Method 2	36
5.2.1. Catalysts Characterization	36
5.2.2. Parabens Degradation	39
5.2.3. Chemical Oxygen Demand (COD) and Total Organic Carbon (TOC) Removals	40
5.2.4. Toxicity Evaluation	42
5.3. Comparison of Catalysts	43
6. MECHANISTIC STUDIES	45
6.1. Effect of pH and Catalyst Loading.....	45
6.2. Effect of Radical Scavengers and Water Matrix	47
7. BACTERIA REMOVAL	55
7.1. Advanced Oxidation Processes	55
7.2. Biofiltration	57
8. CONCLUSIONS	59
9. FUTURE WORK	61
REFERENCES	63
APPENDIX A	75
APPENDIX B	78

LIST OF FIGURES

Figure 2.1 - Generic structural formula of parabens	5
Figure 2.2 – Illustration of different reaction mechanisms in photocatalytic ozonation.....	8
Figure 4.1 – <i>E. Coli</i> quantification and confirmation tests: (a) membranes after filtration, (b) oxidase test, (c) indol test.	22
Figure 5.1 – X-ray diffraction patterns for TiO ₂ , 5% N-TiO ₂ and 15% N -TiO ₂ using synthesis method 1.....	26
Figure 5.2 – Raman spectra of method 1 TiO ₂ catalysts.	28
Figure 5.3 – Tauc’s plot of 10% N-TiO ₂	29
Figure 5.4 – Propylparaben (a), butylparaben (b) and benzylparaben (c) degradation (%) and Transferred Ozone Dose (mg L ⁻¹) during UV/N-TiO ₂ reactions using method 1 catalysts Erro! Marcador não definido.0	
Figure 5.5 – Methylparaben degradation (%) and Transferred Ozone Dose (mg L ⁻¹) during UV/O ₃ and UV/O ₃ /N-TiO ₂ reactions using N-doped method 1 catalysts	Erro! Marcador não definido.1
Figure 5.6 – Chemical oxygen demand removals during and total organic carbon removals after 120 min of UV/O ₃ /TiO ₂ and UV/O ₃ reactions using method 1 N-doped catalysts. Erro! Marcador não definido.	
Figure 5.7 – X-ray diffraction patterns for TiO ₂ , 5%N-TiO ₂ and 5%NS -TiO ₂ using synthesis method 2.....	36
Figure 5.8 – Raman spectra of method 2 TiO ₂ catalysts.	37
Figure 5.9 – Tauc’s plot of method 2 N-TiO ₂	38
Figure 5.10 – Methylparaben degradation (%) and Transferred Ozone Dose (mg L ⁻¹) during UV/O ₃ and UV/O ₃ /TiO ₂ reactions using N-doped (left) and NS-codoped (right) method 2 catalysts.....	39
Figure 5.11 – Chemical Oxygen Demand removals during and Total Organic Carbon removals after 120 min of UV/O ₃ and UV/O ₃ /TiO ₂ reactions using N-doped and NS-codoped method 2 catalysts. ..	41
Figure 6.1 – Methylparaben (a), ethylparaben (b), propylparaben (c), butylparaben (d) and benzylparaben € degradation over 120 min reactions with pH adjustment using a buffer mixture or sodium hydroxide (NaOH), using 140 mg L ¹ of catalyst and the original conditions (unaltered pH and 70 mg L ¹ of catalyst) using method 1 10% N-TiO ₂	46

Figure 6.2 - Methyl-, ethyl-, propyl-, butyl- and benzylparaben degradation as function of TOD over 120 min photocatalytic ozonation reactions using method 1 10% N-TiO₂ in solutions containing only ultrapure water (original) or with the addition of 13mM of isopropanol, 5mM of potassium iodide (KI), 20 mg L⁻¹ of humic acid or 125 mg L⁻¹ of sodium chloride (NaCl), sodium sulfate (Na₂SO₄), sodium bicarbonate (NaHCO₃) and humic acid..... 48

Figure 6.3 – 4-Hydroxybenzoic acid (a), 2,4-Dihydroxybenzoic acid (b), 1,4-Benzoquinone (c) and hydroquinone (d) concentration evolution during photocatalytic ozonation of parabens solution with or without isopropanol obtained through normalized peak areas from HPLC tests as function of TOD. . 49

Figure 6.4 - Methylparaben and ethylparaben degradation over 120 min N-TiO₂ photocatalytic ozonation reaction and the transferred ozone dose (TOD)..... 52

Figure 7.1 - *E. coli* removal in UV/O₃/N-TiO₂ and UV/O₃ reactions and TOD evolution 56

Figure 7.2 - *E. coli* removal in biofiltration and control tests 57

LIST OF TABLES

Table 3.1 - Overview of CECs degradation studies using TiO ₂ and TiO ₂ +O ₃	13
Table 3.2 - Overview of microorganisms disinfection studies using AOPs and biofiltration	17
Table 5.1 - TiO ₂ catalysts crystallite sizes obtained using Debye-Scherrer equation.	27
Table 5.2 – Chemical oxygen demand and total organic carbon removal, transferred ozone dissolved and partial oxidation yield after 120 min reaction using different processes.....	33
Table 5.3 - <i>L. sativum</i> germination index, <i>A. fischeri</i> luminescence inhibition after 15 min exposure and <i>C. fluminea</i> mortality after 48 h exposure to solutions obtained from 120 min treatment using different process.....	34
Table 5.4 - TiO ₂ catalysts crystallite sizes obtained using Debye-Scherrer equation.	37
Table 5.5 - Estimated band gap energies for method 2 N-TiO ₂ catalysts.....	38
Table 5.6 - Parabens removal after 120 min of photocatalytic oxidation using method 2 N-TiO ₂	39
Table 5.7 - Chemical oxygen demand and total organic carbon removal, transferred ozone dissolved and partial oxidation yield after 120 min reaction using different processes.....	42
Table 5.8 - <i>L. sativum</i> germination index, <i>A. fischeri</i> luminescence inhibition after 15 min exposure and <i>C. fluminea</i> mortality after 48 h exposure to solutions obtained from 120 min treatment using different process.....	42
Table 5.9 - Transferred ozone dissolved, chemical oxygen demand and total organic carbon removal, partial oxidation yield, <i>L. sativum</i> germination index, <i>A. fischeri</i> luminescence inhibition after 15 min exposure and <i>C. fluminea</i> mortality after 48 h exposure of solutions obtained after photocatalytic ozonation reactions.....	43
Table 6.1 - Secondary wastewater (SWW) and river water (RW) characterization.....	51
Table 6.2 – Chloride (Cl ⁻), nitrate (NO ₃ ⁻) and sulfate (SO ₄ ²⁻) concentrations after 120 min photocatalytic reactions using river water (RW) and a secondary wastewater (SWW) spiked with the mixture of 5 parabens.....	52
Table 7.1 - Secondary wastewater (SWW) and river water (RW) characterization.	55
Table 7.2 - TOD evolution during disinfection reactions using AOPs.....	55

NOMENCLATURE

$[O_3]_i$ – Inlet ozone concentration

$[O_3]_o$ – Outlet ozone concentration

μ_{partox} – Partial oxidation yield

D – Crystallite size

e^- - electron

E_{bg} – Band gap energy

E^0 – Standard redox potential

h – Plank's constant

K – Shape factor

L_R – Radical length of sample

$L_{R,B}$ – Radical length of control

N_G – Number of germinated seeds of sample

$N_{G,B}$ - Number of germinated seeds of control

N-TiO₂ – Nitrogen doped titanium dioxide catalyst

NS-TiO₂ – Nitrogen and sulfur codoped titanium dioxide

Q_{gas} – Gas flow rate

t – time

V_{liq} – Volume of liquid

α – Absorption coefficient

B - full width at half maximum peak

λ – Wavelength

ν - light frequency

ACRONYMS

AOP – Advanced oxidation process
BP – Butylparaben
BzP – Benzylparaben
CB – Conduction band
CEC – Contaminant of emergent concern
CFU – colony-forming unit
COD – Chemical oxygen demand
DBP – Disinfection by-product
EP – Ethylparaben
EU – European Union
GHG – Greenhouse gas
GI – Germination index
HPLC – High-performance liquid chromatography
MP – Methylparaben
PHBA - Parahydroxybenzoic acid
PPCP – Pharmaceuticals and personal care product
RRG – Relative radical length
RSG – Relative seed germination
TOC – Total organic carbon
TOD – Transferred ozone dose
TTIP – Titanium (IV) isopropoxide
USA – United States of America
UV – Ultraviolet radiation
UVA – Ultraviolet radiation with wavelengths between 320 and 400 nm
VB – Valence band
WHO – World Health Organization
WWTP – Wastewater treatment plant
XRD – X-ray diffraction

1. INTRODUCTION

1.1. Work Motivation and Scope

The increasing global population is responsible for a great boost in the overall industry, mostly due to the resulting increase in the consume of different products, which are continuously getting more specialized and technologically advanced. Both population and industry are deeply dependent of natural resources. However, these resources do not have the renovation capability in front of the current intake, leading to shortages in different regions of the planet.

Water is one of the most plenty and vital resources on Earth, occupying more than 70% of its surface, but only a small amount is safe for drinking (Molins-Delgado et al., 2015). Additionally, water is also one of the most degraded of the resources, due to the global warming, increasing consume and contamination of multiple water sources responsible for the reduction of water availability, resulting in two thirds of the world population facing water scarcity for at least 1 month in the year (WWAP, 2017).

Besides the reduction of clean water availability, the direct or indirect contact with contaminated water represents an important consequence of water pollution. Annually 3.4 million people die from the result of waterborne and water-related diseases and are estimated that 780 million people still do not have access to an improved water source (Boelee et al., 2019; WHO, 2012)

In this context, treatment and reutilization of water resources becomes a highly important subject and essential for that current and future generations have proper access to clean water. Thus, the analysis and maintenance of water quality are the focus of an increasing number of studies by the scientific community.

The wastewater treatment plants (WWTPs) are the key element in the treatment of contaminated water, making possible its reutilization and turning a previously stablish linear strategy of water consumption into a more circular model. Nowadays, around 80% of the world wastewater is inadequately discharged into water bodies, indicating the inefficiency of these installations. This problem has great consequences, leading to not only a human health hazard but also eutrophication and emissions of methane and other greenhouse gases (GHGs), representing a significant role in global warming (IWA, 2018). Therefore, wastewater reclamation can be a suitable alternative for water reuse strategies (Bixio et al., 2006).

Over 150 000 substances are commercially used nowadays, but only a fraction of these that are released in the environment are constantly monitored (AMAP, 2017). Microorganisms, heavy metals, organic pollutants (e.g. phenols, dioxins) and nutrients (e.g. N, P, K) are usually the targets of water treatment and quality analysis technologies and can be categorized as well-known contaminants (Naidu et al., 2016a; Rodriguez-Narvaez et al., 2017). However, the industrial development and increasing consume of certain products are responsible for the presence of some compounds, known as contaminants of emerging concern (CECs). The CECs are molecules present in pharmaceuticals and personal care products (PPCPs), pesticides, among others, and are only recently released and/or detected in different environments.

These micropollutants existent in water sources, due to their high persistency and recalcitrant characteristics, represent a serious threat to human and environmental health, even if they are only detected typically in concentrations at the ng/L and $\mu\text{g/L}$ range (Ahmed et al., 2017). Many of the CECs have proven or at least the suspect of mutagenic, cancerogenic or reproductive toxicity, and due to its low concentrations, the chronic characteristics of these effects constitute a problem of high concern not only for this, but also future generations. Also, the antibiotics that are being highly consumed and released, in very low concentrations do not have the intended effect, but in controversy result in the formation of high resistance bacteria strains (Bhattacharyya et al., 2019).

Nowadays, CECs are not efficiently regulated at international level, but the European Community and especially Switzerland with the Water Protection Act implemented in 2016, and other countries such as the United States of America and Canada have already begun to take actions to study more closely the consequences and effects of these compounds, as well as the control of their utilization and release in the environment (Eggen et al., 2014; FOEN, 2015; Taheran et al., 2018).

Currently, some attempts are being done to list, gather and motivate the study and investigation of the CECs, for example the NORMAN network supported by the European Commission (EC). This organization is responsible for the harmonization of measurement methods, enhancing the exchange of information, monitoring emerging environmental substances and, in parallel with directives established by the EC, the creation of lists for better organize and categorize these substances (Dulio et al., 2018). Some of these listed substances are, for example, parabens (Methyl, Ethyl, Propyl and Butylparaben), which are very commonly used as preservatives in PPCPs.

Many sources are responsible for the release of these pollutants, being the WWTPs one of the most substantial, since human's excretion have a large impact on this effect (Taheran, 2018). WWTPs are not currently designed for these contaminants removal nor the usual technologies are globally capable to totally degrade these substances. This can be explained by the wide spectrum of these substances with different physicochemical properties, such as the refractory characteristics of the CECs for the treatment methods used in WWTPs.

Once in surface waters, CECs ends up in a variety of niches, such as soil, that is also contaminated by the usage of manure and bio-solids from sewage treatment plants, which is an important matter for agriculture reuse. For instance, in Portugal, more than 87% of its produced sludge is currently being applied in agriculture activities (Kelessidis et al., 2012; Naidu et al., 2016b). Other important endpoint for these contaminants are evidently groundwater and seas, where then are spread between other water bodies and ecosystems, been currently detected in the most isolated zones like polar regions and mountain glaciers (Ferrario et al., 2017).

In front of the growing presence and awareness of the CECs, a few technologies have already been applied in some treatment facilities for the degradation of these substances. Activated carbon and membrane filtration methods, such as nanofiltration and reverse osmosis, are examples of these technologies, currently used in Switzerland and Germany at full scale. Despite of the satisfactory removal rates, studies indicate that the ultimate abatement of the CECs is not yet accomplished (Casas et al., 2015; Luigi Rizzo et al., 2019; Salimi et al., 2017). Thus, the parallel research of other methods is strongly motivated in recent years, being the advanced oxidation processes (AOPs) a group of technologies with high value.

Among AOPs, ozonation, photolysis, Fenton and photocatalysis methods are the ones getting more attention nowadays and are based on the generation of highly reactive radicals, more importantly hydroxyl radicals ($\cdot\text{OH}$), that are responsible for the degradation of the contaminants (Gomes et al., 2017a; Salimi et al., 2017). Besides the usage of these single methods, combinations between them present higher degradation rates of a broader range of CECs. On this way, the utilization of photocatalytic ozonation will be the focus of this study.

These process are also used for elimination of different pathogenic contaminants, such as bacteria, fungi and virus, and will be also evaluated in this study. Alongside AOPs, the application of invasive bivalves as biofiltration host for pollutants removal will also be assessed.

1.2. Thesis Objectives

The following study focused in the investigation of advanced oxidation processes (AOPs), with emphasis on photocatalytic ozonation, and the use of invasive bivalves for biofiltration process. Photocatalytic ozonation were studied for the degradation of CECs, namely parabens, using nitrogen doped and nitrogen-sulfur codoped TiO₂ catalysts.

The initial and treated solutions by photocatalytic ozonation were submitted to ecotoxicity tests over a wide range of species, clams, bacteria and plants. These ecotoxicity tests allow to infer about the toxicity level after application of the oxidation process comparing to the initial mixture of parabens.

The effect of different parameter over photocatalytic reactions and the contaminants were also studied to better comprehend the mechanisms for parabens removal and possible factors existent in real water treatment scenarios.

Oxidation processes and biofiltration were applied for the removal of *Escherichia coli* using 2 different water matrices, river water and the secondary effluent from a WWTP. *Corbicula fluminea*, invasive Asian bivalve species, was applied in the biofiltration processes.

1.3. Thesis structure

The following studied is divided in 8 chapters. The first chapter include the introduction and principal objectives of the research. Chapters 2, 3 and 4 contains the theoretical background, state of the art and materials and methods, respectively, involved in the study. The chapters 5, 6 and 7 represents the results and discussion of the three main studied section. The fifth chapter is dedicated for the study of the different catalysts applied in photocatalytic ozonation reaction for the degradation of the mixture of 5 parabens and the analysis of the resulting solutions. In chapter 6 different parameters and its effects in the photocatalytic ozonation reactions were evaluated. Chapter 7 is represented the advanced oxidation and biofiltration tests for the removal of *E. coli*. The conclusions obtained from this study are present in chapter 8.

2. THEORETICAL BACKGROUND AND FRAMEWORK

2.1. Parabens

Among the innumerable pollutants classified as CECs, parabens are a well-known group, being focus of an increasing number of studies. Parabens are a series of alkyl esters of parahydroxybenzoic acid (PHBA). Due to their antimicrobial properties, are widely used as preservatives in food and PPCPs, mainly cosmetics and pharmaceuticals (Nowak et al., 2018).

Parabens are differentiated by its substituent group, being some of the most commons methyl-, ethyl-, propyl-, butyl- and benzylparaben (Figure 2.1). Their properties are directly influenced by the substituent group and the chain size of the molecule, as the case of its antimicrobial performance and water solubility, which a higher chain length results in a higher inhibition of microbial growth and a lower hydrophilicity (Błedzka et al., 2014).

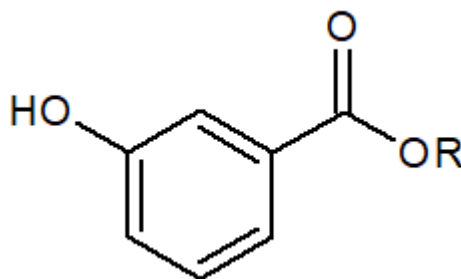


Figure 2.1 - Generic structural formula of parabens

These pollutants are currently regulated in different countries for different products. In the European Union (EU), only methyl- and ethylparaben are permitted as food additives and just in some specific uses, having different limits depending on the end use. The United States Food and Drugs Administration (FDA), for pharmaceuticals and food products, the use of parabens is limited to a maximum concentration of 1.0% and 0.1% respectively (Lee et al., 2019). For the use in cosmetics, the EU has a limit of 0.4% for single parabens and 0.8% for mixtures, and the FDA recommends the same concentration, but since 2014 EU lowered to 0.14% as the maximum content of ethyl- and butylparaben (Nowak et al., 2018).

The stricter recommendations and regulations of these contaminants is a response to the increasing concern about its endocrine disrupting potential and other possible health hazards. In the last 20 years, several studies have been published indicating the parabens carcinogenic potential and hormonal activity (Darbre et al., 2004; Oishi, 2001). These compounds have already been found in different body fluids and tissues, including tumors, which indicates a relation between parabens and cancer, and is a direct result of its widespread use, been found in high

quantity of urine samples in many tests made in different countries (Jamal et al., 2019; Liao et al., 2013; Nowak et al., 2018). In fact, studies have shown that different parabens, *in vitro*, promote the multiplication of MCF-7 human breast cells and indicate that its oestrogenic activity increases with a higher chain length (Darbre et al., 2003, 2002).

Even been biodegradable in most cases, analysis between the influent and effluent of several WWTPs shown that these pollutants still leave these facilities in concentrations in the ng/L and µg/L ranges, entering the water cycle (Błędzka et al., 2014; Lu et al., 2018). These results demonstrate that the WWTPs actual technologies are not capable to totally degrade parabens and represents a major point source.

2.2. Microorganisms

Microorganisms are commonly used in current secondary wastewater treatments, but some pathogenic species, including bacteria, viruses, protozoa and helminths, can represent an important health hazard when released in water bodies (Wen et al., 2009). These microorganisms are the major cause of innumerable waterborne diseases, leading to millions of deaths every year, mainly due to diarrhea and infections, and are already the leading cause of malnutrition as result of poor food digestion (Pichel et al., 2019).

Escherichia coli is a well-known enteric bacteria, present in the gastrointestinal tract of humans and all warm-body animals. Despite its usual harmless characteristic, some strains are dangerous to human health, such as Shiga-toxin producing *E. coli*, specially O157:H7 serotype, which causes more than 2.8 million acute illness cases worldwide annually (Gerba et al., 2004; Majowicz et al., 2014). Due to its common presence in waterbodies, *E. coli* can be used for the evaluation of water quality and safety for different uses, being the most common bacterial indicator for fecal pollution (Osuolale et al., 2017). The World Health Organization (WHO) determines that, in all water intended for drinking, no *E. coli* must be detected in 100 mL (WHO, 1997).

2.3. Photocatalytic Ozonation

The growing concern and proof of the negative effects of parabens and other CECs, allied with its high persistence and the inability of WWTPs to totally remove these contaminants, leads to the investigation of different new technologies. In this context, advanced oxidation methods rise as an important alternative to solve this problem.

These processes involve the production of different radicals (e.g. ·OH, Cl·, O₃·) capable to remove a large variety of organic molecules. AOPs have been proved to be highly effective and

less detrimental to the environment, leading to the formation of smaller molecules or, being the most desired result, total mineralization of the initial pollutants, producing water and CO₂. There are different technologies that are categorized as AOPs, such as photocatalytic ozonation, which is an integrated process involving photocatalysis and ozonation in simultaneous.

The photocatalytic process can be first categorized as homogeneous or heterogeneous. The last one is based in the use of a semiconductor solid catalysts, more frequently TiO₂. This has some advantages over homogeneous process, for example the possible selective degradation of specific compounds and the use of moderate conditions. Besides, the use of heterogeneous catalysts allows its recovery after the reaction and reuse.

Photocatalysis basically implies the activation of the catalyst by photon radiation, for example through UV or, more preferentially, solar radiation. The activation of the semiconductor material is essentially dependent of the band gap between its conduction (CB) and valence bands (VB), that determines the minimum photon energy ($h\nu$) necessary. The absorption of the photon results in the excitation of one electron (e^-) from the VB to the CB, leaving a positive hole (h^+) in the first one. The e^- can reduce an electron acceptor, such as O₂, forming its respective radical, O₂ \cdot^- . The h^+ are responsible for the oxidation of molecules in the surface of the catalyst, for example water, also forming other radicals, in this case hydroxyl (\cdot OH) (Kumar et al., 2002).

In these reactions, the recombination of the pair e^- and h^+ is a possibility that needs to be prevented to enhance the process efficiency. This can be obtained by providing oxygen, but, in the case of photocatalytic ozonation, also by ozone presence, which is a very efficient electron acceptor and results in the production of other highly active radicals (O₃ \cdot^-).

Ozonation by itself is a very common water treatment process due to its high oxidizing characteristics ($E^0 = 2.08$ eV), being very effective on the degradation of electron-rich molecules (e.g. aromatic structures, double bonds) (Ghuge et al., 2018). Ozone can react with the contaminants through direct reactions or indirectly, by producing highly oxidative \cdot OH (Xiao et al., 2015).

The low solubility and stability of ozone in water, align with its capability of only partly degrade most contaminants, not achieving total mineralization, impose some difficulties for its application at large scale (Mehrjouei et al., 2015).

The combination of both ozonation and photocatalysis is a promising method with important synergic effects. Ozone, as a very efficient electron acceptor, can reduce the electron-hole recombination of the catalyst and adsorb on its surface, producing more radicals (Xiao et al.,

2015). The catalyst is then responsible for the acceleration of the ozone decomposition into hydroxyl radicals, resulting in a process capable to eliminate more quickly and efficiently a wider range of contaminants, compared with single technologies (Ghughe et al., 2018). The principal mechanisms involved in the radicals formation are present in Figure 2.2.

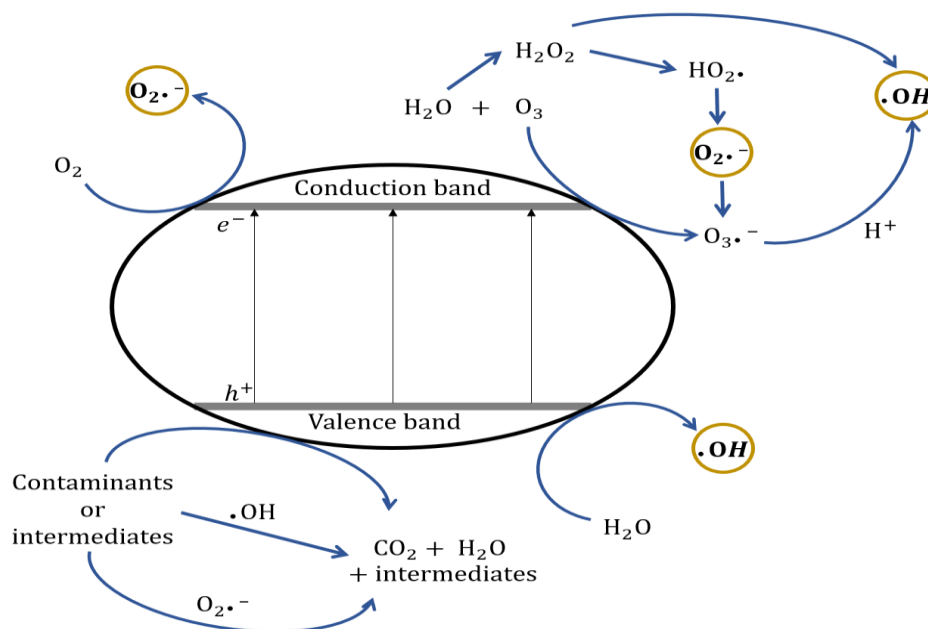


Figure 2.2 – Illustration of different reaction mechanisms in photocatalytic ozonation.

As said, TiO₂, specially anatase-phase, is the most commonly used catalyst in photo-assisted processes, due to its low cost and toxicity, high stability properties and, more importantly, it's very photoactive compared with other semiconductors. However, one of the major disadvantages of TiO₂ is that, with a band gap energy of 3.2 eV, only ultraviolet (UV) radiation is capable to activate it, under the 300-390 nm wavelength (Centi et al., 2014; Petala et al., 2015). The incoming solar irradiation that reaches Earth surface is composed by only 3-5% of UV radiation, which means that this technology is, in its original configuration, highly dependent of an artificial photon source, representing a higher cost of the overall process.

Thus, mechanisms to decrease the band gap energy of TiO₂ and shift its activity into the solar spectrum (>400 nm) are an important case of study to make photocatalytic-based processes more efficient and cheaper. In this context, doping has become a technique of high interest, involving the incorporation of different compounds, such as metal (e.g. Cu, Fe, Ag) and non-metal (e.g. N, B, C) elements, capable to interact with the CB and VB of the catalyst and modify its band gap energy (Fisher et al., 2013; Pham et al., 2017; Rimoldi et al., 2018).

Besides physicochemical contaminants, the use of AOPs is vastly studied for water disinfection and pathogenic microorganisms removal. The inactivation of different species has been

investigated, including bacteria and its spores, virus and fungi, been *Escherichia coli* the most studied bacteria (Demirel et al., 2018).

Regarding bacteria, the oxidative radicals are capable of disrupt the cell wall membrane, causing leakage of potassium ions and consequently flow of genetic and protein material, which finally results in cellular death (Ganguly et al., 2018). $\cdot\text{OH}$ are partly responsible for the anti-bacterial activity of AOPs but the presence of reactive hydrogen peroxide plays an important role in the lipid peroxidation of the cellular wall, leading to its disruption (Maness et al., 1999).

The actual disinfection processes used in WWTPs, such as chlorination, are capable to eliminate these microorganisms to some extent, but its main disadvantages the production of harmful disinfection byproducts (DBPs) (e.g. haloacetic acid, trihalomethanes) and resistance of some species (Chong et al., 2011). Single ozonation is already used since the 1970s as post-tertiary wastewater treatment, resulting in a lower DBPs formation compared with chlorination, but this process is limited to low ozone concentration since higher dosages result in higher production of DBPs, principally bromate, which is strictly regulated ($10 \mu\text{g L}^{-1}$) in many countries due to its carcinogenicity (Soltermann et al., 2017; Wert et al., 2007).

The use of photocatalysts for the removal of microorganisms is yet limited to laboratory and pilot scale, but the high degradation efficiencies of a wide spectrum of contaminants and inorganic mineralization at moderate conditions demonstrate a great potential (Mecha et al., 2017a). The combination of both photocatalysis and ozonation is not totally explored to this day, but the possibility of an increasing removal efficiency and the mineralization using lower amounts of ozone, preventing DBPs formation and microorganisms regrow, are some of the high interesting synergic advantages of this process.

2.4. Biofiltration

The application of different species for biofiltration purposes is a low-cost method for the removal of different contaminants, both chemical and biological. Bivalves, more importantly invasive species, are a commonly used class of mollusks due to its high availability, resistance and filtration rates, as well as the need for the removal of this species from invaded ecosystems due to environmental and economic impacts (Gomes et al., 2018b). The Asian clam *Corbicula fluminea* causes, besides the biodiversity reduction, losses of billions of dollars in the USA annually in pest management strategies, mostly due to biofouling and pipes clogging (Pimentel et al., 2005).

Bivalves have been extensively applied for chemicals degradation, but for the removal of microorganisms is not yet totally explored. Different pathogenic microorganisms have been studied in biofiltration test, with the Asian clam showing clearance rates up to 97 mL h⁻¹ bivalve⁻¹ in the case of *Escherichia coli*, being one of the most investigated pathogens (Silverman et al., 1995). The use of invasive bivalves, such as *C. fluminea* for the removal of pathogens rises as an environmental- and economical-friendly method, introducing a circular economy concept for both pest management and water treatment.

2.5. Toxicity Assessment

The potential health hazards of not only the CECs, but pollutants in general that are released in the environment is an important fact that motivates water treatment studies. Different contaminants have toxicological effects over humans and other species, being toxicity a vital parameter to evaluate a treatment efficiency (Cvetnic et al., 2019).

The effects of these compounds vary for each species, and due to the impossibility to directly assess it over humans, different trophic levels need to be studied to make more precise predictions. Many organisms may be used but, regarding water treatment, fish, bacteria, algae and mollusks are more commonly applied in biotoxicity tests (Movahedian et al., 2005).

According to the characteristics of the contaminant, acute or chronic effects may be analyzed, and due to its constant and low concentration, PPCPs and most CECs likely have more important chronic toxic effects over long periods. These tests need to be conducted over controlled conditions and evaluate parameters such as reproduction decrease, mass or size increase. Acute toxicity mostly verifies mortality rates using different conditions and concentrations (OECD, 2018; Quinn et al., 2008).

Some research has been conducted to evaluate parabens toxicity, but a complete toxicological assessment of the initial contaminants and its by-products after different treatments is yet to be done (Gomes et al., 2019a).

3. STATE OF THE ART

3.1. Parabens Degradation

In this decade, the study of the integrated process of photocatalytic ozonation has been intensified as a promising alternative technology for the degradation of innumerable contaminants. In front of this, the use of doped catalysts has been proved to efficiently degrade contaminants in different water matrices, but its application has been mainly focused in photocatalytic oxidation reactions, thus more complete and broader tests needs to be conducted to optimize the technology.

Sólis et al., 2015 applied TiO₂ doped with different amounts of nitrogen in photocatalytic ozonation assays for the degradation of a mixture of clopyralid, picloram and triclopyr using UVA radiation. When compared with the un-doped TiO₂, the doped catalyst resulted in higher contaminants conversion and mineralization, 99% and 80%, respectively, in 60 min. Toxicity was evaluated, and after 30 min of photocatalytic ozonation treatment, 100% survival rates of *Daphnia parvula* were obtained, and also in a 60 min treatment, 100% root growth (L/L_{Blank}) of *Lactuca sativa* and *Solanum lycopersicum* seeds.

Mecha et al., 2017 studied both photocatalytic ozonation and photocatalysis using Cu, Ag and Fe doped TiO₂ and single ozonation for the degradation of spiked phenols in deionized water and a secondary wastewater effluent. The integrated process applied in the effluent solution resulted in up to 72% and 82% lower energy requirements using UV radiation when compared with, respectively, ozonation and photocatalysis alone. Tests using solar radiation were also conducted for the photocatalytic processes, and photocatalytic ozonation required at least a 70% lower collector area than the single process. Un-doped TiO₂ had the lowest energy requirement under UV radiation but the highest collector area under solar light, 37% lower than iron doped catalyst, which indicates, as intended, the shift of the photoactivity window of the doped catalyst.

Regarding parabens, different studies demonstrate the ability of the single technologies to degrade these contaminants, but most of them involve only one paraben and the integrated technology is not yet totally explored. Gomes et al., (2017) showed that the use of noble metal doped TiO₂ (Pd, Pt, Au and Ag) with ozone led to a lower transferred ozone dose (TOD), up to 66%, necessary for the total degradation of a mixture of 5 parabens using Ag-TiO₂ and a chemical oxygen demand (COD) and total organic carbon (TOC) removals of, respectively, 23% and 12% higher when compared with single ozonation. *Allivibrio fischeri* bacteria, *Corbicula fluminea* clams and *Lepidium sativum* seeds were used for toxicological tests, resulting on no

mortality of Asian clams after 72h, 43.4% of bacteria luminescence inhibition and a 112% germination index when Ag-TiO₂ was used as catalyst.

An overview of researches involving different topics discussed and studied in this section is present in Table 3.1.

Table 3.1 - Overview of CECs degradation studies using TiO₂ and TiO₂+O₃

Contaminant	Catalyst Synthesis	Experimental Conditions	Results	Reference
Picloram, clopyralid and triclopyr	N-TiO ₂ catalysts were prepared by sol-gel method using titanium isopropoxide (TTIP) and triethylamine as doping agent, followed by a precipitation in an autoclave at 80 °C for 12h, centrifugation, drying overnight and calcination at 500 °C for 4 h.	<ul style="list-style-type: none"> • Ti:N ratio from 1:0-1:2 with bandgaps of 2.99-3.14 eV; • 1.0 L reactor covered by aluminum foil, equipped with 4 15 W emitting in the range 350-400 nm and a photon flux at 6.86×10^{-5} Einstein min⁻¹ L⁻¹; • O₂, N₂ or O₂/O₃ was fed at 30 L h⁻¹; pH=4.0; T=20°C; [N-TiO₂] =0.5 g L⁻¹; • Ultrapure water spiked with contaminants at 5 ppm each • Toxicity tests were conducted using <i>Daphnia parvula</i>, <i>Lactuca sativa</i> and <i>Solanum lycopersicum</i>. 	<ul style="list-style-type: none"> • Doped catalyst obtained a higher conversion of the contaminants compared with pure TiO₂; • 1:1.6 was the best Ti:N with almost total contaminant removal and 80% mineralization in 60 min; • Toxicity presented an increase at early stages, but total survival rates were obtained after complete degradation of the parent contaminants. 	(Solís et al., 2015)
Methylparaben, ethylparaben, propylparaben, butylparaben and benzylparaben	TTIP was used as titanium source for all catalysts; Au-TiO ₂ prepared by sol-gel method using KAuCl ₆ as doping agent, followed by a 24 h thermal treatment at 45 °C and calcination for 2 h at 400 °C; Ag-TiO ₂ , Pd-TiO ₂ and Pt-TiO ₂ prepared by photo-deposition using as doping agent AgNO ₃ , PdCl ₂ and H ₂ PtCl ₆ , respectively, irradiation for 100 min for silver and 6 h for palladium and platinum and dried at 65-120 °C for 12 h.	<ul style="list-style-type: none"> • 2.0 L glass reactor continuously stirred equipped with 3 UVA lamps; Photon flux at 5.75×10^{-7} Einstein min⁻¹ L⁻¹; • Ozone produced by an ozone generator from pure O₂ stream; • Concentration of 10 mg L⁻¹ of each contaminant using ultrapure water as solvent; The concentration of catalyst in each test is 70 mg L⁻¹; • <i>A. fischeri</i>, <i>C. fluminea</i> and <i>L. sativum</i> were used for toxicity evaluation. 	<ul style="list-style-type: none"> • 0.5%Ag-TiO₂ and 0.5%Pt-TiO₂ resulted in total contaminants removal with 40 and 64 mg L⁻¹ of TOD • TiO₂, 0.5%Ag-TiO₂ and 0.5%Pt-TiO₂ resulted in the lowest bacteria inhibition rates, 36.3%, 43.4% and 44.2%, respectively. All doped catalyst resulted in higher germination index, mostly 0.5%Ag-TiO₂, with 112%. All <i>C. fluminea</i> resulted in no mortality after 72 h. 	(Gomes et al., 2017a)
Diuron	N-TiO ₂ catalysts were prepared by sol-gel method using TTIP and triethylamine as doping agent, followed by a precipitation in an autoclave at 80 °C for 12h, centrifugation, drying overnight and calcination at 500 °C for 4 h.	<ul style="list-style-type: none"> • Ozonation, photocatalysis and photocatalytic ozonation tests were conducted; • 1.0 L reactor covered by aluminum foil, equipped with four black light lamps of 15 W emitting in the range 350-400 nm and a photon flux at 3.60×10^{-5} Einstein min⁻¹ L⁻¹; • 30 L h⁻¹ gas flow rate of O₂ or O₂/O₃; • Toxicity was evaluated using <i>A. fischeri</i> bacteria. 	<ul style="list-style-type: none"> • All processes had similar diuron removals; • Photocatalytic ozonation resulted in the lowest bacteria inhibition, around 20%, and the highest TOC removal, 85%, after 3 h; • In photocatalysis the inhibition increased through the process, reaching up to 85% after 9 h for 30 min exposure. 	(Solís et al., 2016)
Phenol	TiCl ₃ was used as Ti precursor and Fe(NO ₃) ₃ , AgNO ₃ and Cu(NO ₃) ₂ nitrates were used as doping agent for Fe-TiO ₂ , Ag-TiO ₂ and Cu-TiO ₂ catalysts at 2% wt.; The solutions were prepared and then stirred for 20 h at room temperature, centrifuged and the precipitates were dried for 10 h at 100 °C and calcinated at 500 °C for 4 h.	<ul style="list-style-type: none"> • Secondary wastewater and synthetic water prepared with deionized water and phenol (5 mg L⁻¹) were used; • Ozone was produced using air fed generator; • UV-Vis photocatalysis was studied in a 700 mL reaction vessel equipped with a medium pressure mercury lamp; • Solar photocatalysis was also studied in a tubular reactor; • Cytotoxicity was evaluated using MTT assay. 	<ul style="list-style-type: none"> • Photocatalytic ozonation had a lower energy requirement, up to 72% and 82% lower than single ozonation and photocatalysis, respectively; • Fe-TiO₂ and Ag-TiO₂ had higher average oxidation state variations, indicating higher mineralization rate; • Fe-TiO₂ and TiO₂ improved cell viabilities in both processes, achieving in UV tests 80% and 76%, and in solar tests 69% and 58%, respectively. 	(Mecha et al., 2017b)

Methylparaben	<p>*Aeroxide P-25 (70% anatase, 30% rutile), *Kronos Vlp 7000 (>85% anatase) and *Kronos Vlp 7001 (>85% anatase). Both Kronos catalysts are carbon doped.</p>	<ul style="list-style-type: none"> • 0.3 L borosilicate glass reactor under a solar simulator with a 150 W xenon ozone-free lamp and an output irradiance of 7.5 W m⁻²; • Catalyst loading from 0.1-1.0 g L⁻¹; pH= 5.2; • A volume of 30% H₂O₂ was inserted when the oxidant was necessary; • <i>Artemia franciscana</i> and <i>Artemia nauplii</i> were used for toxicity evaluation. 	<ul style="list-style-type: none"> • [P-25] = 0.5 g L⁻¹ resulted in the highest paraben degradation rate. No improvement was verified with the increase of the catalyst load; • H₂O₂ had a negative effect on the reaction rate using P-25; • Paraben degradation was completed in 35 min using P-25 catalyst, lower efficiencies were obtained for the Kronos 7000 and 7001 catalysts (40% and 20% removal in 45 min, respectively); • Higher reaction rates were obtained in acidic conditions (~5.2); • P-25 catalysts resulted in higher mineralization, with more than 40% of TOC removal after 240 min and total paraben degradation. <p>(Velegraki et al., 2015)</p>
Ethylparaben	<p>N-TiO₂ catalysts were prepared by annealing a sol-gel method at 450-800 °C under flowing ammonia while TiO₂ catalyst were calcinated in air at the same temperature range.</p>	<ul style="list-style-type: none"> • Photocatalysis were conducted under a solar simulator with a 100 W xenon ozone-free lamp with a 280 nm cut-off filter, with an incident irradiation of 1,3 x 10⁻⁴ Einstein m⁻² s⁻¹; • Visible light experiments were performed using a 420 nm cut-off filter, with an incident irradiation of 7 x 10⁻⁵ Einstein m⁻² s⁻¹; • Ultrapure water with humic acid or bicarbonates, bottled water and wastewater were used to simulate different matrix. 	<ul style="list-style-type: none"> • Doped catalyst with calcination at 600 °C resulted in higher apparent reaction rates and paraben conversion, either for solar or UV radiation; • 750 mg L⁻¹ N-TiO₂ was found to be the optimum concentration; • Humic acid had a detrimental effect on paraben degradation; • H₂O₂ enhanced the contaminant degradation. <p>(Petala et al, 2015)</p>
Diuron, 2-phenylphenol, MCPA and terbuthylazine	<p>TiO₂ and B-TiO₂ catalysts were synthesized by sol-gel method, using tert-butyl titanate as Ti precursor and boric acid as doping agent. Ammonia aqueous solution were added to the solution and then stirred, the resulting suspensions were centrifuged, and the solids were washed, dried at 60 °C overnight, grinded and calcinated at 500 °C for 30 min.</p>	<ul style="list-style-type: none"> • 3, 6, 9, and 12 wt.% B-TiO₂ and TiO₂ were prepared; • Photocatalysis were conducted in a 250 mL pyrex flask under a solar simulator equipped with a 1500 W air-cooled xenon lamp and a 300 nm cut-off filter; Irradiation intensity of 550 W m⁻²; T= 25-40 °C; • Ozone generator was used to produce an ozone-oxygen gaseous stream and fed to the reactor at 10 L h⁻¹ and [O₃] =5 mg L⁻¹; • Concentrations of each contaminant were 5 mg L⁻¹; Catalyst loading in each experiment was 0,33 g L⁻¹. 	<ul style="list-style-type: none"> • Doped catalyst leaching was detected, resulting in up to 70% of total boron loss; Contaminants adsorption were higher in doped TiO₂ catalysts; • Photocatalytic ozonation resulted in higher degradation rates and mineralization, reaching total depletion in 60 min and 65%-75% TOC removal after 2 h. Faster mineralization occurred with doped catalysts. <p>(Quiñones et al., 2015)</p>

3.2. Bacteria Removal

Alternative disinfection methods for the removal of pathogenic coliform bacteria, more importantly *Escherichia coli*, is a highly researched subject due to the disadvantages of nowadays technologies. Regarding AOPs, single ozonation is already in use in some WWTPs due to its lower DBPs formation, but the use of photocatalyst presents a potential reduction in costs and bacterial regrowth, improving the overall efficiency. Despite the number of researches involving catalysts, the integrated process of photocatalytic ozonation is yet to be fully explored. The same can be said for the use of the invasive bivalves *Corbicula fluminea* in biofiltration processes, being a highly available and low-cost alternative of a yet unused material, representing both an economical and environmental end use.

The comparison of the single and integrated AOPs is an important study to evaluate the synergic effects of photocatalytic ozonation. Mecha et al., (2017a) compared O_3 , TiO_2/O_2 and TiO_2/O_3 using both UV and solar irradiation, metal doped catalysts (Ag, Cu and Fe) and different water matrix (spiked water and secondary wastewater) for *E. coli* inactivation. In spiked water tests using UV radiation, all catalysts reached total *E. coli* inactivation within 15 min using ozone, but under solar radiation, doped catalyst were more photoactive, with Fe- TiO_2/O_3 also reaching total *E. coli* disinfection in 15 min. Using wastewater, all photocatalytic ozonation tests completely removed *E. coli*, while single ozonation and photocatalytic oxidation obtained only up to 0.839 and 0.796 under solar radiation and 0.839 and 1.000 log reductions under UV radiation, respectively.

Gomes et al., (2018a) also compared single ozonation and photocatalytic oxidation, using noble metal doped catalysts, with biofiltration using the Asian clams for the disinfection of water spiked with *Escherichia coli* at 10^3 - 10^4 CFU mL^{-1} . Tests using >20 clams L^{-1} were able to totally remove bacteria under 6 h, but only using 60 clams L^{-1} no bacterial regrowth was obtained. For AOPs, ozonation using 0.16 mgO_3 L^{-1} of TOD and Ag- and Pd- TiO_2 without light in 20 min also reached total bacterial removal with no regrowth. Analysis of the soft tissue and shells of the clams after treatment revealed only residual amounts of bacteria, indicating that *Corbicula fluminea* can fully metabolize it.

Current disinfection technologies can lead to condition or the formation of components that allow bacterial regrowth after treatment. Araña et al., 2002 applied TiO_2 commercial catalyst and its mixture with activated carbon for wastewater disinfection containing 1.5×10^5 CFU 100 mL^{-1} of total coliforms under solar light using air or an air-ozone mixture. Using only air, only solar irradiation led to a higher disinfection, 3.5×10^3 CFU 100 mL^{-1} , after 2 h treatment, but

the analysis of the treated solutions after 48 h showed that TiO₂ had a 10 times lower microorganisms regrowth, with a total coliforms of 2.8×10^5 CFU 100 mL⁻¹. When an air-ozone mixture was used, all tests had higher total coliforms reductions, and photocatalysis resulted in total disinfection with no regrowth after 48 h.

Table 3.2 summarizes the use of AOPs and biofiltration studies for the removal of pathogens.

Table 3.2 - Overview of microorganisms disinfection studies using AOPs and biofiltration

Process	Catalyst Synthesis	Experimental Conditions	Results	Reference
Photolysis, ozonation, photocatalytic oxidation and photocatalytic ozonation	Ag, Cu, Fe doped and undoped TiO ₂ catalysts were prepared by sol-gel method using titanium (III) chloride as titanium source and silver, copper and iron nitrates (2.0 wt.%) as doping agents and stirred for 20 h at room temperature. The resulting suspensions were washed, dried at 100 °C for 10 h and calcinated at 500 °C for 4 h	<ul style="list-style-type: none"> • Tests were conducted for <i>Escherichia coli</i>, <i>Salmonella</i> species, <i>Shigella</i> species, and <i>Vibrio cholerae</i> disinfection; • 0.7 L annular quartz photochemical reactor covered by aluminum foil, a medium pressure mercury lamp (Heraeus TQ 150 W) with a light intensity of 70 mW cm⁻² and a water circulation system at 30 °C was used for UV radiation tests; • Borosilicate glass tubular reactor equipped with a parabolic solar collector for was used for solar radiation tests. The feed water was recirculated using a pump and the average solar radiation intensity was 37.6 mW cm⁻²; • Ozone was produced in a generator using dry compressed air; • Spiked synthetic water (SW) with 10³ CFU mL⁻¹ of each culture and, secondary wastewater (SWW) was used on tests; • [TiO₂] = 0.5 g L⁻¹; 	<ul style="list-style-type: none"> • UV and solar radiation only resulted in, respectively, 55%-69% and 28%-38% disinfection efficiencies in SW; • TiO₂ in the dark had a disinfection efficiency in SW of 9.5% and, using 1.0 g L⁻¹, 21.2%; • Total disinfection of SW and SWW was achieved in 15 min for all catalysts with ozone under UV radiation • Under solar radiation, in SW, >99% efficiencies were obtained for Fe-TiO₂ in 15 min and for Ag-TiO₂ in 30 min. For SWW, Ag-TiO₂ and Fe-TiO₂ resulted in total disinfection under 15 min; • Using SWW under UV, ozonation and photocatalytic oxidation obtained, respectively, 0.839 and up to 1.000 using Ag-TiO₂ <i>E. coli</i> log reductions. Under solar light, the log reductions were 0.839 and 0.796 for the same processes; • After 24 h of the treatment, ozonation and photocatalysis had a bacterial reactivation up to, respectively, 5% and 3% under UV and 5% and 11.9% under solar radiation. The integrated process had no bacterial regrowth; 	(Mecha et al, 2017a)
Biofiltration, ozonation and photocatalytic oxidation	Titanium (IV) isopropoxide (TTIP) was used as titanium source for all catalysts. Au-TiO ₂ was prepared by sol-gel method using KAuCl ₆ as doping agent, followed by a 24 h thermal treatment at 45 °C and calcination for 2 h at 400 °C; Ag-TiO ₂ and Pd-TiO ₂ were prepared by photo-deposition with UV-reduction, using as doping agents AgNO ₃ and PdCl ₂ , respectively, irradiation for 100 min for Ag-TiO ₂ and 6 h for Pd-TiO ₂ and Pt-TiO ₂ , followed by drying at 65-120 °C for 12 h.	<ul style="list-style-type: none"> • <i>Corbicula fluminea</i> was used in biofiltration essays. Tests were conducted in 500 mL biofilters with 5, 10, 20 and 30 clams, kept under continuous aeration and at 20 ± 2 °C; • Solutions contained distilled water spiked with <i>Escherichia coli</i> at 10³-10⁴ CFU mL⁻¹; • Oxidation experiments were conducted in a 2.0 L glass reactor equipped with 3 lamps (Philips TL 6WBLB) emitting UVA radiation with a photon flux of 5.75 x 10⁻⁵ Einstein min⁻¹ L⁻¹, maintained at continuous magnetic stirring and at 25 ± 1 °C; • Ozone was produced from a pure oxygen stream (99.9%) and the inlet and outlet ozone gas concentrations were measured by ozone analyzers (BMT 963 and 964 vent, BMT). Gas flow rate was 0.2 L min⁻¹; • [TiO₂] = 0.07 g L⁻¹; 	<ul style="list-style-type: none"> • Tests using >10 clams reached total <i>E. coli</i> removal under 24 h and 20 clams led to the maximum removal yield, with total removal in 6 h; • Bacterial regrow was found in all treated solutions except for the maximum clam population (30 clams); • Tests using only clams shells indicated no adsorption after 24 h of contact; • Soft tissue after biofiltration contained <2% of <i>E. coli</i>; • Clams were left aerated in water after biofiltration for 48 h and no bacteria release was found; • Ozonation using 0.16 mgO₃ L⁻¹ of transferred ozone dose (TOD) was able to totally remove <i>E. coli</i> with no regrowth detected; • Ag and Pd doped catalyst had the best performances and totally removed bacteria in 20 min without the use of UV light, with no regrowth detected; 	(Gomes et al., 2018a)

Photocatalytic oxidation	<p>N-TiO₂ was prepared by sol-gel method. Ammonia was added dropwise to a TTIP solution at 0 °C under stirring. The resulting precipitate was washed, centrifuged, dried and calcinated at 450°C at different times (10-40 min). Undoped catalyst was prepared using demineralized water instead of ammonia. Anatase TiO₂ PC50 and PC100 catalysts were used for comparison.</p>	<ul style="list-style-type: none"> • Tests were conducted in 2.2 L glass reactor equipped with a 250 W lamp with a UV filter and maintained under stirring and at 30 °C; • Solutions were prepared with 500 mL of wastewater collected prior chlorination and 10 mL of a physiological solution containing 10⁷ CFU 100 mL⁻¹ of <i>Escherichia coli</i>; • [TiO₂] = 0.025-0.5 g L⁻¹; 	<ul style="list-style-type: none"> • 30 min of calcination resulted in catalysts with the lowest bandgap (2.5 eV) • 0.2 g L⁻¹ was the optimum catalyst loading • N-TiO₂ was the most effective regarding bacteria inactivation, 89.47% after 10 min treatment using 0.2 g L⁻¹ of the catalyst. Total <i>E. coli</i> inactivation was achieved under 60 min using the same catalyst amount; 	(Rizzo et al., 2014)
Biofiltration	-	<ul style="list-style-type: none"> • Solutions were prepared with river water filtrated using a tangential flow system and spiked with indigenous bacteria, including <i>Escherichia coli</i>; • Each 400 mL beaker with 200 mL of the prepared solution and a single clam, <i>Corbicula fluminea</i>, or mussel, <i>Anodonta californiensis</i> of varying sizes, kept at 15 °C for 12 h; • After laboratory tests, bivalve soft tissue was removed and dried at 50 °C for 4 h to obtain dry weight; • Field tests were conducted in the studied river in 17 pools of water, being measured the bivalve's densities. Indigenous bacteria were also inoculated into 4 pools (10³-10⁴ CFU 100 mL⁻¹); 	<ul style="list-style-type: none"> • On dry weight basis, <i>C. fluminea</i> had higher <i>E. coli</i> clearance rates; • <i>E. coli</i> concentration showed a negative correlation with the bivalve density (Spearman's $\rho = -0.6$) • Concentrated pools of water containing bivalves had a decrease in <i>E. coli</i> concentration of 1-1.5 log after 24 h 	(Mecha et al., 2017a)
Photolysis, Photocatalytic oxidation and photocatalytic ozonation	*Degussa P-25 and its mixture with activated carbon, AC-TiO ₂ (13 wt.% activated carbon).	<ul style="list-style-type: none"> • Wastewater containing a total coliforms concentration of 1.5 x 10⁵ CFU 100 mL⁻¹ was treated; • 250 mL glass reactors, continuously stirred and air (100 mL min⁻¹) or air-ozone bubbled (80-20 mL min⁻¹); • Reactions were carried out under solar light; • [TiO₂] = 2 g L⁻¹, [AC-TiO₂] = 2.3 g L⁻¹ and [AC] = 0.3 g L⁻¹; 	<ul style="list-style-type: none"> • Using air, after 2 h, single solar irradiation treatment resulted in the lower coliforms concentration, 3.5 x 10³ CFU 100 mL⁻¹, but TiO₂ had a lower bacterial regrowth after 48 h; • Ozone addition improved all treatments, with TiO₂ and AC-TiO₂ leading to total bacteria inactivation after 2 h and 1 h reactions, respectively, and no regrowth after 48 h; • Regarding total organic carbon and chemical oxygen demand, only air reactions had higher removals, specially AC-TiO₂, with 67.8% and 63.6%, respectively; 	(Araña et al., 2002)
Photocatalytic oxidation	*Degussa P-25 was modified using different amounts of urea. 1.0 g of P-25 was mixed with 0.25-0.75 g of urea and added to an ethanol solution under stirring. The precipitate was then calcinated at 380 °C for 2 h.	<ul style="list-style-type: none"> • <i>Escherichia coli</i> (ATCC 25922) suspension was prepared in a saline solution with 10³-10⁴ CFU mL⁻¹; • Tests were conducted in microplates containing 1 mL of bacteria suspension and 1 mL of photocatalyst suspensions (0.125 or 0.500 mg L⁻¹) with a 11 W black-light UVA lamp; 	<ul style="list-style-type: none"> • All catalysts led to almost complete bacteria inactivation (>95%) in 5 min using the highest catalyst load; • (0.5 g)N-TiO₂ led to more than 90% of <i>E. coli</i> inactivation within 5 min treatment with 0.125 mg L⁻¹ catalyst load; • No bacterial regrow was found in treated solutions after 24 h; 	(Monteiro et al., 2015)

4. MATERIALS AND METHODS

4.1. Catalysts Synthesis

4.1.1. Method 1

TiO₂ catalysts from method 1 were prepared by sol-gel method. Under constant stirring and at 40 °C, 19.10 mL of titanium (IV) isopropoxide was mixed with 16.10 mL of glacial acetic acid and, after 30 min, 19.10 mL of isopropyl alcohol was added. Another solution containing 30 mL of distilled water, 1 mL of nitric acid and, in the case of the doped catalysts, ammonia at different amounts according to its ratio (2.5%, 5%, 10% and 15% w/w) was prepared and, after 2 h, was slowly added to the first. The resulting solution was maintained at the same temperature for 48 h, dried at 70 °C during 12 h and then calcinated at 450 °C for 3 h. The undoped TiO₂ was prepared by the same way but without addition of ammonia.

4.1.2. Method 2

Sol-gel method was also used to prepare method 2 catalysts. 5 mL of tetrabutyl titanate was added to a 20 mL anhydrous ethanol solution and kept under stirring at room temperature. Another solution was prepared with 10 mL of distilled water, 10 mL of anhydrous ethanol, an amount of glacial acetic acid and, for the doped catalysts, urea according to the respective molar ratio. In the case of NS-TiO₂, thiourea was used instead of urea. The first solution was added dropwise into the second solution under vigorous stirring and room temperature. After homogenization, the solution was kept under slow stirring for 24 h, dried at 70 °C during 12 h and calcinated at 450 °C. The undoped TiO₂ was prepared by the same way but without addition of urea.

4.2. Catalysts Characterization

4.2.1. Specific Surface Area (S_{BET})

Catalysts Brunauer–Emmet–Teller specific surface area (S_{BET}) were determined using nitrogen (−196 °C) with an accelerated surface area and porosimetry analyzer (ASAP 2000, Micromeritics) (Gomes et al., 2017).

4.2.2. X-Ray Diffraction

X-ray diffraction (XRD) analysis made through a diffractometer (Bruker D8 Advance) with Cu K α radiation (2.2 kW ceramic tube) and a 1D LynxEye detector (Silicon Drift Detector) covering an angle of $\sim 3^\circ$ and with $\sim 25\%$ energy resolution was used for the evaluation of catalysts crystalline structures.

4.2.3. Raman Spectroscopy

Raman spectra were obtained using Raman FT-IR (Renishaw).

4.3. Asian Clams Gathering

Corbicula fluminea clams were collected from a canal located in Mira, Portugal (N40°25'06.90"/W8°44'13.18") through sieving of the sediment in a 5 mm mesh bag and kept in field water during transportation. In the laboratory, *C. fluminea* clams were gradually acclimated during 1 week at controlled temperature (20 ± 2 °C), continuous aeration and under a photoperiod of 16 h of light and 8 h of dark. After acclimation, clams were kept in dechlorinated water, which was continuously renewed (2-3 times per week) (Gomes et al., 2018a).

4.4. Experimental Procedures

4.4.1. Parabens Oxidation Reactions

Tests performed in dark or under UV radiation were carried out in a 2 L glass reactor with a thermostatic bath kept at 25 ± 1 °C and under continuous magnetic stirring at 700 rpm, which was previously established to ensure chemical regime (Martins et al., 2009). The reactor was equipped with 3 UVA lamps (Philips TL 6 W BLB, tube diameter of 16 mm) emitting mainly at 365 nm.

Single and photocatalytic ozonation reaction was performed during 120 min and photocatalytic oxidation during 180 min. In photocatalytic tests, 5 min before the lamps turned on and placed inside the reactor, a 2 L ultrapure water solution containing 10 mg L⁻¹ of each paraben and 70 mg L⁻¹ of the catalyst was introduced into the reactor to test the catalysts adsorption capacity. Samples were taken during reaction for further analysis.

Ozone was produced from pure oxygen (99.9 %) by an ozone generator (802N, BMT), and the outlet gaseous stream was passed through a potassium iodide solution as an ozone scavenger. The inlet gas flow rate (Q_{gas}) was maintained at 0.2 L min⁻¹. The inlet ($[\text{O}_3]_i$) and outlet ($[\text{O}_3]_o$)

ozone concentration, in mg L⁻¹, was measured in two ozone analyzers (BMT 963 and BMT 964, BMT, respectively). Transferred ozone dose (TOD) was calculated according to Eq. (1):

$$TOD = \int_0^t \frac{Q_{gas}}{V_{liq}} \times ([O_3]_i - [O_3]_o) \times dt \quad (1)$$

TOD is expressed in mg O₃ L⁻¹ and V_{liq} corresponds to the volume of the liquid solution in the reactor.

4.4.2. Bacteria Disinfection Tests

Escherichia coli removal tests were conducted using biofiltration with *C. fluminea* and both single and photocatalytic ozonation. 2 different water matrices were used: a secondary wastewater effluent from WWTP and from a river located in Portugal Center region. River water was collected from at least a 0.5 m depth due to the higher oxygen concentration and its bacterial growth relation at the river surface. All water matrices were collected, transported and stored in 5-6 L plastic containers.

Oxidation methods were conducted following the same techniques and using the same apparatus as the parabens degradation tests, using 2 L solutions in each reaction. River water and the wastewater were treated in 30 min and 120 min reactions, respectively, due to its expected different *E. coli* concentrations. Samples were taken prior, during and post reactions and storage in sterilized plastic containers.

Biofiltration tests were performed in 1.0 L glass biofilters maintained at controlled temperature (20 ± 2 °C) with a volume solution of 0.75 L, continuous aeration and under a photoperiod of 16 h of light and 8 h of dark, with a clam concentration 60 clams L⁻¹. Duplicates and a control with only the solutions were used in all tests. Bacterial removal was evaluated during 24 h, with samples being taken during the tests and storage in sterilized plastic containers.

Membrane filtration method was used for bacteria quantification tests, according to ISO 9308-1:2014. The collected samples were diluted in order to achieve plate counts below 150 CFU. For river tests, instead of dilutions, higher sample volumes were used due to the lower bacteria concentration. 0.45 µm cellulose nitrate membranes and, when needed, sterilized water was used for the samples filtration. Tests were performed in duplicate. Filters were then plated in lauryl sulphate agar and incubated at 37 ± 0.2 °C for 24 h. After incubation, the yellow colonies, which could correspond to *E. coli*, were counted and the results reported as colony forming units (CFU) per mL (Gomes et al., 2019b).

For *E. coli* confirmation tests, 5 yellow colonies from each plate, resulting in total 10 colonies for each sample, in the range of 15-150 CFU were selected, inoculated in tryptic soy agar and incubated at 37 ± 0.2 °C for 24 h. Colonies samples were taken and tested against oxidase enzyme, changing color to blue when its positive. Negative colonies were then inoculated in buffered peptone water and incubated at 44 °C during 24 h. Finally, drops of indole reagent were added to the inoculated samples and the surface of the confirmed *E. coli* suspension turned red after agitation. Samples with negative oxidase and positive (red) indole were taken as a proportional indication of the actual initial *E. coli* colonies in each sample (Figure 4.1).

Plates with no bacterial growth after filtration may not ensure total *E. coli* removal. Regrowth tests were conducted after 24 h, using the same filtration technique as described before, to guarantee that no viable cells are present in the solution.

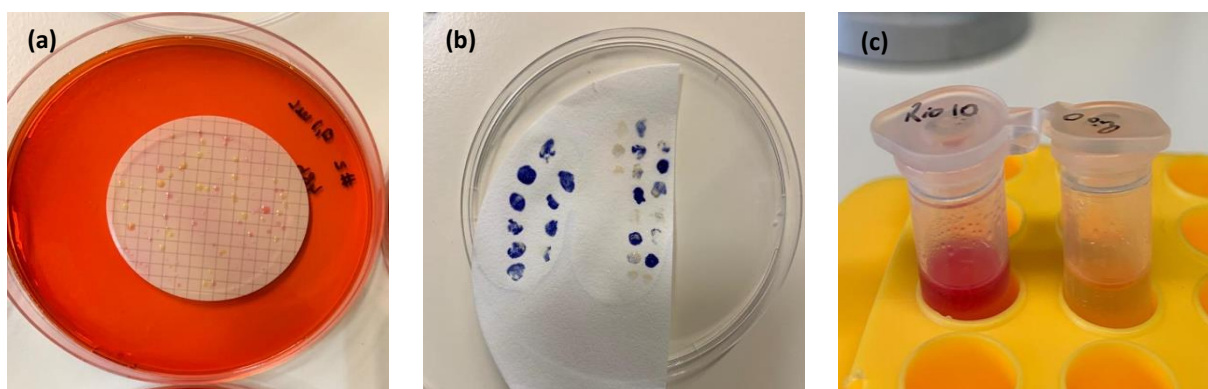


Figure 4.1 - *E. Coli* quantification and confirmation tests: (a) membranes after filtration, (b) oxidase test, (c) indole test.

4.5. Analytical Methods

4.5.1. High-Performance Liquid Chromatography (HPLC)

High-performance liquid chromatography (HPLC) (UFLC, Shimadzu) was used for the determination of each paraben and byproducts concentration during reactions. 20 μL of each sample was directly injected and a mixture of 50% methanol and 50% acidic water (0.1% orthophosphoric acid) was used as mobile phase (0.5 mL min^{-1}). The column used was a C18 (SiliaChrom) kept at 40 °C and compounds detection was assessed at 255 nm. The retention times of the peaks of each compound were determined by comparison with standard solutions. Peaks areas were used for analysis of parabens degradation and byproducts formation (Gomes et al., 2017a).

4.5.2. Chemical Oxygen Demand (COD)

Chemical oxygen demand (COD) was determined by standard method 5220D, representing the oxygen quantity needed to chemical degrade the organic matter contained in a solution (Clesceri et al., 1999). Each glass vial was filled with a solution containing 1.5 mL of a digestion solution ($K_2Cr_2O_7$), 3.5 mL of acidic solution (H_2SO_4) and 2.5 mL of the sample. Each solution was tested in duplicate and with a control using ultrapure water instead of the sample.

Vials were then put in thermoreactors (ECO25 – Velp Scientifica) at 150 °C for 2 h and, after cooled down at room temperature, absorbances were measure at 445 nm in a WTW photolab S6 photometer. Potassium hydrogen phthalate was used to prepare a COD calibration curve within the range 0-125 mg $O_2 L^{-1}$, present in Appendix B (Gomes et al., 2017b).

4.5.3. Total Organic Carbon (TOC)

The total organic carbon of solutions was used as measure of its mineralization level. Samples were analyzed in a TOC analyzer (TOC-V CPN model, Shimadzu, Japan) coupled to an autosampler (model V-ASI, Shimadzu, Japan) (Gomes et al., 2017b). TOC measurement was made through nondispersive analysis after oxidative combustion.

4.5.4. Ionic Chromatography

Cl^- , NO_3^- and SO_4^- ions were quantified by ionic chromatography using a Millipore, Actions Water Analyzer equipped with a conductivity detector Waters 431.

4.6. Toxicity evaluation

4.6.1. *Lepidium sativum*

Phytotoxicity was evaluated using *Lepidium sativum* germinated seeds and its radicle growth, which were used to calculate the germination index (GI). In each test, 10 *L. sativum* seeds were placed over filter paper in petri dishes and 5 mL solution were added, guarantying an evenly dispersion of the seeds. Tests were conducted in duplicate and blank controls with distilled water were used. Samples were put in an oven for 48 h at 27 °C.

After incubation, germinated seeds were counted and measured its radicle length. Relative seed germination and radicle growth (RSG and RRG, respectively), and germination index (GI) were calculated according to Eq. (2-4):

$$RSG (\%) = \frac{N_G}{N_{G,B}} \times 100 \quad (2)$$

$$RRG (\%) = \frac{L_R}{L_{R,B}} \times 100 \quad (3)$$

$$GI (\%) = \frac{RSG \times RRG}{100} \quad (4)$$

Where N_G and $N_{G,B}$ are the number of germinated seeds in samples and blank control, respectively, and L_R and $L_{R,B}$ are the radicle length of the same solutions. The phytotoxicity was evaluated through GI, according to the (Trautmann and Krasny, 1997) criteria.

4.6.2. *Allivibrio fischeri*

Allivibrio fischeri bacteria was used to evaluate sample's toxicity through its luminescence inhibition. Samples were inoculated with the bacteria suspension at 15 °C in a LUMISTherm (HACH) and LUMISTox 300 equipment from Dr. Lange GmbH (HACH) was used for luminescence direct measurement after 15 min of incubation and compared with a blank control, consisting in NaCl solution (2%) with the bacteria. Tests were conducted in duplicate and the solutions pH were previously corrected to a 6.5-7.5 range.

4.6.3. *Corbicula fluminea*

The Asian clam, *Corbicula fluminea*, was applied for toxicity evaluation. 10 individuals, previously acclimated as described before, were put in plastic containers with 500 mL of solutions for 48 h at controlled temperature (20 ± 2 °C), continuous aeration and under a photoperiod of 16 h of light and 8 h of dark. Clams mortality was verified every 24 h through the resistance to valve opening when a force was applied or siphoning activity (Gomes et al., 2014).

5. PHOTOCATALYTIC OZONATION FOR PARABENS REMOVAL

In this section, the results of photocatalytic ozonation tests regarding the degradation of a parabens mixture with different TiO₂ catalysts, as well as the comparison with single technologies will be evaluated. Each test was conducted using the same apparatus, with a duration of 180 min for UV/TiO₂ and 120 min for UV/O₃ and UV/TiO₂/O₃. Samples were taken during reaction. Transferred Ozone Dose (TOD), Chemical Oxygen Demand (COD), Total Organic Carbon (TOC), contaminants degradation evolution and the toxicity of the treated solutions comparing to the initial ones were analyzed.

5.1. Method 1

5.1.1. Catalysts Characterization

All characterization tests were conducted at the University Rovira i Virgili (Tarragona, Spain) and, due to logistics, a complete analysis of all catalysts was not possible in due time. Figure 5.1 displays the patterns obtained from X-ray diffraction tests from TiO₂, 5% N-TiO₂ and 15% N-TiO₂.

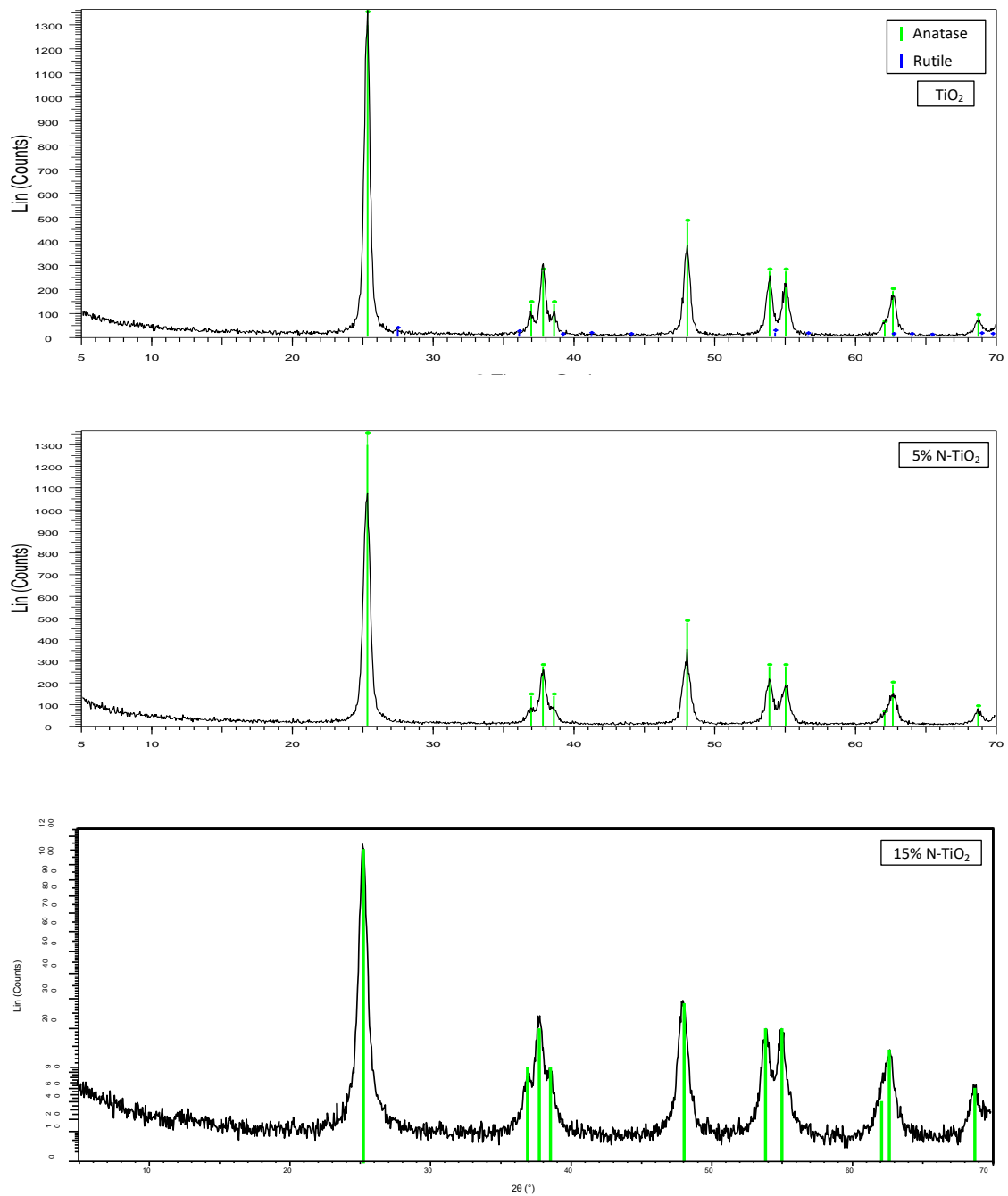


Figure 5.1 - X-ray diffraction patterns for TiO_2 , 5% N- TiO_2 and 15% N - TiO_2 using synthesis method 1.

Method 1 TiO_2 undoped catalyst crystalline phase is predominantly anatase but with a small presence of also a rutile phase. The catalyst doping resulted in a total anatase phase, indicating a high crystallinity. Crystallite sizes (D) were determined by the Debye-Scherrer equation, Eq. (5), and are present in Table 5.1.

$$D = \frac{K\lambda}{\beta \cos \theta} \quad (5)$$

Where K is a shape factor, usually 0.9, λ is the wavelength of the X-ray radiation (Cu $K\alpha = 0.154$ nm), β is the full width at half maximum peak in radians and θ is the diffraction angle at (101) anatase peak.

Table 5.1 - TiO₂ catalysts crystallite sizes obtained using Debye-Scherrer equation.

Catalyst	Crystallite size (nm)
TiO ₂	19.56
5% N-TiO ₂	15.30
15% N-TiO ₂	17.05

Doped N-TiO₂ presented a lower crystallite size, which is expected due to the broader and lower intensity of the first diffraction peak at 25.3°, which represents (101) plane of catalyst's anatase phase. The decrease of crystallite sizes as result of nitrogen doping has been detected in other studies and may be due to substitution of oxygen atoms by nitrogen, which has a higher ionic radius, causing distortions and destabilizing the crystallites (Bokhimi et al., 2007; Kalantari et al., 2016; Qiu et al., 2019). Lower crystallite sizes are generally related to an increase in superficial area and photocatalytic activity (Ibrahim et al., 2019; Sanchez-martinez et al., 2018). In fact, BET analysis of 10% N-TiO₂ resulted in a observed surface area of 80.6 m² g⁻¹, which is considerably higher compared to the most common commercial TiO₂ catalysts, Degussa P25, having a reported surface area of around 55 m² g⁻¹ (Han et al., 2018; Raj et al., 2009).

Nitrogen substitution on catalyst lattice may also lead to a small shift (~0.3°) of (101) anatase peak in doped catalysts, but it was not observed (Lee et al., 2013). Higher resolution diffraction spectras should be obtained to better analyze this parameter.

No additional peak for the doping agent was observed in doped TiO₂ XRD spectras, which may be due to a small amount of nitrogen in the catalyst lattice or to substitution of oxygen sites (Barkul et al., 2016).

Raman spectroscopy tests (Figure 5.2) conducted demonstrate the typical 6 modes of anatase TiO₂ that are Raman active at 143 (E_g), 196 (E_g), 395 (B_{1g}), 515 (A_{1g} + B_{1g}) and 638 (E_g) cm⁻¹, confirming that anatase is the principal phase in the doped catalyst (Komaraiah et al., 2019). Different from XRD results, no peak corresponding to rutile phase was detected in the undoped catalyst spectra, possibly due to its small presence.

5% N-TiO₂ first peak presented a small shift, appearing at 144 cm⁻¹. This small blue shift have been reported in different studies and may be a result of changes of the oxygen stoichiometry in the presence of nitrogen, being a indication of its incorporation in the catalyst lattice (Rizzo

et al., 2014). This peak intensity was also higher compared with undoped TiO₂, which, concordantly to XRD measurements, may be due to defects on the crystallites caused by nitrogen substitution and can be associated with a decrease in both crystallite and particle sizes (Qiu et al., 2019; Zhang et al., 2000).

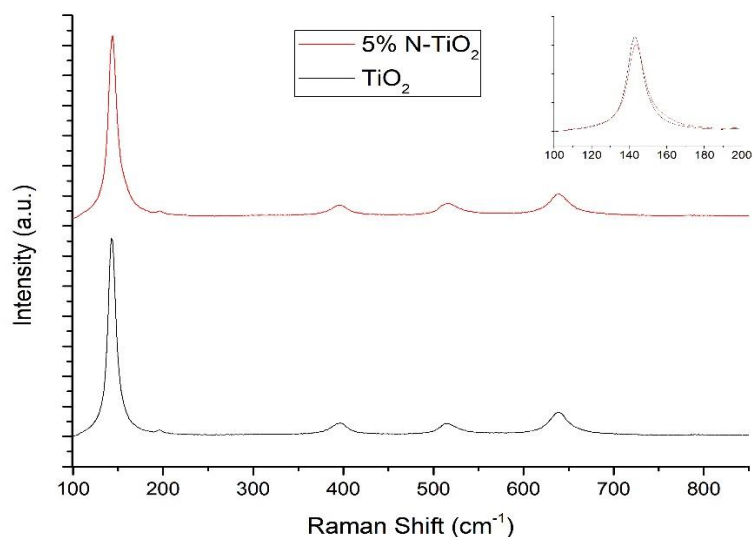


Figure 5.2 - Raman spectra of method 1 TiO₂ catalysts.

To investigate the optical properties improvement of nitrogen doping, 10% N-TiO₂ was analyzed in UV-Visible spectroscopy. The band gap energy (E_{bg}) was calculated using Tauc's plot as $(\alpha h\nu)^n$ versus $h\nu$ (Figure 5.3), based on Tauc's rule $(\alpha h\nu)^n = B(h\nu - E_{bg})^n$ where α is the absorption coefficient, B is an energy independent constant, h is the Planck's constant, ν is the light frequency and n indicates the type of optical transition, which is $n=1/2$ for direct allowed transition (López et al., 2012; Shkir et al., 2018). The final E_{bg} was obtained by the intersection point of the tangent line where $(\alpha h\nu)^{1/2}$.

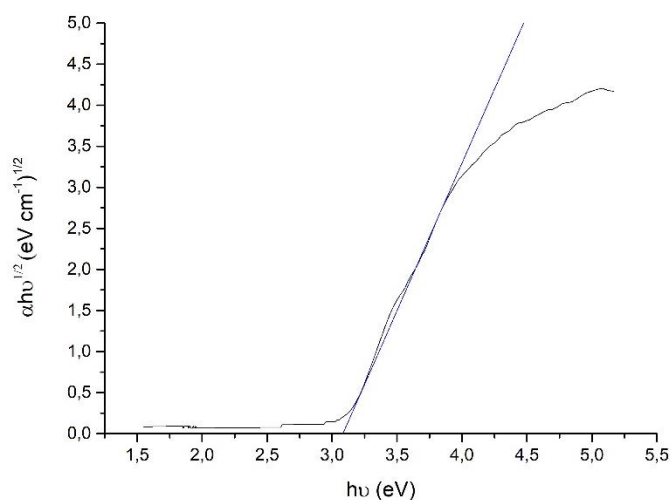


Figure 5.3 - Tauc's plot of 10% N-TiO₂.

The estimated band gap energy for 10% N-TiO₂ was 3.08 eV. The commercial TiO₂ Degussa P25 reported band gap estimated with the same graphic method is 3.26 eV, concluding that method 1 doped catalyst present a narrowing of its E_{bg} (López et al., 2012). This is caused by the presence of nitrogen atoms in the catalyst lattice, which is a result of mixed oxygen and nitrogen 2p states, being the last located above oxygen 2p valence band leading to a red shift in the absorption spectrum to visible range and reducing the electron-hole recombination (Gomes et al., 2019c). However, the difference is not so sharp which can be related with the small fraction of nitrogen that can be doped at the TiO₂ lattice. Therefore, this can be one of the reasons for low performance on the parabens degradation by photocatalytic oxidation.

5.1.2. Parabens Degradation

The concentrations evolution of methylparaben (MP), ethylparaben (EP), propylparaben (PP), butylparaben (BP) and benzylparaben (BzP) were obtained using high-performance liquid chromatography (HPLC). Firstly, photocatalytic oxidation tests were conducted to better understand the catalysts role on parabens degradation and its photoactivity. In Figure 5.4 are present the PP, BP and BzP depletion evolution, as the more readily degraded contaminants, over the 180 min reactions under UV radiation.

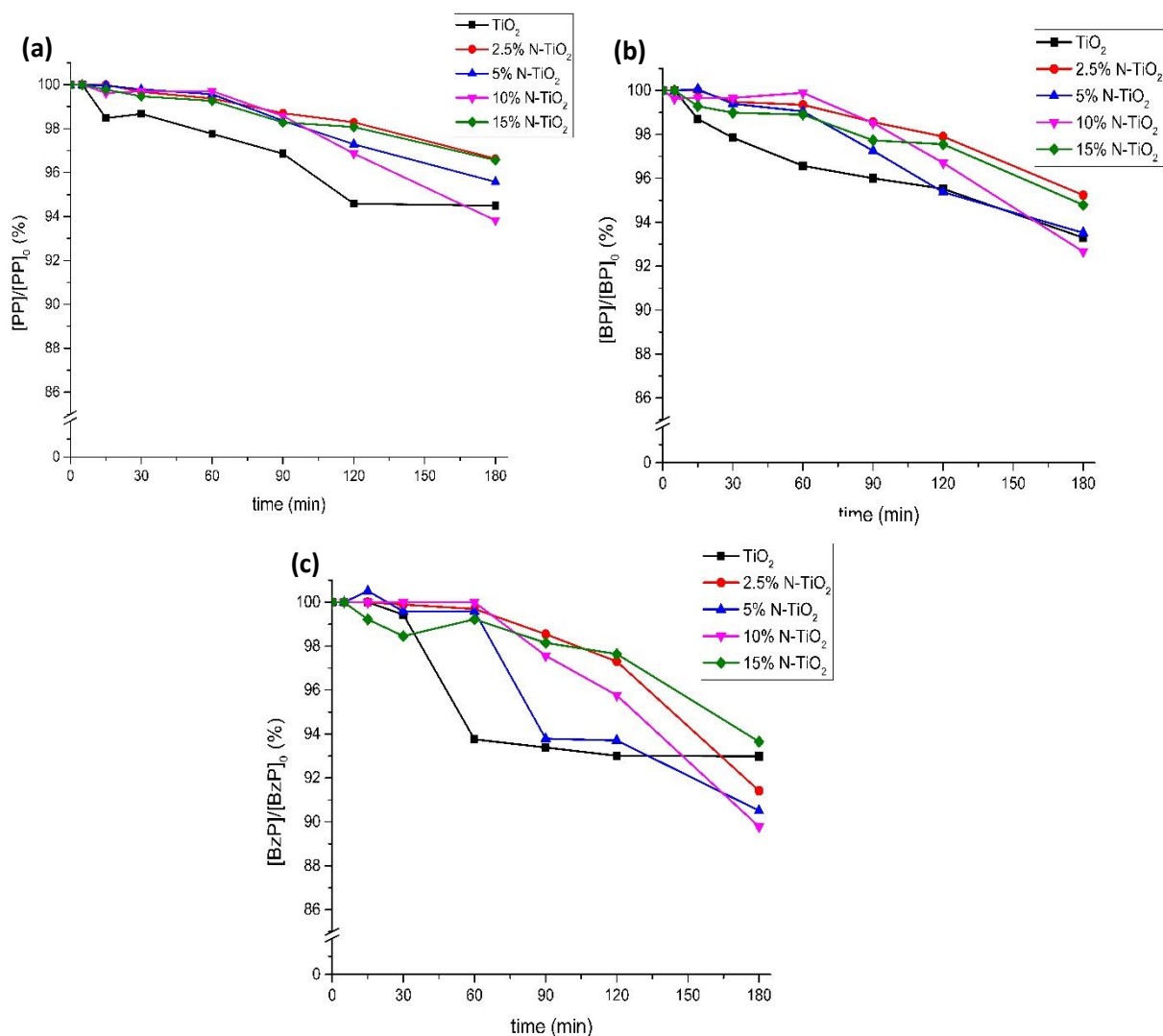


Figure 5.4 – Propylparaben (a), butylparaben (b) and benzylparaben (c) degradation (%) and Transferred Ozone Dose (mg L^{-1}) during UV/N- TiO_2 reactions using method 1 catalysts.

As can be observed, method 1 catalyst present a low photoactivity under UV radiation regarding paraben depletion as UV/N- TiO_2 reactions resulting in only up to 10% benzylparaben removal after 180 min. The degradation rate decreased with a decreasing chain length, with less than 5% removal for propylparaben. Catalyst doping had no significant improvement in the performances, with only slightly higher removals for 10% and 5% N- TiO_2 .

Subsequently, UV/ O_3 and UV/N- TiO_2 / O_3 reactions were conducted for the degradation of the parabens mixture and evaluated in parallel with the transferred ozone dose (TOD), being methylparaben represented in Figure 5.5 and the remaining parabens in Appendix A.

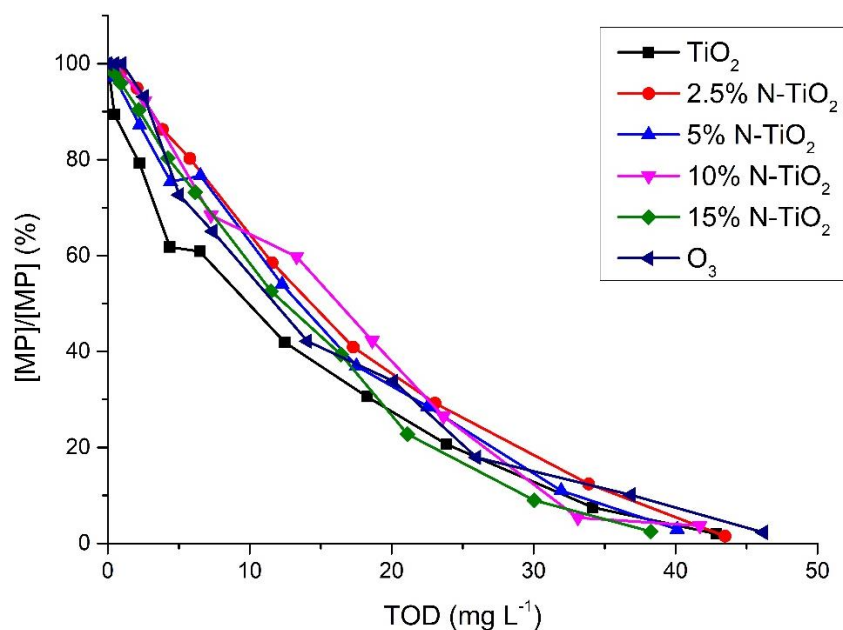


Figure 5.5 - Methylparaben degradation (%) and Transferred Ozone Dose (mg L^{-1}) during UV/O₃ and UV/O₃/N-TiO₂ reactions using N-doped method 1 catalysts.

Near total parabens depletion (>98%) was obtained in all reactions with 120 min duration, specially butyl- and benzylparaben. These 2 contaminants are more readily degraded due to the higher chain length, which implicates in more active sites, and a higher electronic density in the case of benzylparaben, making it more susceptible to ozone attack.

Single photolytic ozonation led to higher TOD amounts compared with catalytic reactions, 46.19 mg L^{-1} after 120 min. The better performances using photocatalyst can be explained by the generation of highly oxidative radicals (e.g. $\bullet\text{OH}$, $\bullet\text{O}_2^-$) by the catalysts. The lower TOD implies a decrease in the overall cost of the process due to the lower ozone production and, consequently, energy costs, making its application more viable at large scale.

Regarding the doping of photocatalysts, an increasing dosage of nitrogen resulted in a lower TOD when compared with the undoped photocatalyst in almost all reactions. 10% and 15% N-TiO₂ led to, respectively, 94.66% and 97.42% of methylparaben removal using 33.11 and 38.25 mg L^{-1} of TOD. This represents a decrease of up to 28.32% and 23.87% of ozone consumption for almost the same level of paraben depletion compared with single ozonation and pure TiO₂ photocatalytic ozonation, respectively.

5.1.3. Chemical Oxygen Demand (COD) and Total Organic Carbon (TOC) Removals

In Figure 5.6 are represented the chemical oxygen demand and total organic carbon removals after 120 min reactions of solution containing all 5 parabens.

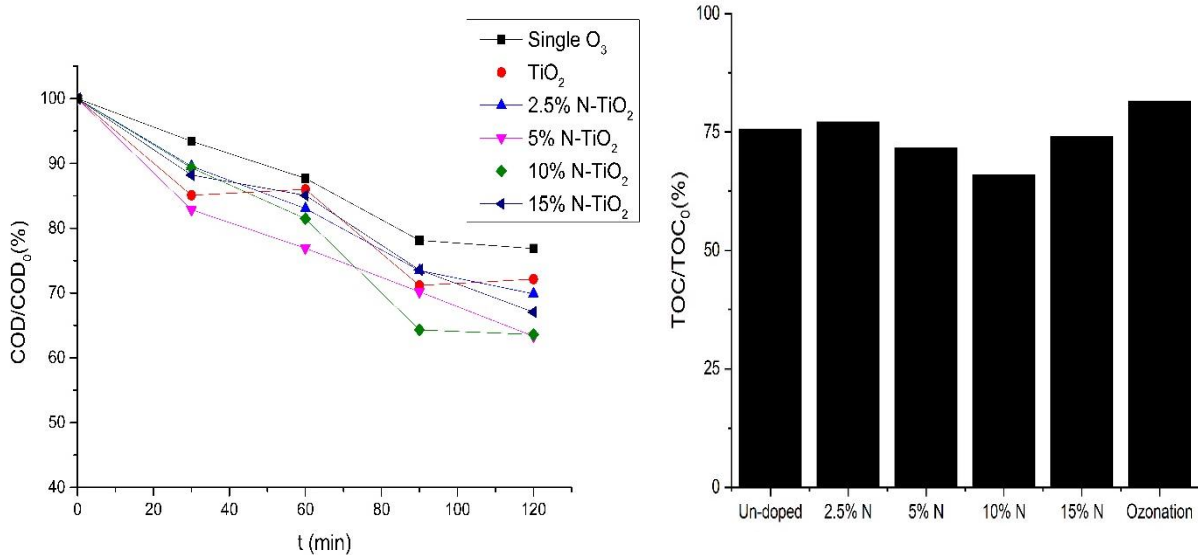


Figure 5.6 – Chemical oxygen demand removals during and total organic carbon removals after 120 min of UV/O₃/TiO₂ and UV/O₃ reactions using method 1 N-doped catalysts.

As can be observed, ozonation by itself led to a lower COD removal, around 23% after 120 min, when compared with all UV/N-TiO₂/O₃ reactions, indicating the presupposed higher capacity of the photocatalytic ozonation to reach a higher oxidation level. The nitrogen doping also improved the COD removal, with an increasing dosage of nitrogen leading to a higher efficiency. In fact, 10% N-TiO₂ reached its maximum removal (35.69 %), with no significant further increase, before the end of the reaction, at 90 min.

Regarding TOC, the increasing amount of nitrogen has the same effect found in COD removal. The most efficient reaction, using 10% N-TiO₂, resulted in a reduction of 34.11% of the initial 35.88 mg L⁻¹ of TOC, being almost the double when compared with photolytic ozonation, which led to a 18.53% removal. Even with an almost complete paraben degradation, TOC and COD total removal are not accomplished, meaning that the parabens oxidation lead to the formation of refractory by-products

To understand better the selectivity of the different processes regarding mineralization and oxidation, the partial oxidation yield ($\mu_{COD_{partox}}$) was calculated following Eq. (6) and (7) (Hellenbrand et al., 1997):

$$COD_{partox} = \left(\frac{COD_0}{TOC_0} - \frac{COD}{TOC} \right) \times TOC \quad (6)$$

$$\mu_{COD_{partox}} = \frac{COD_{partox}}{COD_0 - COD} \quad (7)$$

The partial oxidation yield may lead to values between 1, meaning that COD removal is due to partial oxidation, and 0, which represents total mineralization. The calculated parameter and related data are summarized in Table 5.2.

Table 5.2 – Chemical oxygen demand and total organic carbon removal, transferred ozone dissolved and partial oxidation yield after 120 min reaction using different processes.

Process	COD removal (%)	TOC removal (%)	TOD (mg L ⁻¹)	$\mu_{COD_{partox}}$
O ₃ +TiO ₂	27.86	24.39	42.90	0.12
O ₃ +2.5%N-TiO ₂	30.12	22.88	43.49	0.24
O ₃ +5%N-TiO ₂	36.68	28.43	40.12	0.22
O ₃ +10%N-TiO ₂ *	35.69	34.11	33.11	0.04
O ₃ +15%N-TiO ₂	32.94	25.98	38.25	0.21
O ₃	23.11	18.53	46.19	0.20

*Results after 90 min reaction.

Photolytic and photocatalytic ozonation led to overall similar $\mu_{COD_{partox}}$, except for reactions with TiO₂ and 10% N-TiO₂. 10% N-TiO₂ result indicate that 96% of COD removed was mineralized, producing only carbon dioxide and water. The undoped catalyst also resulted in a high mineralization, 88% of the removed COD, but its overall COD and TOC removal is considerably smaller compared with the other photocatalytic reactions.

These summarized results confirm the existence of an optimal nitrogen dosage, which may possibly be explained by a balance of the different effects of the nonmetal on the catalyst performance. Nitrogen may lead to a decrease in the bandgap energy and an increase in ozone decomposition with a consequent higher oxidative radical formation, but an increasing amount also result in a higher particle size and a lower specific area, decreasing the process efficiency (Cong et al., 2007; Dhanya et al., 2013; Solís, 2015).

5.1.4. Toxicity Evaluation

Toxicity tests were conducted using *Aliivibrio fischeri*, *Lepidium sativum* and *Corbicula fluminea*, representing 3 different trophic levels, being demonstrated in Table 5.3. Solutions after 120 min of photolytic or photocatalytic ozonation were used in all test, pH was adjusted when needed and kept at neutral conditions.

Table 5.3 - *L. sativum* germination index, *A. fischeri* luminescence inhibition after 15 min exposure and *C. fluminea* mortality after 48 h exposure to solutions obtained from 120 min treatment using different process.

Process	Germination Index (%) (\pm SD)	Luminescence inhibition (%) after 15 min (\pm SD)	Mortality (%) after 48 h (\pm SD)
O ₃ +TiO ₂	108.6 \pm 5.8	73.9 \pm 0.90	30.0 \pm 28.3
O ₃ +2.5%N-TiO ₂	114.0 \pm 7.6	79.3 \pm 0.85	40.0 \pm 14.1
O ₃ +5%N-TiO ₂	108.4 \pm 18.7	80.2 \pm 0.00	60.0 \pm 28.3
O ₃ +10%N-TiO ₂	115.2 \pm 1.7	84.6 \pm 0.00	45.0 \pm 21.2
O ₃ +15%N-TiO ₂	120.5 \pm 20.2	82.5 \pm 0.02	55.0 \pm 21.2
O ₃	74.6 \pm 19.6	70.0 \pm 0.15	30.0 \pm 14.1

All solutions treated with photocatalytic ozonation led to higher seeds growth, up to almost 50%, comparing to ozonation by itself, representing a lower toxicity in *L. sativum* tests. The single photolytic ozonation can reduce the phytotoxicity of initial parabens mixture (GI= 40%), but still presents moderate phytotoxicity according to (Trautmann and Krasny, 1997) criteria. Globally, the increasing ammonia dosage led to solutions less toxic to *L. sativum*, which can be explained by a possible nitrogen leaching, serving as a seed nutrient and boosting its growth.

A. fischeri presented in all treatments a decrease in the luminescence inhibition compared with the initial paraben solution (99%), but as proposed by Miralles-Cuevas et al., 2017., solutions with inhibition percentages higher than 30% are still considered toxic. Despite this, the presence of nitrogen in photocatalytic ozonation seems to affect the luminescence inhibition of bacteria, since the results for single photolytic ozonation and undoped TiO₂ are very similar.

Comparing single and catalytic ozonation, all catalytic reactions resulted in higher bacteria luminescence inhibition and clam's mortality. Through the analysis of HPLC results after 120 min, the peaks originated during reaction corresponding to unidentified by-products had higher areas, and consequently higher concentrations, in catalytic process than single ozonation. Thus, the higher degradation level of O₃+TiO₂ reactions also lead to higher concentrations of toxic intermediates. Hydroquinone, 1,4-Benzoquinone, 2,4-Dihydroxybenzoic acid and 4-

Hydroxybenzoic acid are some of the most common parabens oxidation aromatic by-products, but ring opening reactions also leads to the formation of other aliphatic compounds, mostly carboxylic acids (Gmurek et al., 2015; Gomes et al., 2017a).

Another explanation for higher toxicities for *A. fischeri* and *C. fluminea* is the already proposed nitrogen leaching. In this case, the produced nitrogenous substances, such as ammonia and nitrates, can contribute to high stress levels for the Asian clams and bacteria bioluminescence inhibition, being aggravated with the increasing doping dosage (Abbas et al., 2018; Oliveira et al., 2015; Rodríguez-Loaiza et al., 2016).

5.2. Method 2

5.2.1. Catalysts Characterization

Method 2 TiO₂, 5% N-TiO₂ and 5% NS-TiO₂ X-ray diffraction patterns and crystallite sizes obtained through Debye-Scherrer equation are represented in Figure 5.7 and Table 5.4, respectively.

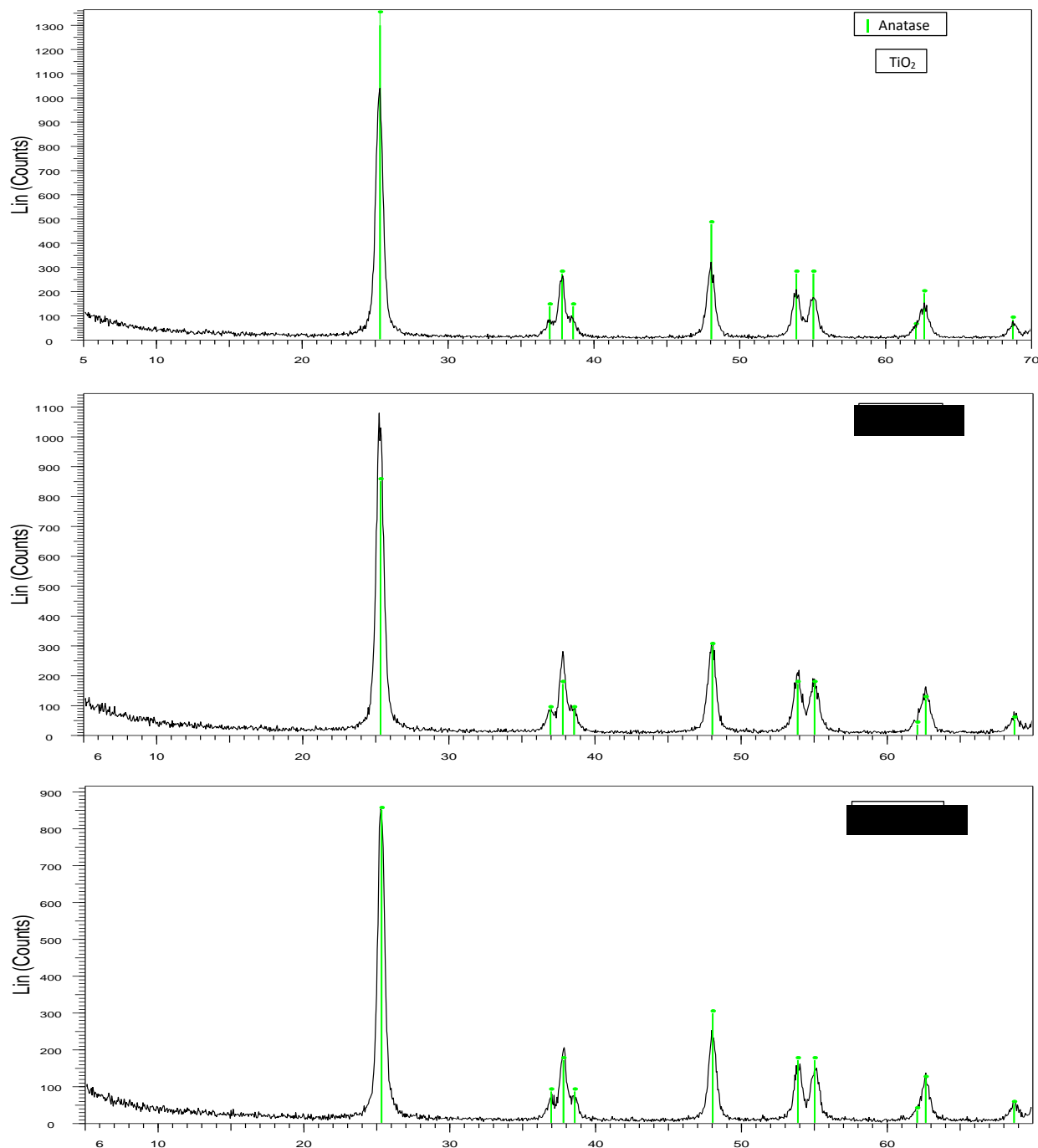


Figure 5.7 - X-ray diffraction patterns for TiO₂, 5% N-TiO₂ and 5% NS -TiO₂ using synthesis method 2.

A complete anatase phase is present in all catalyst and its modifications did not affect the crystalline structure. Observed peaks are in agreement with literature values and are well-defined,

indicating a high crystallinity (Lee et al., 2013). The average crystallite size increased with the addition of urea, which can be a result of poor nitrogen incorporation and deposition on catalyst surface. Codoped NS-TiO₂ has a slightly lower crystallite size, which can be explained due to the higher ionic radius of S²⁻ (170 pm) and resulting crystallite defects formation.

Table 5.4 - TiO₂ catalysts crystallite sizes obtained using Debye-Scherrer equation.

Catalyst	Crystallite size (nm)
TiO ₂	16.76
5% N-TiO ₂	17.60
5% NS-TiO ₂	16.37

Raman spectroscopy results (Figure 5.8) are consistent with XRD and only typical anatase modes are present. The first anatase peak has an increase in its intensity when urea is used and a small decrease using thiourea, which is related to the crystallite average size alterations. These results suggest that method 2 catalyst led to no significant or a negative alteration in the catalyst photoactivity regarding particle and crystallite sizes.

The obtained BET surface areas of nitrogen doped catalysts were 66.8 m² g⁻¹ (TiO₂), 71.3 m² g⁻¹ (2.5% N-TiO₂), 65.8 m² g⁻¹ (5% N-TiO₂) and 66.8 m² g⁻¹ (10% N-TiO₂), indicating only a small enhancement of active surface using low amounts of urea.

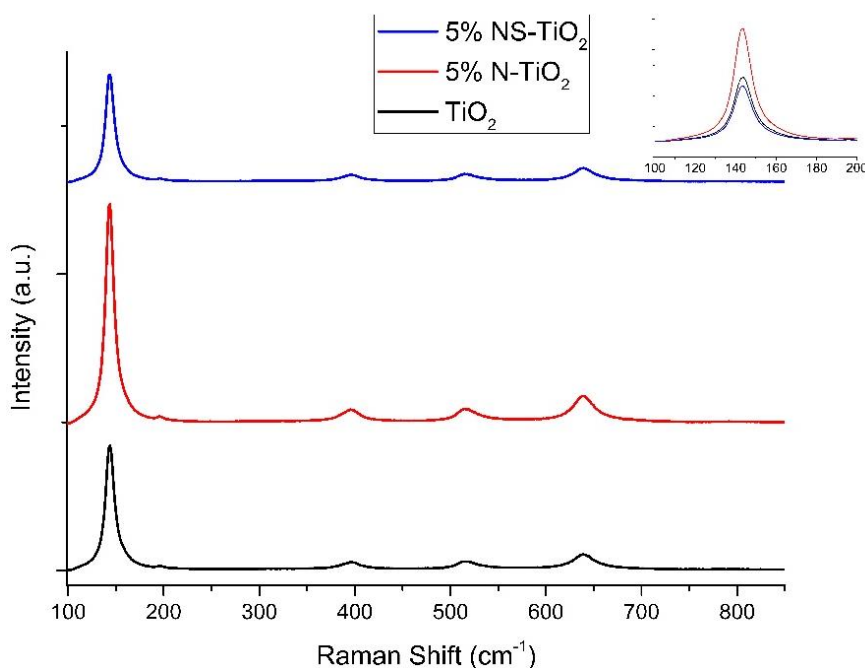


Figure 5.8 - Raman spectra of method 2 TiO₂ catalysts.

The use of urea as doping agent was also evaluated regarding its influence in TiO₂ catalyst. Band gap energy was calculated using Tauc's plot, as described before and are represented in Figure 5.9 and Table 5.5.

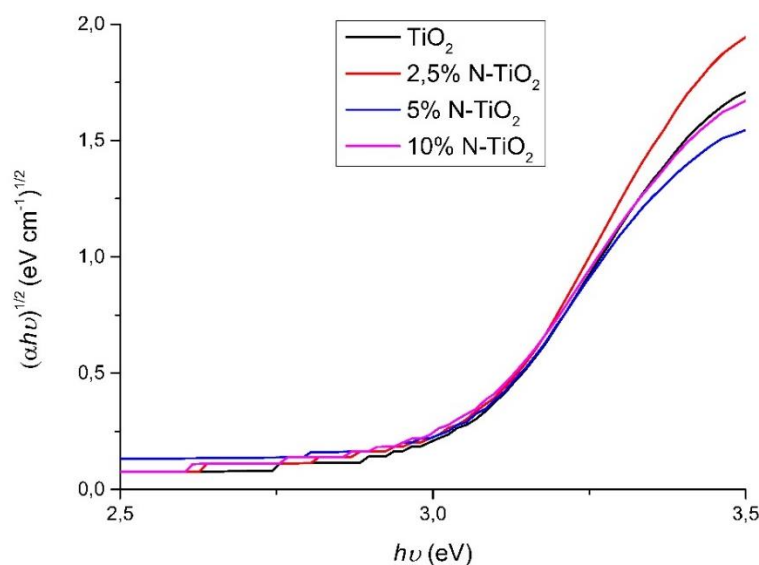


Figure 5.9 - Tauc's plot of method 2 N-TiO₂.

As can be observed urea doping has no significant improvement in band gap energy, with all method 2 N-TiO₂ catalysts analyzed leading to the similar values. Considering all characterization results, urea and thiourea lead to small or negative modifications in TiO₂, indicating a higher particle and crystallite sizes and lower crystallinity.

Table 5.5 - Estimated band gap energies for method 2 N-TiO₂ catalysts.

Catalyst	Band gap energy (eV)
TiO ₂	3.03
2.5% N-TiO ₂	3.04
5% N-TiO ₂	3.01
10% N-TiO ₂	3.01

Comparing both undoped TiO₂, method 2 results demonstrate a higher crystallinity and photoactivity than method 1 catalyst. Both methods have different titanium precursors and solvents, and the obtained characteristics may be due to two main factors. Tetrabutyl titanate has a higher molecular weight and viscosity, which means that it is slowly hydrolyzed and consequently form a higher number of nucleation sites and smaller particles. Regarding the different alcohols used as solvent, it is possible that the zeta-potential of the particles is altered, leading to a different particle sizes during precipitation phase (Chauhan et al., 2018). Moreover, after the characterization it will be seen the performance of the catalysts for parabens mixture degradation through photocatalytic ozonation.

5.2.2. Parabens Degradation

Photocatalytic oxidation tests were conducted, but due to the expected low photoactivity, reactions had a duration time of 120 min and 15% N-TiO₂ and thiourea doped catalysts were not evaluated. The final removal of the most readily attacked parabens, propyl-, butyl- and benzylparaben, for the remaining catalyst are present in Table 5.6.

Table 5.6 - Parabens removal after 120 min of photocatalytic oxidation using method 2 N-TiO₂

Catalyst	Removal (%)		
	Propylparaben	Butylparaben	Benzylparaben
TiO ₂	2.88	3.76	8.48
2.5% N-TiO ₂	7.17	5.61	9.70
5% N-TiO ₂	2.39	2.68	3.99
10% N-TiO ₂	1.30	3.05	7.73

The low photoactivity of the catalyst was confirmed, as also was observed previously using method 1 catalyst. Concordantly to reactions with ozone, parabens removal decrease with the increase of urea doping and 2.5% TiO₂ still resulted in a higher degradation.

In Figure 5.10, A2 and A3 (Appendix A) are represented the removal evolution of methylparaben and remaining parabens during 120 min reaction of single and photocatalytic ozonation using method 2 N-TiO₂ and NS-TiO₂ catalysts.

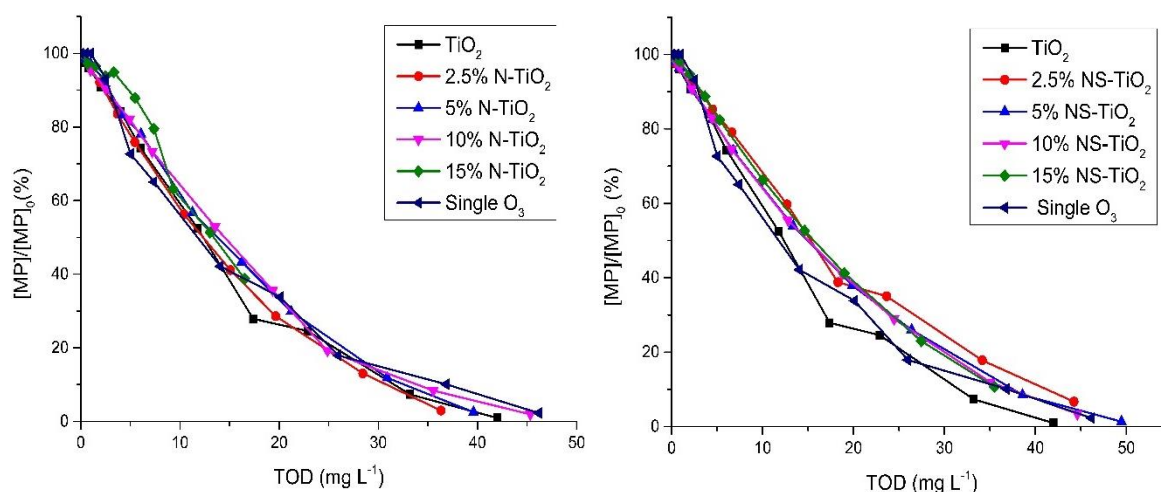


Figure 5.10 - Methylparaben degradation (%) and Transferred Ozone Dose (mg L⁻¹) during UV/O₃ and UV/O₃/TiO₂ reactions using N-doped (left) and NS-codoped (right) method 2 catalysts.

Overall parabens degradation was similar to method 1 catalysts, single ozonation led to the highest TOD after 120 min reaction and almost complete removal was achieved, with the exception of 15% N-TiO₂ reaction. The catalyst with the highest dopage obtained, respectively,

61.22% and 81.60% methyl- and benzylparaben removal, being the last the most readily attacked of the analyzed contaminants.

Urea doping had a positive impact over ozone consume, but a smaller quantity of nitrogen compared with method 1 catalyst achieved better results, with 2.5% N-TiO₂ leading to 36.33 mg L⁻¹ of TOD at the end of the process, which is 15.5% lower than the undoped catalyst. These results are in agreement with XRD and Raman analysis and may be related to an increase in particle size and consequently lower specific area.

Codoped nitrogen and sulfur catalysts led to higher TOD values and were not able to totally remove parabens, with 15% NS-TiO₂ achieving 89.33% of methylparaben removal after 120 min reaction. Undoped catalyst had the highest removals and lower TOD at the end of reaction. This lower efficiency of NS-TiO₂ catalysts may be explained by an inhibiting characteristic of sulfur in the formation of hydroxyl radicals (Todorova et al., 2013).

5.2.3. Chemical Oxygen Demand (COD) and Total Organic Carbon (TOC) Removals

Regarding COD and TOC removals (Figure 5.11) using urea doped catalysts, photolytic ozonation and 15% N-TiO₂ led to the lowest removals, concordantly to parabens abatement and TOD evolution. The undoped catalyst had higher removals, which implies that method 2 doping with urea has a detrimental effect regarding refractory byproducts formation. Moreover, as referred previously the tetrabutyl titanate is slowly hydrolyzed so during the aging step 24h could be not enough time to achieve a well doped catalyst. Contrarily, in method 1 the source of titanium used is hydrolyzed faster and the aging period was 48 h. This also can be the reason of low performance for these catalysts of method 2 on the parabens degradation.

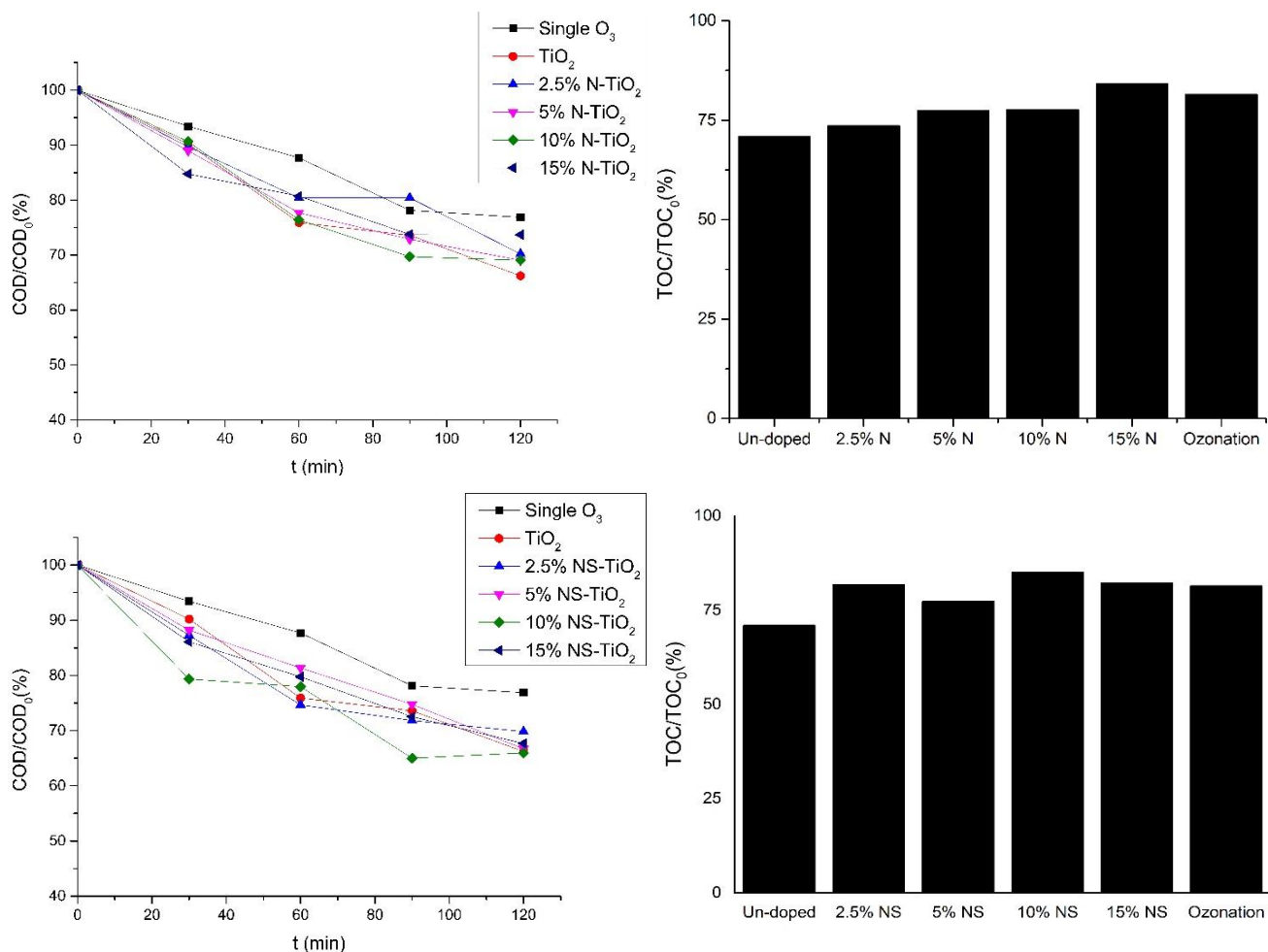


Figure 5.11 – Chemical Oxygen Demand removals during and Total Organic Carbon removals after 120 min of UV/O₃ and UV/O₃/TiO₂ reactions using N-doped and NS-codoped method 2 catalysts.

The lower removals of nitrogen doped catalysts indicate that urea results in a lower incorporation of nitrogen on the catalyst lattice. The prevalence of an interstitial (Ti-O-N) rather than substitutional (Ti-N) incorporation using urea was found in different studies, which may lead to a minor catalytic effect improvement (Ananpattarachai et al., 2009; Smirniotis et al., 2018).

NS-TiO₂ catalysts had almost the same COD removal and resulted in a lower TOC removal compared with the undoped catalyst and single ozonation, except 5% NS-TiO₂, reaffirming the detrimental effect of the additional sulfur doping on the catalysts overall performance.

The mineralization or oxidation selectivity of organic material removal was evaluated according to the partial oxidation yield (Table 5.7). TiO₂ and 2.5% N-TiO₂ had considerably lower yields, resulting in 86% and 89%, respectively, of removed COD mineralized. These catalysts, as demonstrated in the different analysis, had the best overall performances. The doped catalyst, even with slightly smaller COD and TOC removals, present an economical and environmental advantageous lower final TOD and higher mineralization level. The use of thiourea as doping agent showed no actual improvement of catalyst performance and its study was not continued.

Table 5.7 - Chemical oxygen demand and total organic carbon removal, transferred ozone dissolved and partial oxidation yield after 120 min reaction using different processes.

Process	COD removal (%)	TOC removal (%)	TOD (mg L ⁻¹)	$\mu_{COD_{partox}}$
O ₃ +TiO ₂	33.78	29.01	40.03	0.14
O ₃ +2.5%N-TiO ₂	29.80	26.42	35.12	0.11
O ₃ +5%N-TiO ₂	30.97	22.55	39.61	0.27
O ₃ +10%N-TiO ₂	30.95	22.41	42.72	0.28
O ₃ +15%N-TiO ₂	26.30	15.91	16.52	0.39
O ₃ +2.5%NS-TiO ₂	30.17	18.20	44.24	0.40
O ₃ +5%NS-TiO ₂	33.29	22.63	49.47	0.32
O ₃ +10%NS-TiO ₂	34.05	14.88	44.61	0.56
O ₃ +15%NS-TiO ₂	32.32	17.75	35.51	0.45
O ₃	23.11	18.53	46.19	0.20

5.2.4. Toxicity Evaluation

Toxicity tests were conducted as previously described, using *L. sativum*, *A. fischeri* and *C. fluminea* and are present in Table 5.8.

Table 5.8 - *L. sativum* germination index, *A. fischeri* luminescence inhibition after 15 min exposure and *C. fluminea* mortality after 48 h exposure to solutions obtained from 120 min treatment using different process.

Process	Germination Index (%) (\pm SD)	Luminescence inhibition (%) after 15 min (\pm SD)	Mortality (%) after 48 h (\pm SD)
O ₃ +TiO ₂	95.4 \pm 20.6	88.7 \pm 1.76	35.0 \pm 7.1
O ₃ +2.5%N-TiO ₂	112.8 \pm 21.1	87.5 \pm 0.96	20.0 \pm 0.0
O ₃ +5%N-TiO ₂	123.4 \pm 2.4	73.1 \pm 0.95	35.0 \pm 21.2
O ₃ +10%N-TiO ₂	95.9 \pm 5.1	63.0 \pm 0.85	45.0 \pm 7.1
O ₃ +15%N-TiO ₂	94.2 \pm 4.2	95.2 \pm 0.57	40.0 \pm 0.0
O ₃	74.6 \pm 19.6	70.0 \pm 0.15	30.0 \pm 14.1

All treated solutions had a decrease in toxicity compared to the initial parabens solution and the catalyst with smallest amount of nitrogen resulted in less toxic solutions.

10% N-TiO₂ conducted to a lower bacteria luminescence inhibition even when compared to single ozonation. This can be associated to a lower formation of toxic byproducts, as stated before for method 1 results. 15%N-TiO₂ presents the worst result in terms of toxicity over bacteria since

the parabens mixture was not totally removed. Parabens are antimicrobial agents which could justify this result.

Despite the low toxicity to *Corbicula fluminea* clams and high *Lepidium sativum* seeds germination index, 2.5% N-TiO₂ still resulted in a high *A. fischeri* luminescence inhibition. This may be a result to the higher sensibility to different compounds of the bacteria compared to the other studied species. Moreover, the phytotoxicity level decreases, again as occurs for method 1, in the presence of catalyst. The photocatalytic ozonation presents non phytotoxicity on *L. sativum* independently of catalyst considered.

5.3. Comparison of Catalysts

Finally, through the analysis of all catalysts, it's clear that, from method 1, 10% N-TiO₂ had the optimum nitrogen amount resulting in a maximum overall improvement of TiO₂ in photocatalytic ozonation reactions, regarding low TOD usage and high TOC and COD removals. From method 2, the increasing urea doping led to a decrease in the catalysts performances, but, regarding toxicity studies and the reduced TOD after 120 min reactions, 2.5% N-TiO₂ can be selected as a promising catalyst. Due to the better results and its higher availability during this research, further studies will focus on method 1 catalyst, but a future research is needed to completely contemplate urea doped catalysts.

Table 5.9 summarizes the main results obtained from photocatalytic ozonation reactions using both selected catalysts.

Table 5.9 - Transferred ozone dissolved, chemical oxygen demand and total organic carbon removal, partial oxidation yield, *L. sativum* germination index, *A. fischeri* luminescence inhibition after 15 min exposure and *C. fluminea* mortality after 48 h exposure of solutions obtained after photocatalytic ozonation reactions.

Parameter	Method 1	Method 2
	10% N-TiO ₂	2.5% N-TiO ₂
TOD (mg L ⁻¹)	33.11	35.12
COD removal (%)	35.69	29.80
TOC removal (%)	34.11	26.42
$\mu_{COD_{partox}}$	0.04	0.11
Germination Index (%) (\pm SD)	115.2 \pm 1.7	112.8 \pm 21.1
Luminescence inhibition (%) after 15 min (\pm SD)	84.6 \pm 0.00	87.5 \pm 0.96
Mortality (%) after 48 h (\pm SD)	45.0 \pm 21.2	20.0 \pm 0.0

6. MECHANISTIC STUDIES

The previously selected nitrogen doped catalyst will be evaluated in this section regarding the effect of different parameters, such as pH, catalyst loading, radical scavengers and water matrices. Potassium iodide (KI) and isopropanol were studied as ozone and hydroxyl radical's scavengers, respectively. pH was adjusted to neutral conditions (~7) using sodium hydroxide (NaOH) or a buffer mixture of sodium dihydrogen phosphate (NaH_2PO_4) and disodium hydrogen phosphate (Na_2HPO_4). To study the influence of the water matrix, reactions were conducted using a solution containing the mixture of 5 parabens dissolved in a secondary wastewater or river water. Moreover, humic acid and a mixture of sodium chloride (NaCl), sodium sulfate (Na_2SO_4) and sodium bicarbonate (NaHCO_3) as sources of Cl^- , SO_4^{2-} and HCO_3^- were also used, to attest the effect of organic matter and ionic species on the parabens mixture degradation.

6.1. Effect of pH and Catalyst Loading

pH is an important parameter to be evaluated due to its role in ozone decomposition and hydroxyl radicals production (Gomes et al., 2019d). Acidic conditions have a detrimental effect over parabens degradation rate since the main activity was due to the single ozone action and holes act as the principal oxidizing sites, while neutral or basic solution promote hydroxyl radical reactions (Kasprzyk-Hordern et al., 2003; Petala et al., 2015).

Typical pH of parabens mixture is about 5. During parabens degradation reactions, formation of carboxylic acids and other molecules occurs, lowering pH. Thus, initial pH was adjusted using NaOH or, to maintain the neutral pH throughout the entire reaction, a buffer mixture was applied.

The catalyst concentration was also studied by using the double of the previously established amount, 140 mg L^{-1} . A higher catalyst loading represents a higher number of active sites, which may lead to a higher capacity of degrading contaminants and producing oxidative radical species.

Parabens degradation for both pH adjustments, double catalyst loading and for the original conditions, unaltered pH (~5) and 70 mg L^{-1} of catalyst concentration, are present in Figure 6.1. Analysis in parallel with TOD evolution was not possible due to different room temperatures at the time of reactions, which alter the ozone production by the generator. Also due to higher temperatures, a new reaction with the original conditions using method 1 10% N-TiO₂ catalyst was conducted for better comparison with the other tests, which resulted in a higher final TOD compared to the reported in the previously section.

As can be observed, initial neutral pH condition favored parabens degradation. The buffered parabens solution reached total contaminants removal after 60 min, half the time needed for the unaltered solution. The solution adjusted with NaOH presents a faster parabens removal, but due to the pH decrease during reaction, total depletion was achieved after 90 min. The final pH of the buffered solution as expected remained the same as the initial value, while when NaOH was used and for the unaltered pH solution the final pH were 4.19 and 3.90, respectively.

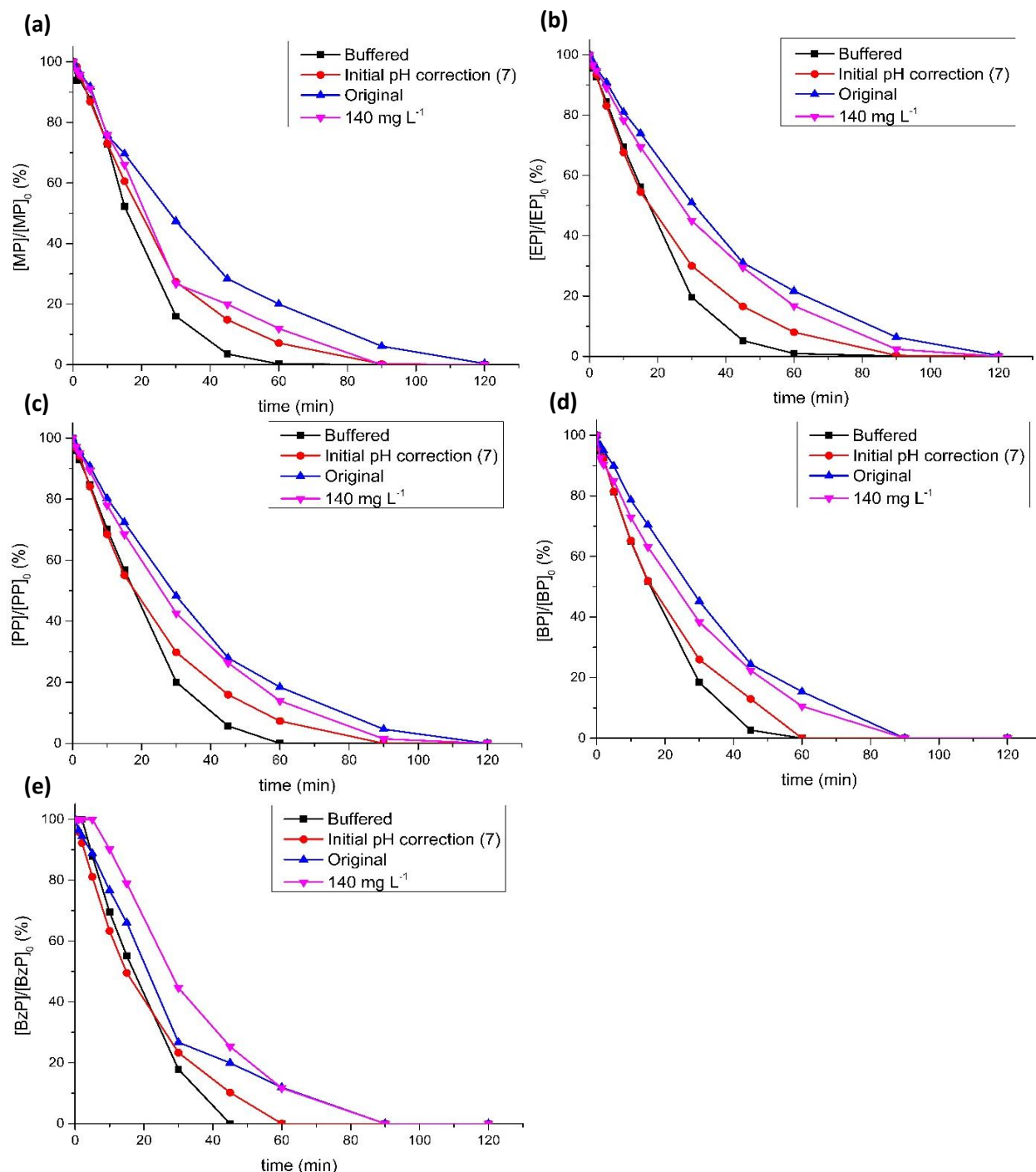


Figure 6.1 – Methylparaben (a), ethylparaben (b), propylparaben (c), butylparaben (d) and benzylparaben (e) degradation over 120 min reactions with pH adjustment using a buffer mixture or sodium hydroxide (NaOH), using 140 mg L⁻¹ of catalyst and the original conditions (unaltered pH and 70 mg L⁻¹ of catalyst) using method 1 10% N-TiO₂.

Besides the increase in ozone decomposition and hydroxyl radical formation, at neutral pH ozonation proceed by radical and molecular ozone reactions, while at lower pH the main route its through only molecular ozone reactions (Mecha et al., 2016). Although the neutral pH resulted in a faster parabens removal, the ozone consumption still needs to be future evaluated as studies indicate that a increase in TOD may occur (Gomes et al., 2019d).

With the exception of methylparaben, no significant improval was observed using a higher catalyst quantity. In photocatalytic reaction at heterogeneous catalytic regimes, the reaction rate depends on the number of active sites capable of absorbing photons, which is proportional to the catalyst concentration. Thus, the fact that increasing N-TiO₂ led to no actual increase in the overall removal rate could be explained by the number of disponible irradiated photons being already fully absorbed by the initial stablished concentration, 70 mg L⁻¹, and at this point a higher quantity of catalyst would only impede light penetration (Petala et al., 2015).

6.2. Effect of Radical Savengers and Water Matrix

Some molecules present in wastewaters may act as radical scavengers during oxidation processes, and more specifically ozonation reactions. Species such as carbonates (CO₃²⁻) and bicarbonates (HCO₃⁻) are considered as hydroxyl radical's and molecular ozone scavengers since they consume the produced •OH and molecular ozone, decreasing the pollutants removal efficiency. However, as these species react with •OH and O₃•, other radicals are produced with a lower oxidative potential (e.g. •CO₃²⁻), but still capable of reacting with pollutants such as parabens (Petala et al., 2015). As hydroxyl radicals are quenched by scavengers, principal reaction pathway changes and consequently the byproducts formed.

To study the roles of the principal oxidative species produced during reactions, isopropanol and potassium iodide were added to solutions. Isopropanol acts as a hydroxyl radical scavenger and KI acts principally as an ozone scavenger but is also able to quench hydroxyl radicals and positive holes. 13.1 mM isopropanol and its mixture with 5 mM of potassium iodide were added to the ultrapure water parabens solutions.

The presence of different ionic species and organic matter was studied using NaCl, Na₂SO₄ and NaHCO₃ as sources of Cl⁻, SO₄²⁻ and HCO₃⁻ at 125 mg L⁻¹, and 20 mg L⁻¹ of humic acid, that acts as an analog of the organic matter present in wastewaters and natural waters. Parabens concentration evolution during reactions with different conditions mentioned using ammonia doped selected catalyst are shown in Figure 6.2.

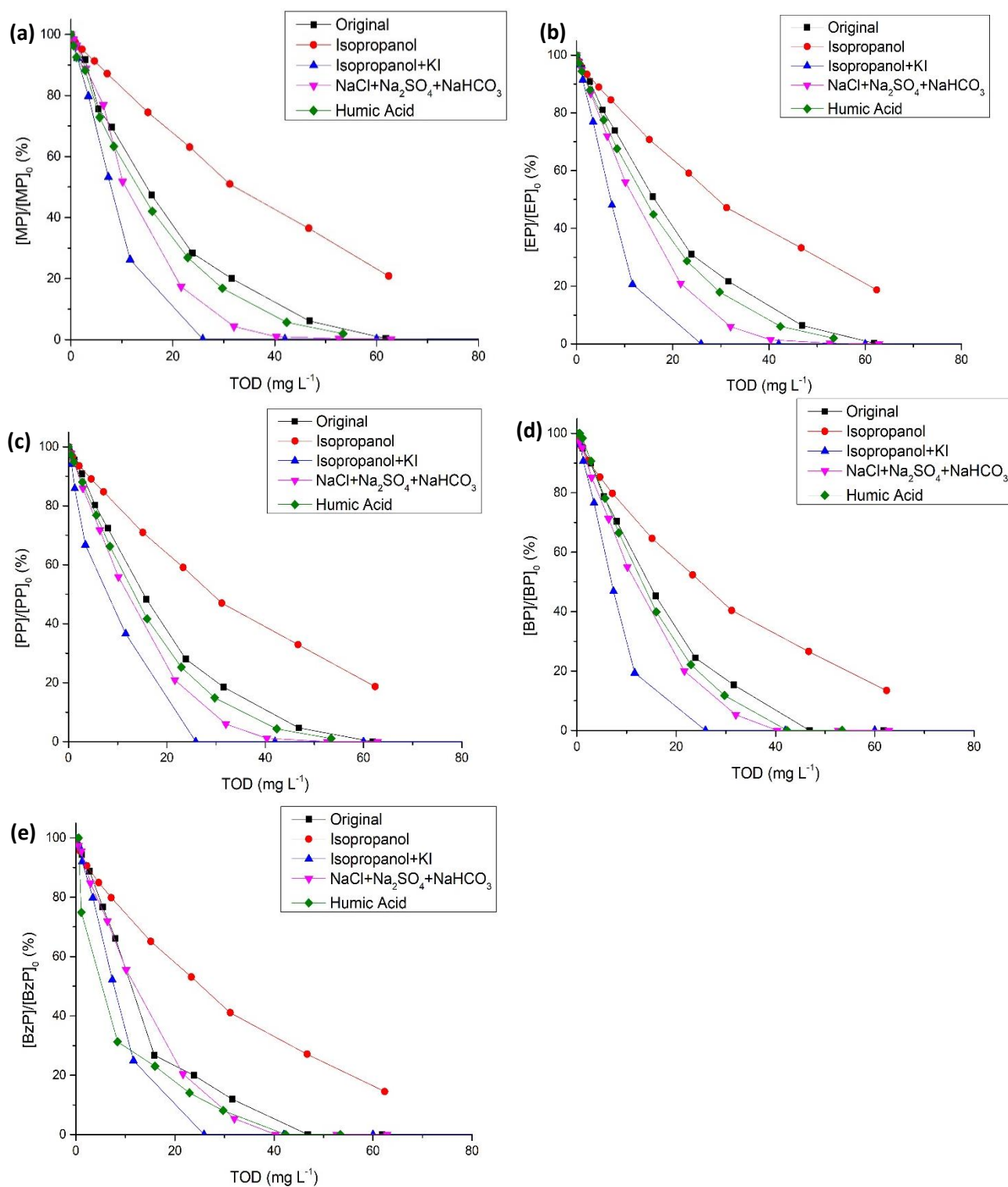


Figure 6.2 - Methylparaben (a), ethylparaben (b), propylparaben (c), butylparaben (d) and benzylparaben (e) degradation as function of TOD over 120 min photocatalytic ozonation reactions using method 1 10% N-TiO₂ in solutions containing only ultrapure water (original) or with the addition of 13mM of isopropanol, 5mM of potassium iodide (KI), 20 mg L⁻¹ of humic acid or 125 mg L⁻¹ of sodium chloride (NaCl), sodium sulfate (Na₂SO₄), sodium bicarbonate (NaHCO₃) and humic acid.

The solution containing isopropanol was not able to achieve total parabens removal during 120 min reaction. Thus, hydroxyl radicals, as expected, play an important role in parabens degradation reactions as hydroxylation is the known main reaction pathway (Velegraki et al., 2015).

Although, is important to notice that even with the hydroxyl radical scavenger, photocatalytic ozonation reaction achieved up to 79.16% as in case of methylparaben depletion, which indicates that other radicals favorably formed due to the absence of $\bullet\text{OH}$ can considerably degrade these contaminants. Ozone is an electrophilic molecule, meaning that can easily attack the high electronic density contaminants such as parabens due to its benzenic ring, also forming hydroxylated by-products (e.g. hydroquinone, 2,4-Dihydroxybenzoic acid).

To better understand the by-products formation when isopropanol is used, hydroquinone (HQ), 1,4-Benzoquinone (1,4-BzQ), 2,4-Dihydroxybenzoic acid (2,4-DHBA) and 4-Hydroxybenzoic acid (4-HBA) were analyzed using HPLC, present in Figure 6.3 using the normalized peak areas detected as function of the TOD.

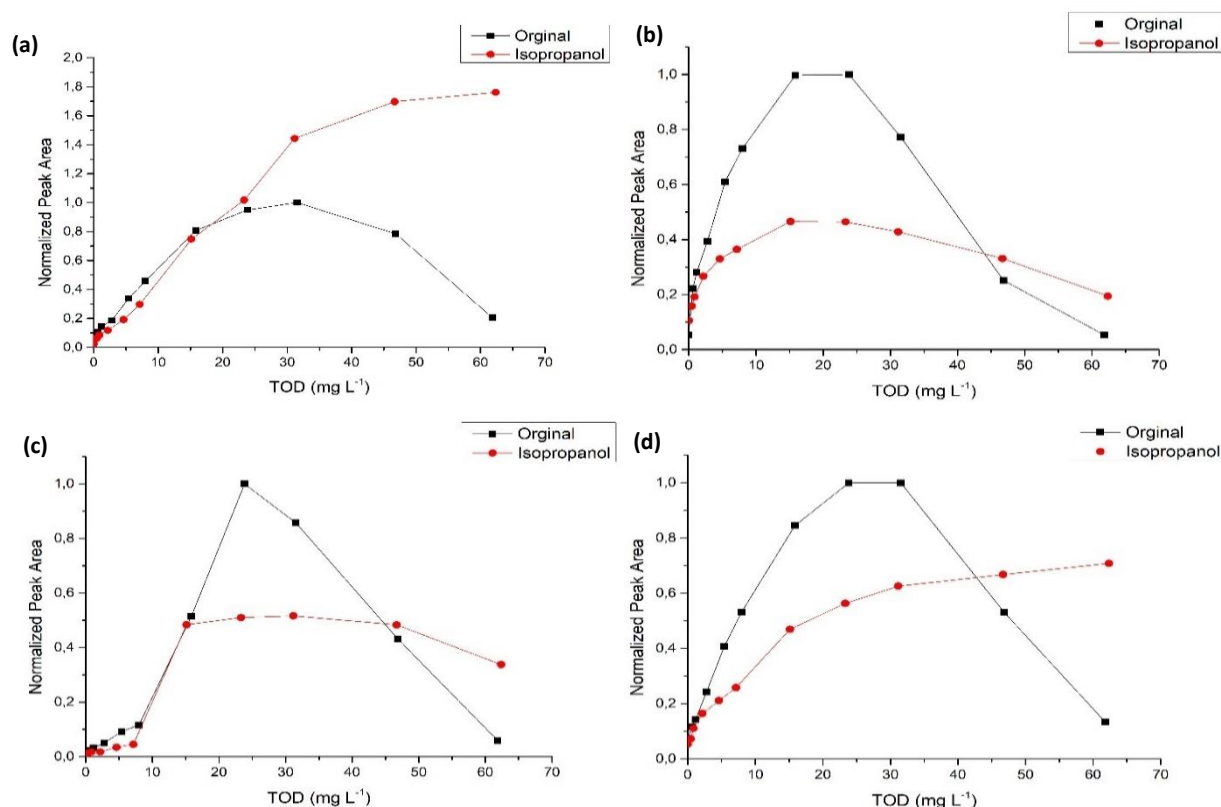


Figure 6.3 – 4-Hydroxybenzoic acid (a), 2,4-Dihydroxybenzoic acid (b), 1,4-Benzoquinone (c) and hydroquinone (d) concentration evolution during photocatalytic ozonation of parabens solution with or without isopropanol obtained through normalized peak areas from HPLC tests as function of TOD.

The presence of isopropanol resulted in a lower formation of these by-products, except for 4-HBA, but also a lower removal rate was observed due to the absence of hydroxyl radicals. Thus, total removal was not possible during the 120 min of reaction. Decarboxylation and dealkylation reactions have been suggested in different studies as the main route for the formation of these by-products through parabens photodegradation (Frontistis et al., 2017; Gomes et al., 2019). The consequent decarboxylation of 4-HBA is also related to the formation of

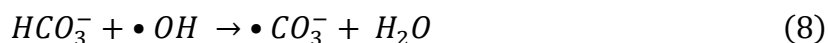
hydroquinone, which is corroborated by the fact that hydroquinone peak areas rapidly increase when the 4-HBA peaks starts to decrease.

When both isopropanol and potassium iodide were mixed with the parabens solution, contaminants were removed at a higher rate, achieving complete elimination under 30 min reaction and using 25.89 mg L⁻¹ of TOD. Even with KI being a radical scavenger, when I⁻ reacts with hydroxyl radicals, •OHI⁻ is formed and, due to the natural acidic characteristic of the parabens solution, decomposes producing •I, which is very electrophilic and able to attack the paraben's benzenic ring (Gomes et al., 2019d). Iodide radicals can also interact with low chain aliphatic alcohols, such as isopropanol, reducing its detrimental effect as a •OH scavenger (Rodríguez et al., 2015). Through the analysis of the HPLC results, the known by-products (HQ, BzQ, 4-HB and 2,4-DHB) were not detected, indicating that the presence of •I may change the reaction pathway, leading to the formation of other substances namely some halogenated organic compounds.

The quenching of ozone eliminates its competition with hydroxyl radicals for contaminants degradation, which promotes a higher interaction between parabens and •OH. Also, as ozone is not present to act as electron receiver, free e⁻ exist in the medium, capable of directly degrade parabens or also produce superoxide radicals (•O₂⁻) through oxygen reduction (Gomes et al., 2017b). The described radicals formed act as adjuvants, obtaining the higher degradation rate observed.

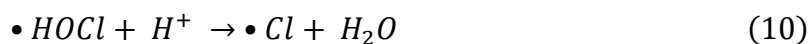
The addition of humic acid resulted in only a slight improval in parabens degradation. The organic matter can act as an ozone scavenger, which suggests that, through the obtained results, hydroxyl radicals have an imperative participation in parabens removal, and the small improvement can be a result of the already explained lower competition between ozone and •OH for the pollutants removal (Gomes et al., 2019d).

The contaminants removal in the presence of Cl⁻, SO₄²⁻ and HCO₃⁻ was enhanced and completed under 60 min with 40.32 mg L⁻¹ of TOD. The reported consequences of the presence of these ions in solutions are still controversial. Some studies indicate a detrimental effect due to the ability of these ions to act as hydroxyl radical scavengers, reducing the treatment efficiency (Azerrad et al., 2014; Petala et al., 2015). On the other hand, the reaction between hydroxyl radicals with these ions produce other radicals that still have high oxidizing potential and may have a higher affinity towards some molecules. Petala et al. (2015) indicated that •CO₃⁻ (Eq. 8) acts as a selective and strong oxidant towards aromatic compounds, depending on its substituent group.



Sulfates are also strong oxidizers, with an oxidative potential even higher than hydroxyl, and through its capacity to direct degrade the pollutants and scavenge electrons, preventing electron-hole recombination, are able to improve parabens degradation (Gomes et al., 2019d; Kotzamanidi et al., 2018).

The detrimental effect of chloride ions due to the formation of less oxidizing radicals (Eq. 9-11) through hydroxyl and photogenerated holes scavenging is dependent of the pH and initial concentration of Cl^- (Kotzamanidi et al., 2018). Thus, the conditions of the conducted tests may not be favorable to these undesirable reactions.



Secondary wastewaters are complex systems that contain different compounds that can alter the photocatalytic ozonation reaction, being the degradation of contaminants very dependent on the condition and composition of the water matrix. Thus, to evaluate the degradation of parabens in real conditions, a secondary wastewater (SWW) and river water (RW) were spiked with the 5 studied parabens. The characterization of the initial conditions of the two matrices are present in Table 6.1.

Table 6.1 - Secondary wastewater (SWW) and river water (RW) characterization.

Parameter	RW	SWW
pH	7.25	7.21
COD (mg L ⁻¹)	7.79	19.87
Cl ⁻ (mg L ⁻¹)	14.95	73.85
NO ₃ ⁻ (mg L ⁻¹)	7.27	35.16
SO ₄ ²⁻ (mg L ⁻¹)	9.19	29.70

During HPLC analysis, some peaks mainly corresponding to propyl, butyl- and benzylparaben were not detected, possibly due to complexation of these contaminants with unknown molecules present in the water matrix. Methyl- and ethylparaben degradation over 120 min of photocatalytic ozonation reaction is demonstrated in Figure 6.3 in parallel with the TOD evolution.

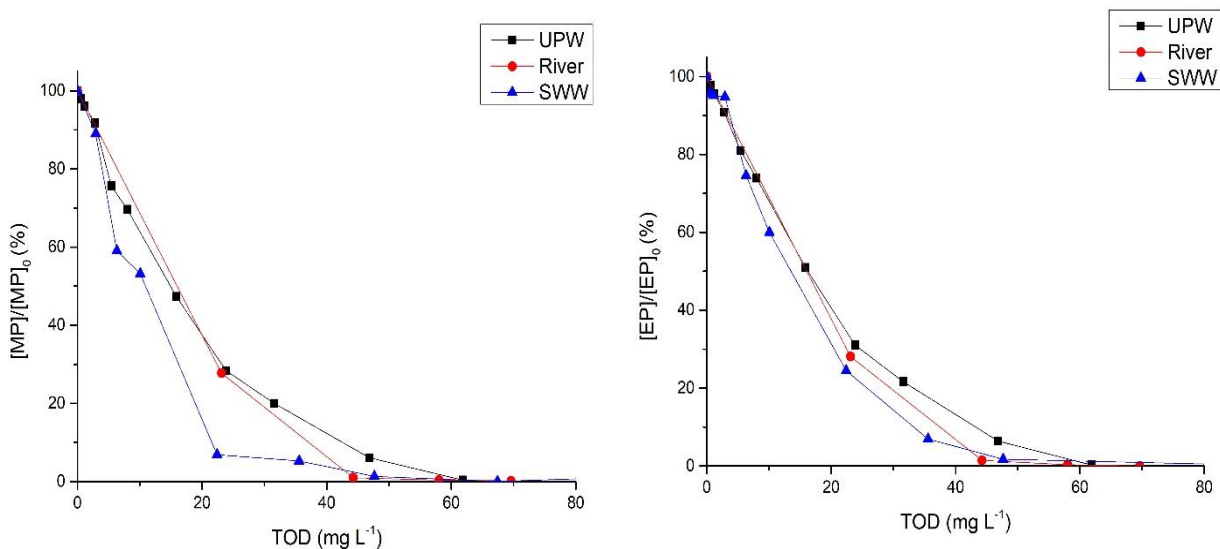


Figure 6.4 - Methylparaben and ethylparaben degradation over 120 min N-TiO₂ photocatalytic ozonation reaction and the transferred ozone dose (TOD)

As it can be observed, parabens degradation is not greatly affected by the different water matrix used. In fact, specially methylparaben, a faster removal using the secondary wastewater occurs. This can be possibly explained by the higher concentration of SO₄²⁻ and other ionic species, as formerly discussed, that are able to produce highly oxidative radicals and thus enhancing the pollutant removal. As the formation of •Cl is favored at acidic conditions, the reaction between hydroxyl radicals and chloride ions lead mainly to the formation of •HOCl, which has a lower oxidative potential.

Comparing the initial and final concentration (Table 6.1 and 6.2) of the 3 anions, chloride had a small increase, which may be related to the neutral pH of the solutions, impeding the radical formation. Sulfate concentration decreased 3.68 and 1.85 mg L⁻¹ in RW and SWW solutions, respectively, indicating that the slightly higher removal rate may be a result of the formation of sulfate radicals. Nitrate had also an increase in its concentration which may be a result of the suspected nitrogen leaching from the catalyst, producing nitrogenous substances.

Table 6.2 – Chloride (Cl⁻), nitrate (NO₃⁻) and sulfate (SO₄²⁻) concentrations after 120 min photocatalytic reactions using river water (RW) and a secondary wastewater (SWW) spiked with the mixture of 5 parabens.

Anion	RW	SWW
Cl ⁻ (mg L ⁻¹)	16.94	75.02
NO ₃ ⁻ (mg L ⁻¹)	7.58	35.53
SO ₄ ²⁻ (mg L ⁻¹)	5.52	27.85

The initial total organic carbon (TOC) of the SWW and RW spiked with parabens was 53.31 mg L⁻¹ and 41.75 mg L⁻¹, respectively. By the end of the reactions, SWW and RW had 38.45

mg L⁻¹ and 31.39 mg L⁻¹, representing a 27.87% and 24.81% removals, respectively. Thus, a similar degradation was obtained independent of the matrix and other by-products was formed, representing the residual value.

Toxicity studies were also conducted using seeds of *Lepidium sativum* for both river water and the secondary wastewater spiked with the mixture of 5 parabens. The initial germination indexes were 67.3% and 75.1% for RW and SWW, respectively. After 120 min treatment, the germination indexes increased to 146.0% for RW and 137.8% for SWW, representing a great decrease in the solutions phytotoxicity.

7. BACTERIA REMOVAL

Escherichia coli is an important pathogenic normally present in wastewater. Due to the disadvantages of current technologies for bacteria removal, such as chlorination and its hazardous organochlorine by-products, AOPs rise as efficient solutions for the disinfection of pathogenic contaminants. Thus, UV/O₃/N-TiO₂ and UV/O₃ test were conducted using secondary wastewater and river water to evaluate the efficiency of these methodologies on the removal of *E. coli* at the real conditions. The initial conditions of the secondary wastewater and river water are present in Table 7.1.

Table 7.1 - Secondary wastewater (SWW) and river water (RW) characterization.

Parameter	RW	SWW
pH	7.25	7.24
COD (mg L ⁻¹)	7.79	83.01

The Asian clam *Corbicula fluminea* was also studied through biofiltration tests as a disinfection process, representing a low-cost technology. This process also represents a pest management strategy, as the Asian clam is an invasive species in Portugal, endangering the local biodiversity and causing economic losses for industries due to biofouling and piping clogging. Their use in wastewater treatment would give to this pest an environmental application.

7.1. Advanced Oxidation Processes

For single and photocatalytic ozonation using nitrogen doped catalyst, reactions were conducted using 2 L solutions with a duration of 120 min for the secondary wastewater and, due to the expected lower bacterial content, 30 min for the disinfection of river water. The TOD evolution along the reactions was calculated and shown in Table 7.2.

Table 7.2 - TOD evolution during disinfection reactions using AOPs.

Solution	Time (min)	TOD (mg L ⁻¹)	
		UV/O ₃ /N-TiO ₂	UV/O ₃
RW	0	0.00	0.00
	10	2.98	5.58
	30	9.45	20.54
SWW	0	0.00	0.00
	30	8.52	10.73
	60	14.91	19.34
	90	20.93	27.56
	120	26.74	35.61

The beneficial effect towards ozone consumption when the photocatalyst is added to the medium is evident. Comparing the value at the end of each reaction, the photocatalytic process has a TOD 117% and 33% lower when river water and wastewater are used, respectively. This decrease of transferred ozone has a great economic benefit as one of the principal drawbacks of ozonation is its high ozone production cost.

E. coli colonies present in the samples were quantified and are shown in Figure 7.1 as a function of TOD. Complete bacteria removal was accomplished using both water matrices. Regarding the secondary wastewater, complete disinfection with photocatalytic ozonation was achieved in 120 min with 26.74 mg L⁻¹ of TOD, while the single process was faster, completely removing *E. coli* in 90 min but with a higher TOD, 27.56 mg L⁻¹. In the reaction using river water, no *E. coli* colonies were detected after 10 min, with single and photocatalytic ozonation using 5.58 and 2.98 mg L⁻¹ of TOD, respectively.

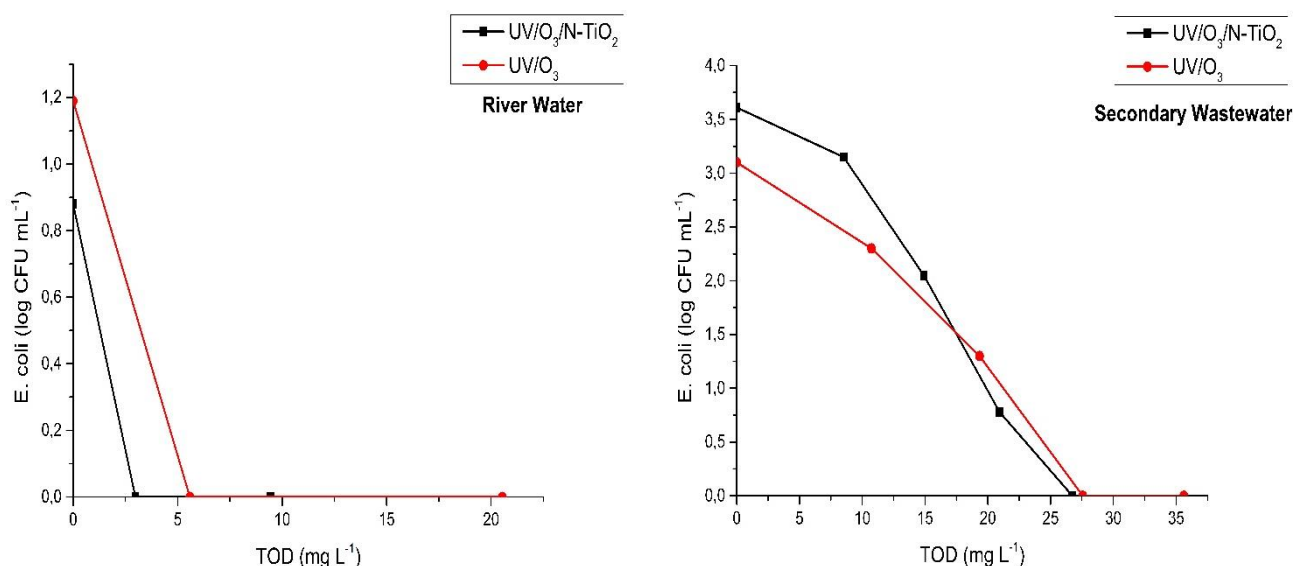


Figure 7.1 - *E. coli* removal in UV/O₃/N-TiO₂ and UV/O₃ reactions and TOD evolution

The samples that presented no colonies of any microorganism were subjected to regrowth tests due to the possibility of some cells to still be present but did not multiply (viable but non-culturable). No bacterial regrowth was observed after 24 h.

Besides the lower bacteria concentration, different factors contribute to the fact that reactions in river water had a higher removal rate. The SWW has a higher COD, thus the organic matter can interfere in the interaction between the oxidative radicals and bacteria. Moreover, the presence of ionic species can inhibit the activities of ozone and/or hydroxyl radical production. Other factor is the intracellular components and remaining cellular debris leached into the solution as microorganisms are being attacked, depositing over the catalyst and absorbing generated photons (Mecha et al., 2017a).

The bacteria inactivation initiates with the rupture of its cellular wall. This occurs due to the existence of different oxidative radicals that can disrupt the phospholipid membrane and attack other cellular defenses, such as antioxidant enzymes (e.g. catalase, superoxide dismutase), causing high oxidative stress and leading to protein fragmentation and loss of cell viability (Bosshard et al., 2010). Hydroxyl radical is suggested by different studies as one of the main responsible for the cellular disruption due to its high oxidative potential, but h^+ and $\bullet O_2^-$ also play an important role (Liu et al., 2019; Wang et al., 2015).

The improved efficiency of the integrated process is due to the higher production of highly oxidative radicals, as ozone act as an electron receiver, reacting with the photogenerated electron, impeding the electron-hole recombination and producing species such as $\bullet O_2^-$ and $\bullet OH$. This synergetic effect allows that the integrated process have an overall lower ozone consumption.

7.2. Biofiltration

To evaluate the use of invasive bivalves in *E. coli* removal, tests were conducted using biofilters containing 750 mL^{-1} of river water with a concentration of 60 clams L^{-1} with a duration of 24 h. River water used in this test was collected in a different location that the used in oxidation processes, presenting a higher bacteria concentration due to being closer to a WWTP discharge. A blank control was performed along the reaction to quantify the bacterial mortality due to other factors besides the clams activity. The results are summarized in Figure 7.2.

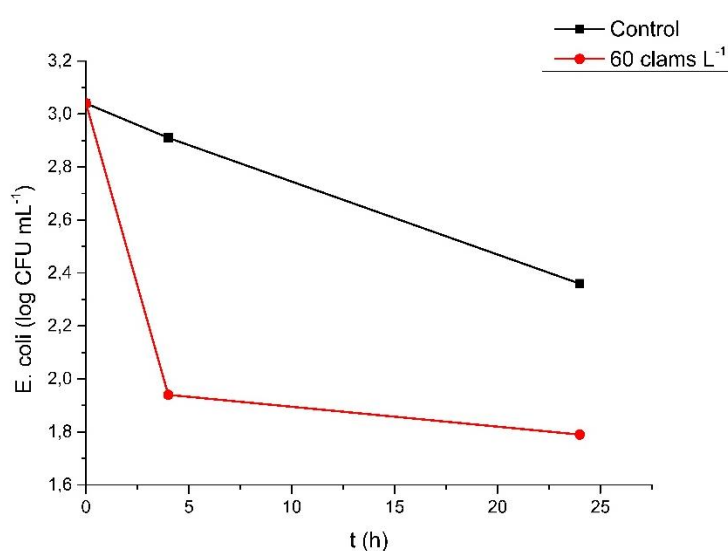


Figure 7.2 - *E. coli* removal in biofiltration and control tests

As can be observed, the control test also presented a decrease in the bacteria population number. These was also found in other studies involving treated effluents, and can be related to

environmental factors (e.g. temperature and oxygen concentration) (Mezzanotte et al., 2016). Toxic substances such as coagulants used in WWTPs can also be responsible for the bacteria removal. Thus, a more complete analysis of the water matrix is needed to determine the exact cause.

Nevertheless, the higher removal rate when *C. fluminea* is evident, achieving a 1.1 log reduction after 4 h. After 24 h the test using clams still had a decrease in the *E. coli* colonies, but at a lower rate, which indicates that the bivalves filtration occurs mainly in the early stage of the test. To elucidate this and obtain a better profile for the bacteria removal by the Asian clams, new tests need to be conducted with a smaller duration but with more samples been taken in shorter times.

Gomes et al., 2018a studied *C. fluminea* in *E. coli* biofiltration tests using spiked distilled water, which permits a better understanding of the mechanism of bacteria removal due to the absence of other influences as found in the present study. It was observed that the bacteria were efficiently metabolized by the bivalves, as only residual amounts of *E. coli* were found in the shells and soft tissue of the Asian clams.

Thus, even not being able to achieve total bacteria removal as the oxidation process, biofiltration was accountable for a considerable *E. coli* clearance level. Added to the fact that it is a still unused highly disponible material, it demonstrates that this process has a great potential as a low-cost water disinfection treatment but also a pest management strategy.

8. CONCLUSION

The use of photocatalytic ozonation and its benefits compared to the single technologies (photocatalytic oxidation and ozonation) was amply explored throughout this work. Initially, nitrogen doped and nitrogen and sulfur codoped TiO₂ catalysts, synthesized according to two sol-gel methods with different dopant amounts, were evaluated for the removal of a mixture of 5 parabens. An increasing nitrogen dosage in method 1 resulted in a lower TOD needed for total parabens depletion and a higher mineralization level was achieved, until an optimum concentration (10% N-TiO₂), with a decrease of the process efficiency with further nitrogen addition. In the case of urea doped catalysts, a small dosage of nitrogen (2.5% N-TiO₂) was more efficient regarding a TOD decrease. The undoped catalyst from method 2 had a higher COD and TOC removals, but 2.5% N-TiO₂ had a lower partial oxidation yield, meaning that the organic matter oxidized is removed toward total mineralization, producing CO₂ and H₂O. The addition of sulfur as doping element had a detrimental effect over the catalysts and all NS-TiO₂ had a worst performance compared with pure TiO₂, with higher ozone usage and lower removals, being promptly excluded from further investigation.

Photocatalytic oxidation tests conducted using N-TiO₂ showed a low photoactivity, with only up to 10% of parabens being removed in 180 min reactions. The doped catalyst still had a slightly higher removal compared to pure TiO₂. Regarding single ozonation, total parabens removal was achieved under 120 min but using a higher TOD and lower TOC and COD removals were obtained compared to pure and nitrogen doped TiO₂. Toxicity tests performed using 3 different species had mixed results, with UV/O₃/N-TiO₂ achieving higher germination index for *L. sativum* but also higher *A. fischeri* luminescence inhibition compared to single ozonation, which may be a result of a higher concentration of toxic by-products and nitrogen leaching from N-TiO₂. Thus, the existence of beneficial synergic effects when both photocatalysis and ozonation are integrated was demonstrated.

The effect of different parameters on parabens degradation and photocatalytic ozonation performance was investigated. The adjustment of the pH towards neutral conditions improved parabens degradation, reaching total removal in 60 min when a buffer is used, which can be related to a higher ozone decomposition and hydroxyl radicals formation. The use of the double catalyst loading had no significant improve in the reaction.

Reaction in the presence of isopropanol was not able to completely remove parabens and led to alterations in by-products formation, demonstrating the important role of hydroxyl radicals in these reactions. This reveals that the main responsible by parabens mixture degradation in

photocatalytic ozonation through nitrogen doped catalyst is the hydroxyl radical. Iodine, sulfate, chloride and carbonate ions induced a higher degradation rate with a lower ozone used, which can be associated to the higher formation of $\bullet\text{OH}$ and other highly oxidative radicals. A higher organic matter concentration, simulated by the addition of humic acid to the solution, had no significant effect over parabens removal.

Secondary wastewater and river water were spiked with the 5 tested parabens to evaluate the effect of real water matrices containing different substances. Both solutions resulted in a lower TOD to obtain a complete parabens removal compared to ultrapure water. The presence of ions such as Cl^- and SO_4^{2-} are suggested to be the main cause for the better performances, as the TOD decreased with a higher initial concentration with these ions.

In the study of the removal of *Escherichia coli*, biofiltration using *Corbicula fluminea*, photocatalytic and single ozonation were revealed as efficient disinfection processes. Using a secondary wastewater and river water, both oxidation processes were compared. Single and photocatalytic ozonation resulted in total bacteria removal with no detected regrowth after 24 h in both matrices, but the use of N-TiO₂ resulted in more efficient relation between ozone consumption and bacteria disinfection, thus also resulting in a more economically efficient process.

Invasive bivalves used in biofiltration tests did not achieved total removal of *E. coli* from river water samples, but resulted in a 1.25 log reduction after 24 h, with a higher clearance rate during the initial hours of the test. The control test without the clams also presented a decrease in bacteria population, which may indicate the presence of a toxic substance.

Thus, comparing the 3 disinfection processes, oxidation technologies have a higher disinfectant power, quickly removing all bacteria, but the costs involving the use of UV radiation and ozone production, even with a lower amount using the catalyst, represent a higher total cost. The use of the invasive species represents an economical and environmental efficient alternative for pathogenic bacteria disinfection but also a pest management technique, avoiding the use of biocides or other strategies that may endanger the environment.

9. FUTURE WORK

From the obtained results of this work, additional studies could be performed to better understand and further optimize this subject. Some suggestions are:

- Perform additional characterization tests in catalysts to better evaluate the nitrogen doping, to understand if the nitrogen is in interstitial or substitutional way in TiO₂ lattice;
- Study photocatalytic ozonation under solar radiation, since the UVA is more expensive radiation than the solar light;
- Study the influence of by-products formed during photocatalytic ozonation and its effects over the toxicity of treated solutions through the wide range of species;
- Evaluate more trophic levels to better understand the toxicity of the treated solutions, and it would be important to infer about the possibility of wastewater;
- Further analyze the obtained solutions from photocatalytic ozonation regarding possible nitrogen leaching;
- Evaluate the influence of different components of water matrices in biofiltration tests and bacterial removal;
- Conduct new biofiltration tests with samples in shorter times and optimize the overall process;
- Application of biofiltration for disinfection of another enteric pathogens, such as viruses, protozoa and other bacteria.

REFERENCES

- Abbas, M., Adil, M., Ehtisham-ul-Haque, S., Munir, B., Yameen, M., Ghaffar, A., Shar, G. A., Asif Tahir, M., & Iqbal, M. (2018). *Vibrio fischeri* bioluminescence inhibition assay for ecotoxicity assessment: A review. *Science of the Total Environment*, *626*, 1295–1309.
- Ahmed, M. B., Zhou, J. L., Ngo, H. H., Guo, W., Thomaidis, N. S., & Xu, J. (2017). Progress in the biological and chemical treatment technologies for emerging contaminant removal from wastewater: A critical review. *Journal of Hazardous Materials*, *323*, 274–298.
- AMAP (Arctic Monitoring and Assessment Programme). (2017). AMAP Assessment 2016: Chemicals of Emerging Arctic Concern. In *Arctic Monitoring and Assessment Programme (AMAP)*. Retrieved from <https://www.amap.no/documents/doc/amap-assessment-2016-chemicals-of-emerging-arctic-concern/1624>
- Ananpattarachai, J., Kajitvichyanukul, P., & Seraphin, S. (2009). Visible light absorption ability and photocatalytic oxidation activity of various interstitial N-doped TiO₂ prepared from different nitrogen dopants. *Journal of Hazardous Materials*, *168*(1), 253–261.
- Araña, J., Melián, J. A., Rodríguez, J. M., Díaz, O., Viera, A., Peña, J., Sosa, P., & Jiménez, V. (2002). TiO₂-photocatalysis as a tertiary treatment of naturally treated wastewater. *Catalysis Today*, *76*(2–4), 279–289.
- Azerrad, S. P., Gur-Reznik, S., Heller-Grossman, L., & Dosoretz, C. G. (2014). Advanced oxidation of iodinated X-ray contrast media in reverse osmosis brines: The influence of quenching. *Water Research*, *62*, 107–116.
- Barkul, R. P., Koli, V. B., Shewale, V. B., Patil, M. K., & Delekar, S. D. (2016). Visible active nanocrystalline N-doped anatase TiO₂ particles for photocatalytic mineralization studies. *Materials Chemistry and Physics*, *173*, 42–51.
- Bhattacharyya, A., Haldar, A., Bhattacharyya, M., & Ghosh, A. (2019). Anthropogenic influence shapes the distribution of antibiotic resistant bacteria (ARB) in the sediment of Sundarban estuary in India. *Science of the Total Environment*, *647*, 1626–1639.
- Bixio, D., Thoeue, C., De Koning, J., Joksimovic, D., Savic, D., Wintgens, T., & Melin, T. (2006). Wastewater reuse in Europe. *Desalination*, *187*(1–3), 89–101.
- Błędzka, D., Gromadzińska, J., & Wasowicz, W. (2014). Parabens. From environmental studies to human health. *Environment International*, *67*, 27–42.

- Boelee, E., Geerling, G., van der Zaan, B., Blauw, A., & Vethaak, A. D. (2019). Water and health: From environmental pressures to integrated responses. *Acta Tropica*, *193*, 217–226.
- Bokhimi, X., & Zanella, R. (2007). *Crystallite Size and Morphology of the Phases in Au / TiO₂ and Au / Ce-TiO₂ Catalysts*. 2525–2532.
- Bosshard, F., Riedel, K., Schneider, T., Geiser, C., Bucheli, M., & Egli, T. (2010). Protein oxidation and aggregation in UVA-irradiated Escherichia coli cells as signs of accelerated cellular senescence. *Environmental Microbiology*, *12*(11), 2931–2945.
- Casas, M. E., & Bester, K. (2015). Can those organic micro-pollutants that are recalcitrant in activated sludge treatment be removed from wastewater by biofilm reactors (slow sand filters)? *Science of the Total Environment*, *506–507*, 315–322.
- Centi, G., & Perathoner, S. (2014). Advanced Oxidation Processes in Water Treatment. In D. Duprez & F. Cavani (Eds.), *Handbook of Advanced Methods And Processes in Oxidation Catalysis* (pp. 251–283). London: Imperial College Press.
- Chauhan, A., Thirumalai, S., & Kumar, R. V. (2018). In-situ fabrication of TiO₂-C core-shell particles for efficient solar photocatalysis. *Materials Today Communications*, *17*(September), 371–379.
- Chong, M. N., Jin, B., & Saint, C. P. (2011). Bacterial inactivation kinetics of a photo-disinfection system using novel titania-impregnated kaolinite photocatalyst. *Chemical Engineering Journal*, *171*(1), 16–23.
- Clesceri, L. S., Greenberg, A. E., & Eaton, A. D. (1999). *Standard methods for the examination of water and wastewater* (20th ed.). Washington, DC: American Public Health Association.
- Cong, Y., Zhang, J., Chen, F., & Anpo, M. (2007). Synthesis and characterization of nitrogen-doped TiO₂ nanophotocatalyst with high visible light activity. *Journal of Physical Chemistry*, *111*(19), 6976–6982.
- Cvetnic, M., Juretic Perisic, D., Kovacic, M., Ukic, S., Bolanca, T., Rasulev, B., Kusic, H., & Loncaric Bozic, A. (2019). Toxicity of aromatic pollutants and photooxidative intermediates in water: A QSAR study. *Ecotoxicology and Environmental Safety*, *169*(October 2018), 918–927.

- Darbre, P. D., Aljarrah, A., Miller, W. R., Coldham, N. G., Sauer, M. J., & Pope, G. S. (2004). Concentrations of Parabens in human breast tumours. *Journal of Applied Toxicology*, *24*(1), 5–13.
- Darbre, P. D., Byford, J. R., Shaw, L. E., Hall, S., Coldham, N. G., Pope, G. S., & Sauer, M. J. (2003). Eostrogenic activity of benzylparaben. *Journal of Applied Toxicology*, *23*(1), 43–51.
- Darbre, P. D., Byford, J. R., Shaw, L. E., Horton, R. A., Pope, G. S., & Sauer, M. J. (2002). Oestrogenic activity of isobutylparaben in vitro and in vivo. *Journal of Applied Toxicology*, *22*(4), 219–226.
- Demirel, C. S. U., Birben, N. C., & Bekbolet, M. (2018). A comprehensive review on the use of second generation TiO₂ photocatalysts: Microorganism inactivation. *Chemosphere*, *211*, 420–448.
- Dhanya, T. P., & Sugunan, S. (2013). Preparation, Characterization and Photocatalytic Activity of N doped TiO₂. *Journal of Applied Chemistry*, *4*(3), 27–33.
- Dulio, V., van Bavel, B., Brorström-Lundén, E., Harmsen, J., Hollender, J., Schlabach, M., Slobodnik, J., Thomas, K., & Koschorreck, J. (2018, December 1). Emerging pollutants in the EU: 10 years of NORMAN in support of environmental policies and regulations. *Environmental Sciences Europe*, Vol. 30.
- Eggen, R. I. L., Hollender, J., Joss, A., Schärer, M., & Stamm, C. (2014). Reducing the discharge of micropollutants in the aquatic environment: The benefits of upgrading wastewater treatment plants. *Environmental Science and Technology*, *48*(14), 7683–7689.
- Ferrario, C., Finizio, A., & Villa, S. (2017). Legacy and emerging contaminants in meltwater of three Alpine glaciers. *Science of the Total Environment*, *574*, 350–357.
- Fisher, M., Keane, D., Fernandez-Ibanez, P., Colreavy, J., Hinder, S., McGuigan, K., & Pillai, S. (2013). Nitrogen and copper doped solar light active TiO. *Applied Catalysis. B, Environmental*, *130*, 8–13.
- FOEN (Federal Office for the Environment). (2015). *Environment Switzerland*. Retrieved from <https://www.bafu.admin.ch/bafu/en/home/state/publications-on-the-state-of-the-environment/environment-switzerland-2015.html>

- Frontistis, Z., Antonopoulou, M., Petala, A., Venieri, D., Konstantinou, I., Kondarides, D. I., & Mantzavinos, D. (2017). Photodegradation of ethyl paraben using simulated solar radiation and Ag₃PO₄ photocatalyst. *Journal of Hazardous Materials*, *323*, 478–488.
- Ganguly, P., Byrne, C., Breen, A., & Pillai, S. C. (2018). Antimicrobial activity of photocatalysts: Fundamentals, mechanisms, kinetics and recent advances. *Applied Catalysis B: Environmental*, *225*(November 2017), 51–75.
- Gerba, C. P., & Pepper, I. L. (2004). Microbial Contaminants. In *Environmental Monitoring and Characterization* (3rd ed.).
- Ghughe, S. P., & Saroha, A. K. (2018). Catalytic ozonation for the treatment of synthetic and industrial effluents - Application of mesoporous materials: A review. *Journal of Environmental Management*, *211*, 83–102.
- Gmurek, M., Rossi, A. F., Martins, R. C., Quinta-Ferreira, R. M., & Ledakowicz, S. (2015). Photodegradation of single and mixture of parabens - Kinetic, by-products identification and cost-efficiency analysis. *Chemical Engineering Journal*, *276*, 303–314.
- Gomes, J. F., Pereira, J. L., Rosa, I. C., Saraiva, P. M., Gonçalves, F., & Costa, R. (2014). Evaluation of candidate biocides to control the biofouling Asian clam in the drinking water treatment industry: An environmentally friendly approach. *Journal of Great Lakes Research*, *40*(2), 421–428.
- Gomes, J. F., Leal, I., Bednarczyk, K., Gmurek, M., Stelmachowski, M., Diak, M., Emília Quinta-Ferreira, M., Costa, R., Martins, R. C. (2017a). Photocatalytic ozonation using doped TiO₂ catalysts for the removal of parabens in water. *Science of the Total Environment*, *609*, 329–340.
- Gomes, J. F., Leal, I., Bednarczyk, K., Gmurek, M., Stelmachowski, M., Zaleska-Medynska, A., Quinta-Ferreira, M. E., Costa, R., Martins, R. C. (2017b). Detoxification of parabens using UV-A enhanced by noble metals - TiO₂ supported catalysts. *Journal of Environmental Chemical Engineering*, *5*(4), 3065–3074.
- Gomes, J. F., Lopes, A., Gonçalves, D., Luxo, C., Gmurek, M., Costa, R., Quinta-Ferreira, R. M., Martins, R. C., & Matos, A. (2018a). Biofiltration using *C. fluminea* for *E. coli* removal from water: Comparison with ozonation and photocatalytic oxidation. *Chemosphere*, *208*, 674–681.

- Gomes, J. F., Matos, A., Quinta-Ferreira, R. M., & Martins, R. C. (2018b). Environmentally applications of invasive bivalves for water and wastewater decontamination. *Science of the Total Environment*, *630*, 1016–1027.
- Gomes, J. F., Frasson, D., Pereira, J. L., Gonçalves, F. J. M., Castro, L. M., Quinta-Ferreira, R. M., & Martins, R. C. (2019a). Ecotoxicity variation through parabens degradation by single and catalytic ozonation using volcanic rock. *Chemical Engineering Journal*, *360* (November 2018), 30–37.
- Gomes, J., Frasson, D., Quinta-Ferreira, R. M., Matos, A., & Martins, R. C. (2019b). Removal of enteric pathogens from real wastewater using single and catalytic ozonation. *Water (Switzerland)*, *11*(1), 1–12.
- Gomes, J. F., Lincho, J., Domingues, E., Quinta-Ferreira, R. M., & Martins, R. C. (2019c). N-TiO₂ Photocatalysts: photocatalysts: A review of their characteristics and capacity for emerging contaminants removal. *Water (Switzerland)*, *11*(2).
- Gomes, J. F., Lopes, A., Gmurek, M., Quinta-Ferreira, R. M., & Martins, R. C. (2019d). Study of the influence of the matrix characteristics over the photocatalytic ozonation of parabens using Ag-TiO₂. *Science of the Total Environment*, *646*, 1468–1477.
- Han, E., Vijayarangamuthu, K., Youn, J. sang, Park, Y. K., Jung, S. C., & Jeon, K. J. (2018). Degussa P25 TiO₂ modified with H₂O₂ under microwave treatment to enhance photocatalytic properties. *Catalysis Today*, *303* (June 2017), 305–312.
- Hellenbrand, R., Mantzavinos, D., Metcalfe, I. S., & Livingston, A. G. (1997). Integration of Wet Oxidation and Nanofiltration for Treatment of Recalcitrant Organics in Wastewater. *Industrial and Engineering Chemistry Research*, *36*(12), 5054–5062.
- Ibrahim, S. A., Nazari, A. S. M., Kamdi, Z., Hatta, M. N. M., Yunos, M. Z., Rus, A. Z. M., & Harun, Z. (2019). Effect of Fe and/or N on the photoactivity of TiO₂ prepared by sol-gel method. *AIP Conference Proceedings*, *2068*(February).
- IWA (International Water Association). (2018). *The Reuse Opportunity: Cities seizing the reuse opportunity in circular economy*. Retrieved from <https://iwa-network.org/publications/the-reuse-opportunity/>
- Jamal, A., Rastkari, N., Dehghaniathar, R., Aghaei, M., Nodehi, R. N., Nasser, S., Kashani, H., & Yunesian, M. (2019). Prenatal exposure to parabens and anthropometric birth outcomes: A systematic review. *Environmental Research*, *173*(August 2018), 419–431.

- Kalantari, K., Kalbasi, M., Sohrabi, M., & Javid, S. (2016). Synthesis and characterization of N-doped TiO₂ nanoparticles and their application in photocatalytic oxidation of dibenzothiophene under visible light. *Ceramics International*, 42(13), 14834–14842.
- Kasprzyk-Hordern, B., Ziólek, M., & Nawrocki, J. (2003). Catalytic ozonation and methods of enhancing molecular ozone reactions in water treatment. *Applied Catalysis B: Environmental*, 46(4), 639–669.
- Kelessidis, A., & Stasinakis, A. S. (2012). Comparative study of the methods used for treatment and final disposal of sewage sludge in European countries. *Waste Management*, 32(6), 1186–1195.
- Komaraiah, D., Radha, E., James, J., Kalarikkal, N., Sivakumar, J., Ramana Reddy, M. V., & Sayanna, R. (2019). Effect of particle size and dopant concentration on the Raman and the photoluminescence spectra of TiO₂:Eu³⁺ nanophosphor thin films. *Journal of Luminescence*, 211 (March), 320–333.
- Kotzamanidi, S., Frontistis, Z., Binas, V., Kiriakidis, G., & Mantzavinos, D. (2018). Solar photocatalytic degradation of propyl paraben in Al-doped TiO₂ suspensions. *Catalysis Today*, 313 (October 2017), 148–154.
- Kumar, P. D., Mohamed, A. R., & Subhash Bhatia. (2002). Wastewater treatment using photocatalysis: Destruction of methylene blue dye from wastewater streams. *Jurnal Kejuruteraan*, 14, 17–30.
- Lee, H. U., Lee, S. C., Choi, S., Son, B., Lee, S. M., Kim, H. J., & Lee, J. (2013). Efficient visible-light induced photocatalysis on nanoporous nitrogen-doped titanium dioxide catalysts. *Chemical Engineering Journal*, 228, 756–764.
- Lee, J. W., Lee, H. K., & Moon, H. B. (2019). Contamination and spatial distribution of parabens, their metabolites and antimicrobials in sediment from Korean coastal waters. *Ecotoxicology and Environmental Safety*, 180(May), 185–191.
- Liao, C., Lee, S., Moon, H. B., Yamashita, N., & Kannan, K. (2013). Parabens in sediment and sewage sludge from the United States, Japan, and Korea: Spatial distribution and temporal trends. *Environmental Science and Technology*, 47(19), 10895–10902.

- Liu, N., Zhu, Q., Zhang, N., Zhang, C., Kawazoe, N., Chen, G., Negishi, N., & Yang, Y. (2019). Superior disinfection effect of *Escherichia coli* by hydrothermal synthesized TiO₂-based composite photocatalyst under LED irradiation: Influence of environmental factors and disinfection mechanism. *Environmental Pollution*, *247*, 847–856.
- López, R., & Gómez, R. (2012). Band-gap energy estimation from diffuse reflectance measurements on sol–gel and commercial TiO₂: a comparative study. *61*, 1–7.
- Lu, J., Li, H., Tu, Y., & Yang, Z. (2018). Biodegradation of four selected parabens with aerobic activated sludge and their transesterification product. *Ecotoxicology and Environmental Safety*, *156*(March), 48–55.
- Majowicz, S. E., Scallan, E., Jones-Bitton, A., Sargeant, J. M., Stapleton, J., Angulo, F. J., Yeung, D. H., & Kirk, M. D. (2014). Global Incidence of Human Shiga Toxin–Producing *Escherichia coli* Infections and Deaths: A Systematic Review and Knowledge Synthesis. *Foodborne Pathogens and Disease*, *11*(6), 447–455.
- Maness, P. C., Smolinski, S., Blake, D. M., Huang, Z., Wolfrum, E. J., & Jacoby, W. A. (1999). Bactericidal activity of photocatalytic TiO₂ reaction: Toward an understanding of its killing mechanism. *Applied and Environmental Microbiology*, *65*(9), 4094–4098.
- Martins, R. C., & Quinta-Ferreira, R. M. (2009). Catalytic ozonation of phenolic acids over a Mn-Ce-O catalyst. *Applied Catalysis B: Environmental*, *90* (1–2), 268–277.
- Mecha, A. C., Onyango, M. S., Ochieng, A., Fourie, C. J. S., & Momba, M. N. B. (2016). Synergistic effect of UV–vis and solar photocatalytic ozonation on the degradation of phenol in municipal wastewater: A comparative study. *Journal of Catalysis*, *341*, 116–125.
- Mecha, A. C., Onyango, M. S., Ochieng, A., & Momba, M. N. B. (2017a). Evaluation of synergy and bacterial regrowth in photocatalytic ozonation disinfection of municipal wastewater. *Science of the Total Environment*, *601–602*, 626–635.
- Mecha, A. C., Onyango, M. S., Ochieng, A., & Momba, M. N. B. (2017b). Ultraviolet and solar photocatalytic ozonation of municipal wastewater: Catalyst reuse, energy requirements and toxicity assessment. *Chemosphere*, *186*, 669–676.
- Mehrjouei, M., Müller, S., & Möller, D. (2015). A review on photocatalytic ozonation used for the treatment of water and wastewater. *Chemical Engineering Journal*, *263*, 209–219.

- Mezzanotte, V., Marazzi, F., Bissa, M., Pacchioni, S., Binelli, A., Parolini, M., Magni, S., Ruggeri, F. M., Radaelli, A. (2016). Removal of enteric viruses and Escherichia coli from municipal treated effluent by zebra mussels. *Science of the Total Environment*, 539, 395–400.
- Miralles-Cuevas, S., Oller, I., Agüera, A., Sánchez Pérez, J. A., & Malato, S. (2017). Strategies for reducing cost by using solar photo-Fenton treatment combined with nanofiltration to remove microcontaminants in real municipal effluents: Toxicity and economic assessment. *Chemical Engineering Journal*, 318, 161–170.
- Molins-Delgado, D., Díaz-Cruz, M. S., & Barceló, D. (2015). Introduction: Personal Care Products in the Aquatic Environment. In M. S. Díaz-Cruz & D. Barceló (Eds.), *Personal Care Products in the Aquatic Environment* (pp. 1–34).
- Monteiro, R. A. R., Miranda, S. M., Vilar, V. J. P., Pastrana-Martínez, L. M., Tavares, P. B., Boaventura, R. A. R., Faria, J. L., Pinto, E., & Silva, A. M. T. (2015). N-modified TiO₂ photocatalytic activity towards diphenhydramine degradation and Escherichia coli inactivation in aqueous solutions. *Applied Catalysis B: Environmental*, 162, 66–74.
- Movahedian, H., Bina, B., & Asghari, G. (2005). Toxicity Evaluation of Wastewater Treatment Plant Effluents Using Daphnia magna. *Iranian Journal of Environmental Health Science & Engineering*, 2(2), 1–4.
- Naidu, R., Espana, A., Andres, V., Liu, Y., & Jit, J. (2016). Emerging contaminants in the environment: Risk-based analysis for better management. *Chemosphere*, 154, 350–357.
- Naidu, R., Jit, J., Kennedy, B., & Arias, V. (2016). Emerging contaminant uncertainties and policy: The chicken or the egg conundrum. *Chemosphere*, 154, 385–390.
- Nowak, K., Ratajczak-Wrona, W., Górska, M., & Jabłońska, E. (2018). Parabens and their effects on the endocrine system. *Molecular and Cellular Endocrinology*, 474(March), 238–251.
- OECD (Organisation for Economic Cooperation and Development). (2018). Section 4: Health Effects. In *OECD Guidelines for the Testing of Chemicals* (p. 16).
- Oishi, S. (2001). Effects of butylparaben on the male reproductive system in rats. *Toxicology and Industrial Health*, 17(2–3), 31–39.

- Oliveira, C., Vilares, P., & Guilhermino, L. (2015). Integrated biomarker responses of the invasive species *Corbicula fluminea* in relation to environmental abiotic conditions: A potential indicator of the likelihood of clam's summer mortality syndrome. *Comparative Biochemistry and Physiology -Part A : Molecular and Integrative Physiology*, *182*, 27–37.
- Osuolale, O., & Okoh, A. (2017). Human enteric bacteria and viruses in five wastewater treatment plants in the Eastern Cape, South Africa. *Journal of Infection and Public Health*, *10*(5), 541–547.
- Petala, A., Frontistis, Z., Antonopoulou, M., Konstantinou, I., Kondarides, D. I., & Mantzavinos, D. (2015). Kinetics of ethyl paraben degradation by simulated solar radiation in the presence of N-doped TiO₂ catalysts. *Water Research*, *81*, 157–166.
- Pham, T. D., & Lee, B. K. (2017). Selective removal of polar VOCs by novel photocatalytic activity of metals co-doped TiO₂/PU under visible light. *Chemical Engineering Journal*, *307*, 63–73.
- Pichel, N., Vivar, M., & Fuentes, M. (2019). The problem of drinking water access: A review of disinfection technologies with an emphasis on solar treatment methods. *Chemosphere*, *218*, 1014–1030.
- Pimentel, D., Zuniga, R., & Morrison, D. (2005). Update on the environmental and economic costs associated with alien-invasive species in the United States. *Ecological Economics*, *52*(3 SPEC. ISS.), 273–288.
- Qiu, P., Sun, X., Lai, Y., Gao, P., Chen, C., & Ge, L. (2019). N-doped TiO₂@TiO₂ visible light active film with stable and efficient photocathodic protection performance. *Journal of Electroanalytical Chemistry*, *844*(May), 91–98.
- Quinn, B., Gagné, F., & Blaise, C. (2008). An investigation into the acute and chronic toxicity of eleven pharmaceuticals (and their solvents) found in wastewater effluent on the cnidarian, *Hydra attenuata*. *Science of the Total Environment*, *389*(2–3), 306–314.
- Quiñones, D. H., Rey, A., Álvarez, P. M., Beltrán, F. J., & Li Puma, G. (2015). Boron doped TiO₂ catalysts for photocatalytic ozonation of aqueous mixtures of common pesticides: Diuron, o-phenylphenol, MCPA and terbuthylazine. *Applied Catalysis B: Environmental*, *178*, 74–81.

- Raj, K. J. A., & Viswanathan, B. (2009). Effect of surface area, pore volume and particle size of P25 titania on the phase transformation of anatase to rutile. *Indian Journal of Chemistry - Section A Inorganic, Physical, Theoretical and Analytical Chemistry*, 48(10), 1378–1382.
- Rimoldi, L., Pargoletti, E., Meroni, D., Falletta, E., Cerrato, G., Turco, F., & Cappelletti, G. (2018). Concurrent role of metal (Sn, Zn) and N species in enhancing the photocatalytic activity of TiO₂ under solar light. *Catalysis Today*, 313(November 2017), 40–46.
- Rivera-Utrilla, J., Bautista-Toledo, I., Ferro-García, M. A., & Moreno-Castilla, C. (2001). Activated carbon surface modifications by adsorption of bacteria and their effect on aqueous lead adsorption. *Journal of Chemical Technology and Biotechnology*, 76(12), 1209–1215.
- Rizzo, L., Sannino, D., Vaiano, V., Sacco, O., Scarpa, A., & Pietrogiacomini, D. (2014). Effect of solar simulated N-doped TiO₂ photocatalysis on the inactivation and antibiotic resistance of an E. coli strain in biologically treated urban wastewater. *Applied Catalysis B: Environmental*, 144, 369–378.
- Rizzo, Luigi, Malato, S., Antakyali, D., Beretsou, V. G., Đolić, M. B., Gernjak, W., Heath, E., Ivancev-Tumbas, I., ... Fatta-Kassinos, D. (2019, March 10). Consolidated vs new advanced treatment methods for the removal of contaminants of emerging concern from urban wastewater. *Science of the Total Environment*, Vol. 655, pp. 986–1008.
- Rodríguez-Loaiza, D. C., Ramírez-Henao, O., & Peñuela-Mesa, G. A. (2016). Assessment of toxicity in industrial wastewater treated by biological processes using luminescent bacteria. *Actualidades Biológicas*, 38(105), 211–216.
- Rodríguez-Narvaez, O. M., Peralta-Hernandez, J. M., Goonetilleke, A., & Bandala, E. R. (2017). Treatment technologies for emerging contaminants in water: A review. *Chemical Engineering Journal*, Vol. 323, pp. 361–380.
- Rodríguez, E. M., Márquez, G., Tena, M., Álvarez, P. M., & Beltrán, F. J. (2015). Determination of main species involved in the first steps of TiO₂ photocatalytic degradation of organics with the use of scavengers: The case of ofloxacin. *Applied Catalysis B: Environmental*, 178, 44–53.
- Salimi, M., Esrafil, A., Gholami, M., Jonidi Jafari, A., Rezaei Kalantary, R., Farzadkia, M., Kermani, M., & Sobhi, H. R. (2017). Contaminants of emerging concern: a review of new approach in AOP technologies. *Environmental Monitoring and Assessment*, 189(8).

- Sanchez-martinez, A., Ceballos-sanchez, O., Koop-santa, C., & López-mena, E. R. (2018). N-doped TiO₂ nanoparticles obtained by a facile coprecipitation method at low temperature. *Ceramics International*, 44(5), 5273–5283.
- Shkir, M., & Yahia, V. G. I. S. (2018). Microwave-synthesis of - La³⁺ doped PbI₂ nanosheets (NSs) and their characterizations for optoelectronic applications. *Journal of Materials Science: Materials in Electronics*, 29(18), 15838–15846.
- Silverman, H., Achberger, E. C., Lynn, J. W., & Dietz, T. H. (1995). Filtration and utilization of laboratory-cultured bacteria by *Dreissena polymorpha*, *Corbicula fluminea*, and *Carunculina texasensis*. *Biological Bulletin*, 189(3), 308–319.
- Smirniotis, P. G., Boningari, T., Damma, D., & Inturi, S. N. R. (2018). Single-step rapid aerosol synthesis of N-doped TiO₂ for enhanced visible light photocatalytic activity. *Catalysis Communications*, 113(February), 1–5.
- Solís, R. R., Javier Rivas, F., Gimeno, O., & Pérez-Bote, J. L. (2015). Photocatalytic ozonation of pyridine-based herbicides by N-doped titania. *Journal of Chemical Technology and Biotechnology*, 91(7), 1998–2008.
- Solís, R. R., Rivas, F. J., Martínez-Piernas, A., & Agüera, A. (2016). Ozonation, photocatalysis and photocatalytic ozonation of diuron: Intermediates identification. *Chemical Engineering Journal*, 292, 72–81.
- Soltermann, F., Abegglen, C., Tschui, M., Stahel, S., & von Gunten, U. (2017). Options and limitations for bromate control during ozonation of wastewater. *Water Research*, 116, 76–85.
- Taheran, M., Naghdi, M., Brar, S. K., Verma, M., & Surampalli, R. Y. (2018, December 1). Emerging contaminants: Here today, there tomorrow! *Environmental Nanotechnology, Monitoring and Management*, Vol. 10, pp. 122–126.
- Todorova, N., Vaimakis, T., Petrakis, D., Hishita, S., Boukos, N., Giannakopoulou, T., Giannouri, M., Antiohos, S., Trapalis, C. (2013). N and N,S-doped TiO₂ photocatalysts and their activity in NO_x oxidation. *Catalysis Today*, 209(2), 41–46.
- Trautmann, N. M., & Krasny, M. E. (1997). “Composting in the classroom. Retrieved April 10, 2019, from <http://compost.css.cornell.edu/schools.html>

- Velegraki, T., Hapeshi, E., Fatta-Kassinos, D., & Poullos, I. (2015). Solar-induced heterogeneous photocatalytic degradation of methyl-paraben. *Applied Catalysis B: Environmental*, 178, 2–11.
- Wang, W., Huang, G., Yu, J. C., & Wong, P. K. (2015). Advances in photocatalytic disinfection of bacteria: Development of photocatalysts and mechanisms. *Journal of Environmental Sciences (China)*, 34, 232–247.
- Wen, Q., Tutuka, C., Keegan, A., & Jin, B. (2009). Fate of pathogenic microorganisms and indicators in secondary activated sludge wastewater treatment plants. *Journal of Environmental Management*, 90(3), 1442–1447.
- Wert, E. C., Rosario-Ortiz, F. L., Drury, D. D., & Snyder, S. A. (2007). Formation of oxidation byproducts from ozonation of wastewater. *Water Research*, 41(7), 1481–1490.
- WHO (World Health Organization). (1997). *Guidelines for drinking-water quality* (Vol. 3).
- WHO (World Health Organization). (2012). UN-Water Global Analysis and Assessment of Sanitation and Drinking-Water: The Challenge of Extending and Sustaining Services. In *UN Water Report*.
- WWAP (United Nations World Water Assessment Programme). (2017). Wastewater - The Untapped Resources. In *The United Nations World Water Development Report. Wastewater. The Untapped Resource*.
- Xiao, J., Xie, Y., & Cao, H. (2015). Organic pollutants removal in wastewater by heterogeneous photocatalytic ozonation. *Chemosphere*, 121, 1–17.
- Zhang, W. F., He, Y. L., Zhang, M. S., Yin, Z., & Chen, Q. (2000). *Raman scattering study on anatase TiO₂ nanocrystals*. 3–8.

APPENDIX A

Parabens removal during UV/O₃/TiO₂ and UV/O₃ reactions

Method 1

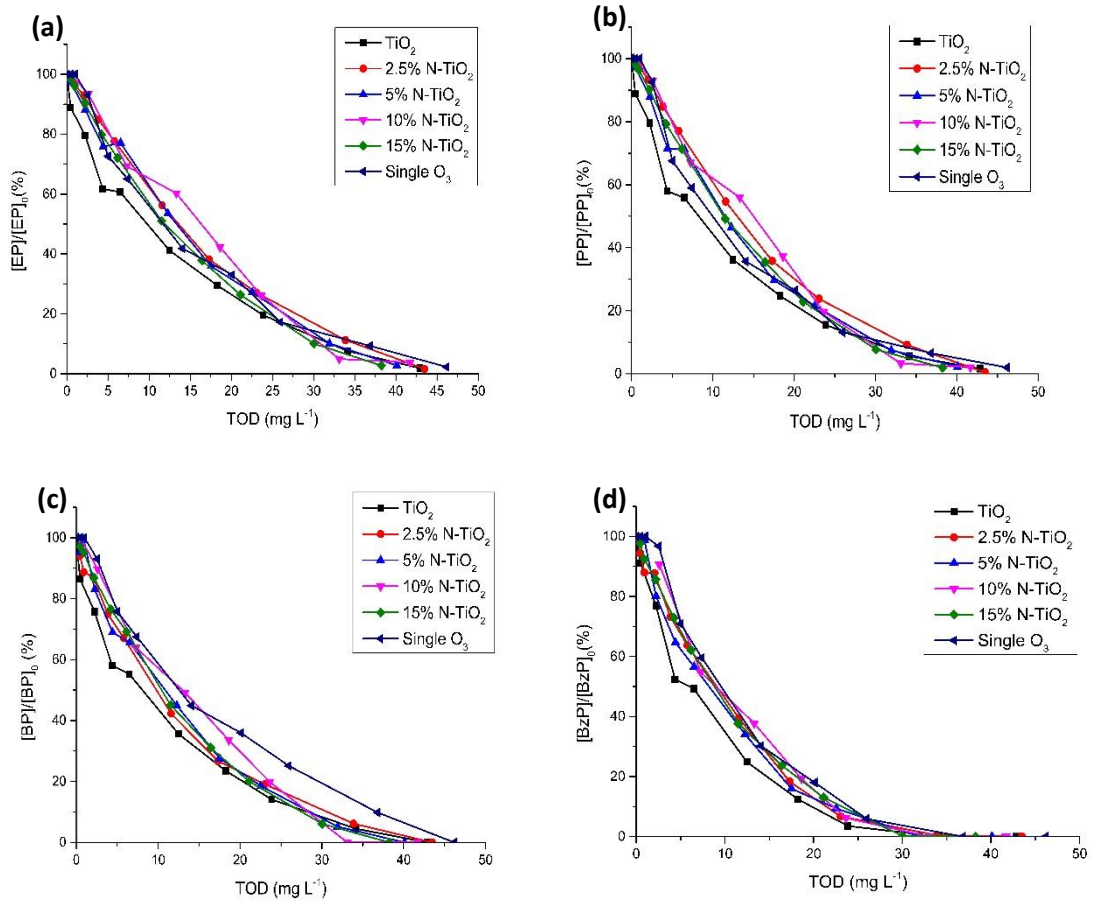


Figure A1 - Ethylparaben (a), propylparaben (b), butylparaben (c) and benzylparaben (d) degradation as a function of TOD during single and photocatalytic ozonation reactions using method 1 TiO₂ and N-TiO₂.

Method 2

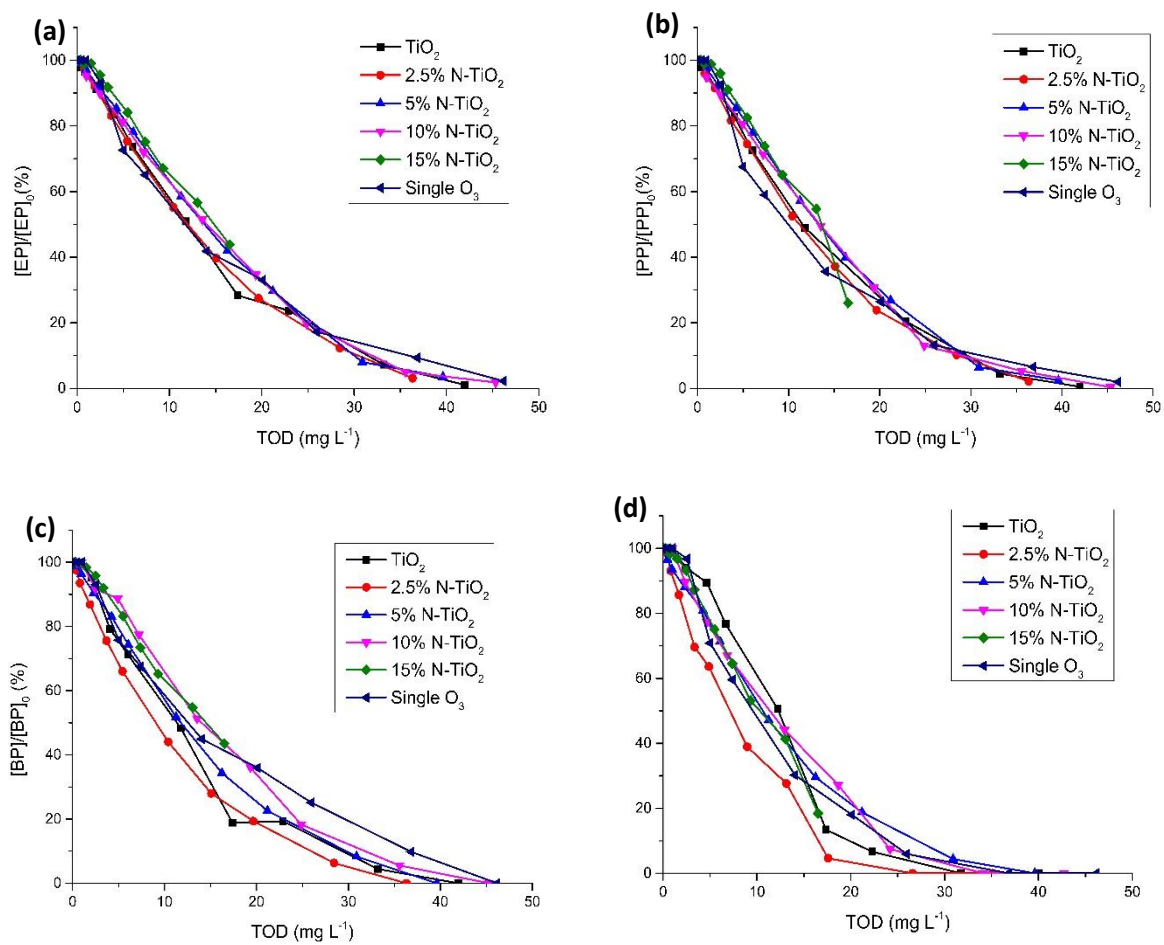


Figure A2 - Ethylparaben (a), propylparaben (b), butylparaben (c) and benzylparaben (d) degradation as a function of TOD during single and photocatalytic ozonation reactions using method 2 TiO₂ and N-TiO₂.

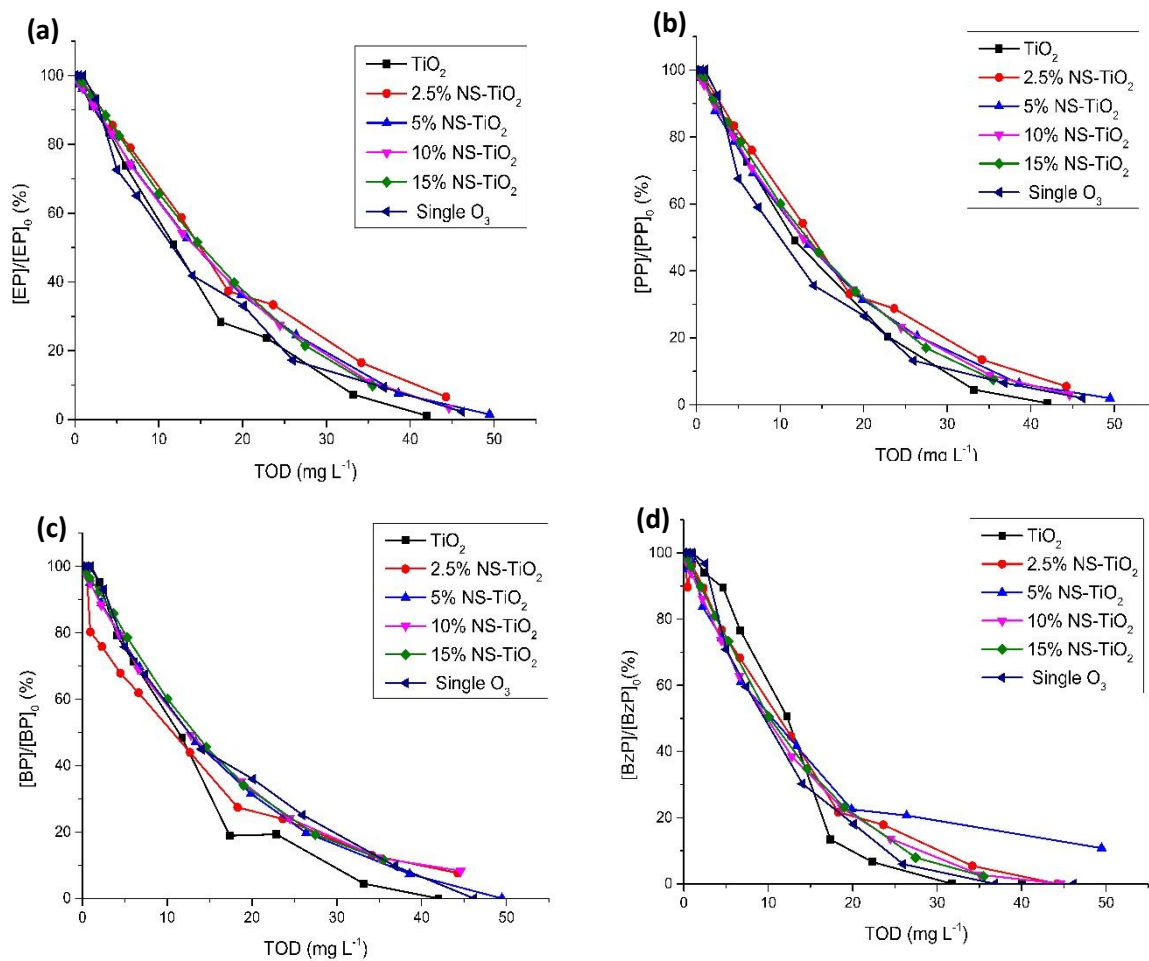


Figure A3 - Ethylparaben (a), propylparaben (b), butylparaben (c) and benzylparaben (d) degradation as a function of TOD during single and photocatalytic ozonation reactions using method 2 TiO_2 and NS- TiO_2 .

APPENDIX B

Calibration curve for chemical oxygen demand (COD)

